Magnetism as seen with X Rays

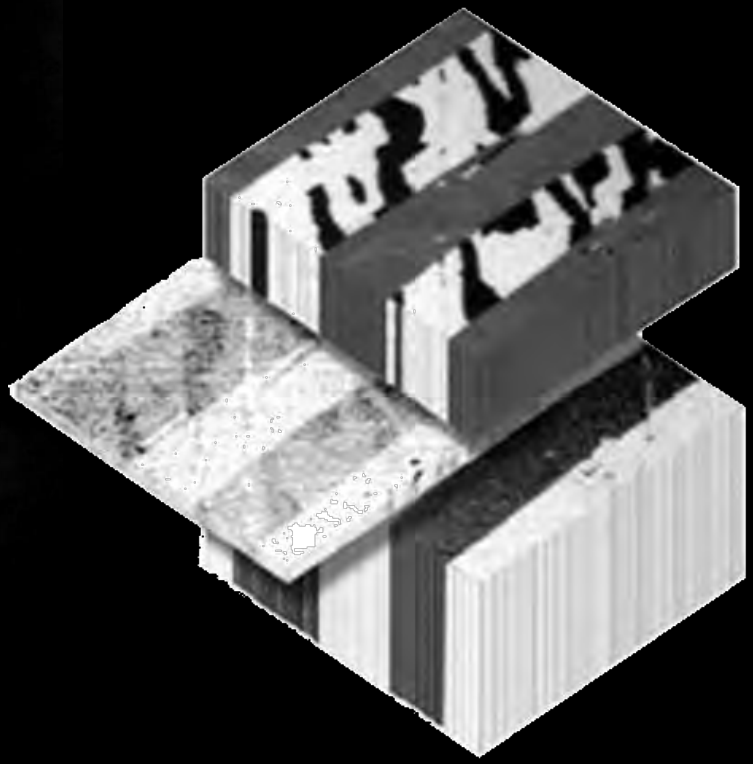

Elke Arenholz

Cornell High Energy Synchrotron Source, CHESS

and

Department of Material Science and Engineering, Cornell University

What to expect:

+ Magnetic Materials Today
+ Magnetic Materials Characterization Wish List
+ Soft X-ray Absorption Spectroscopy – Basic concept and examples
+ X-ray magnetic circular dichroism (XMCD)
    - Basic concepts
    - Applications and examples
    - Dynamics: X-Ray Ferromagnetic Resonance (XFMR)
+ X-Ray Linear Dichroism and X-ray Magnetic Linear Dichroism (XLD and XMLD)
+ Magnetic Imaging using soft X-rays
+ Ultrafast dynamics

Magnetic Materials Today: Permanent/Hard Magnetic Materials

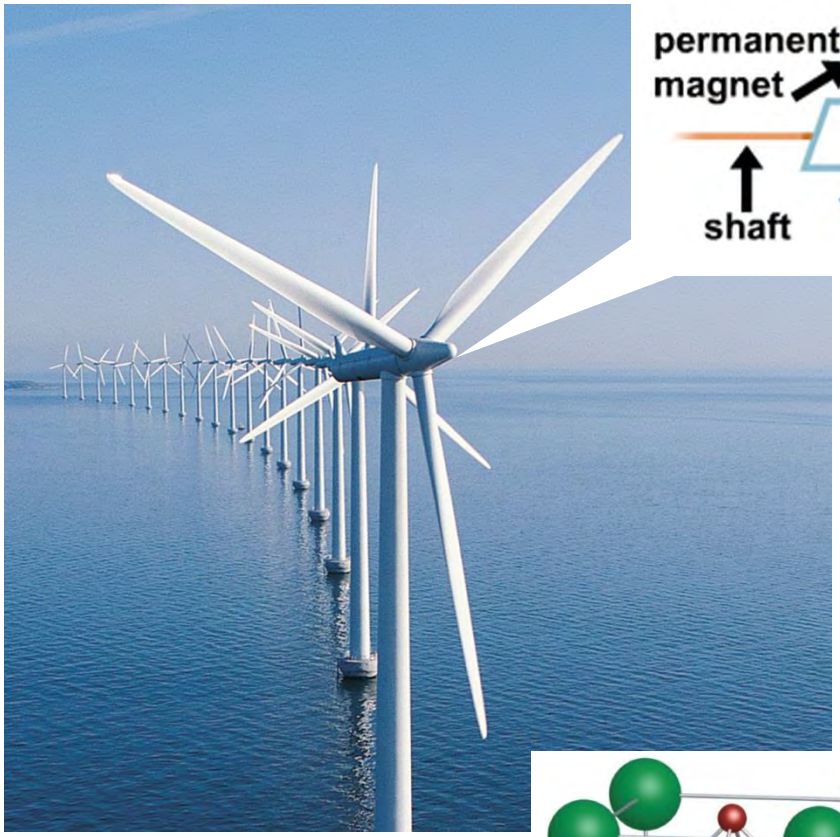

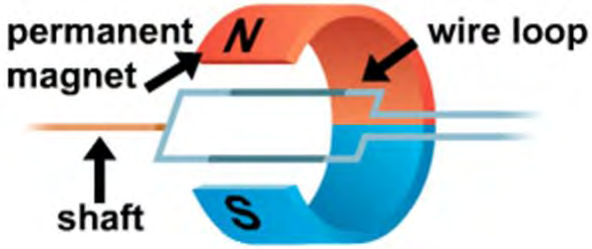

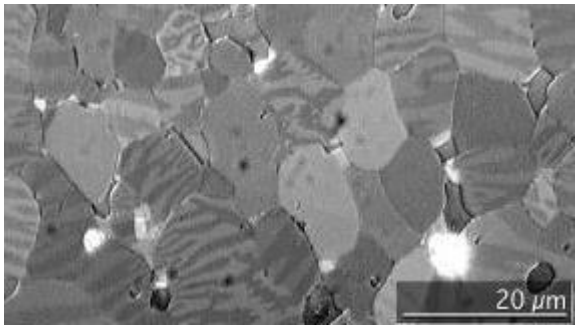

Controlling grain and domain structure on the micro- and nanoscale

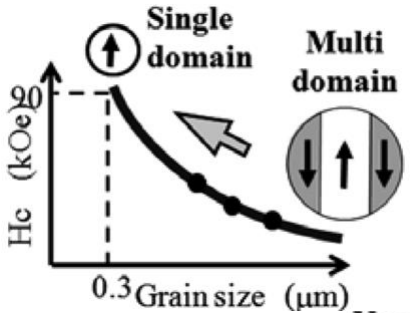

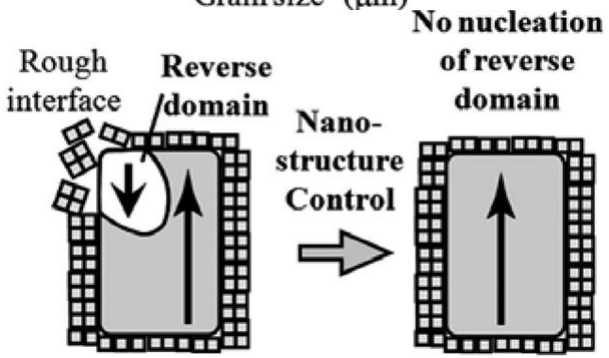

Engineering magnetic anisotropy on the atomic scale

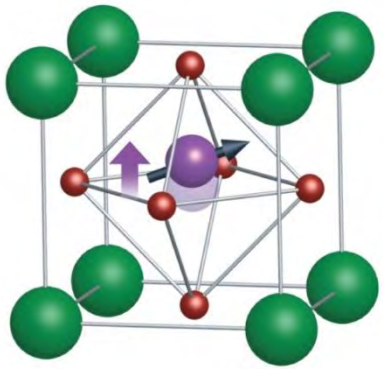

Magnetic Materials Today: Magnetic Nanoparticles

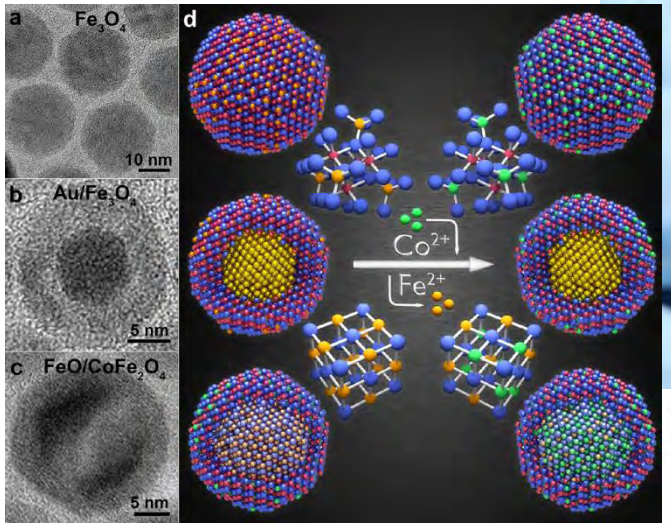

Tailoring magnetic nanoparticles for environmental applications

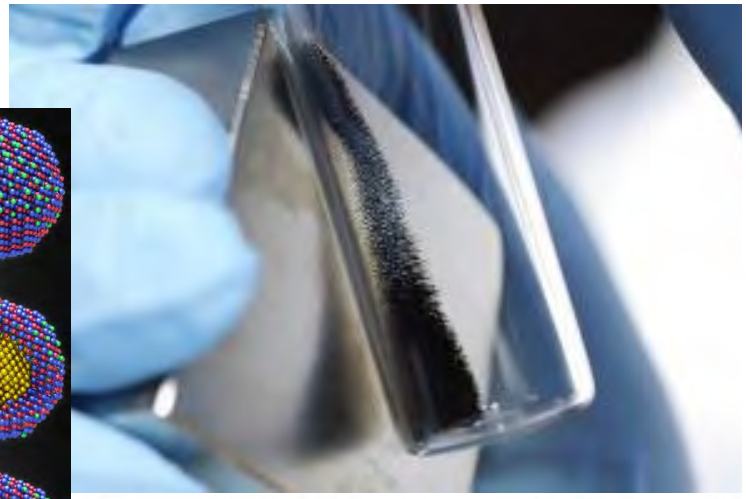

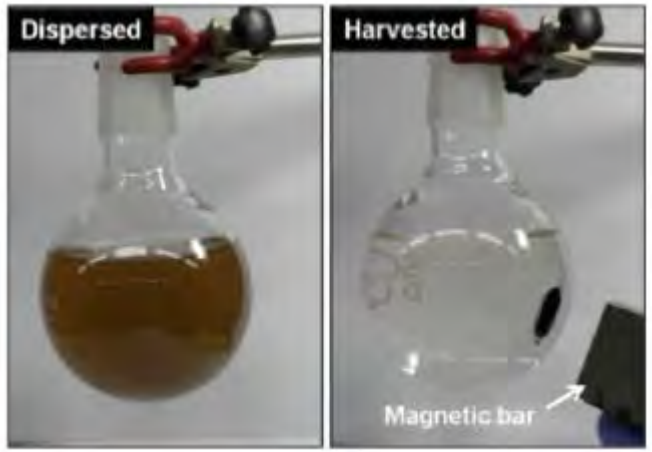

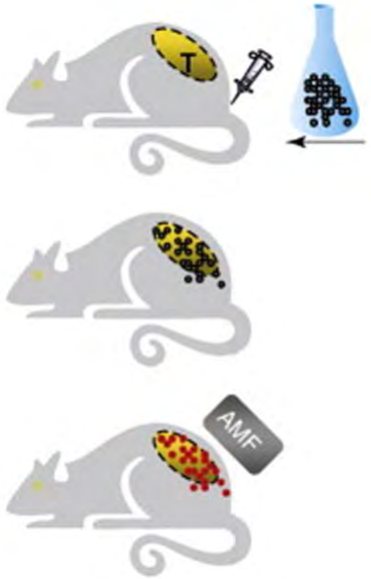

Optimizing magnetic nanoparticles for biomedical applications

Magnetic Materials Today: Magnetic Thin Films

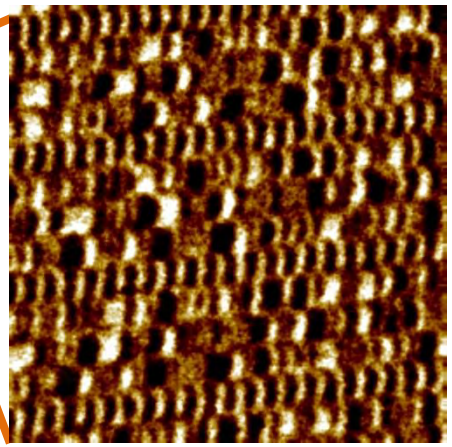

Magnetic domain structure on the nanometer scale

Magnetic coupling at interfaces

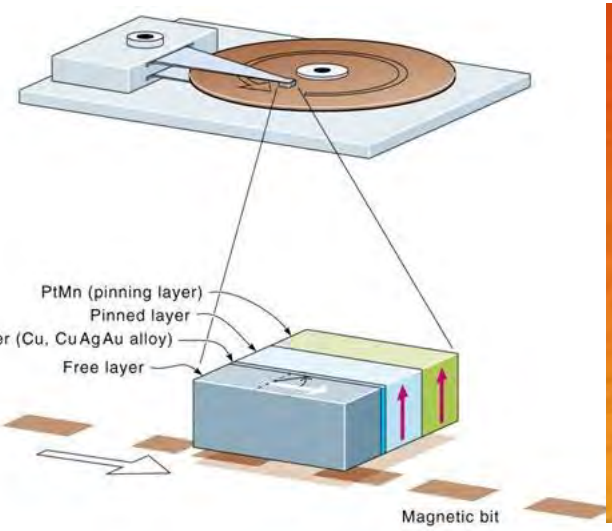

Ultrafast magnetization reversal dynamics

GMR Read Head Sensor

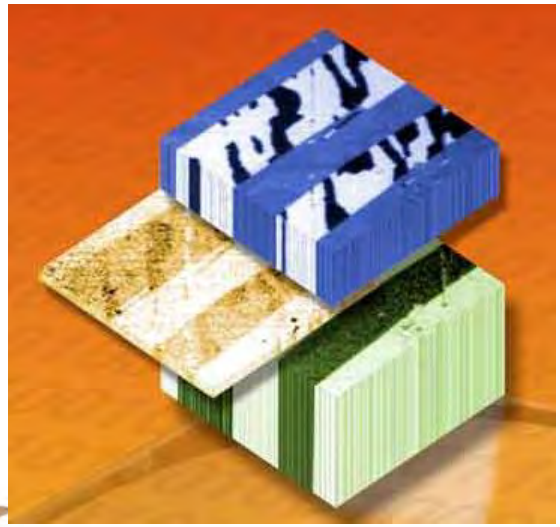

Unique magnetic phases at interfaces

Magnetic Materials Characterization Wish List

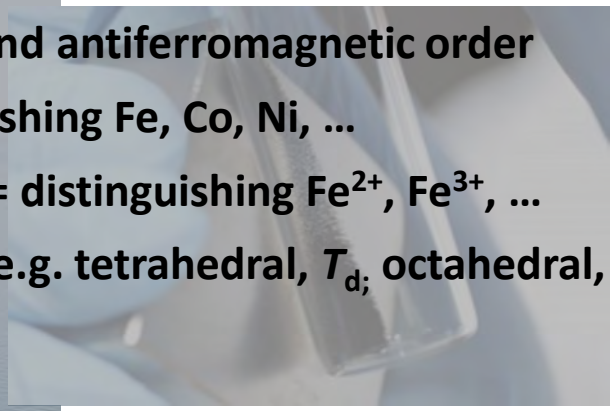

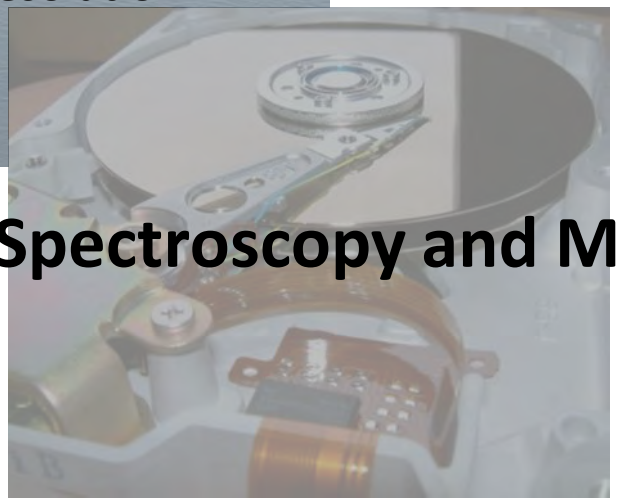

+ Sensitivity to ferromagnetic and antiferromagnetic order
+ Element specificity = distinguishing Fe, Co, Ni, …
+ Sensitivity to oxidation state = distinguishing Fe^{2+}, Fe^{3+}, …
+ Sensitivity to site symmetry, e.g. tetrahedral, T_d, octahedral, O_h
+ Nanometer spatial resolution
+ Ultra-fast time resolution

Soft X-Ray Spectroscopy and Microscopy

Spectroscopy

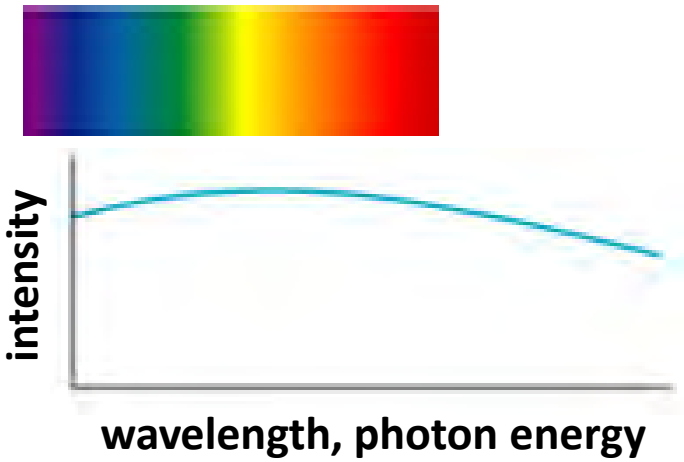

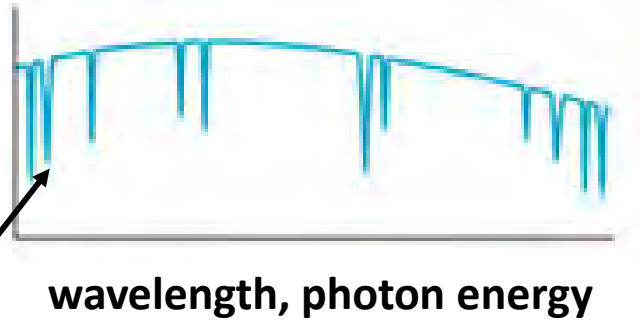

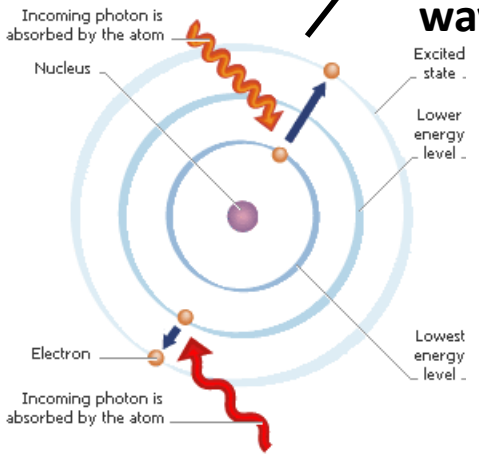

Soft X-Ray Spectroscopy (hν ≈ 500-1000eV, λ ≈ 1-2nm)

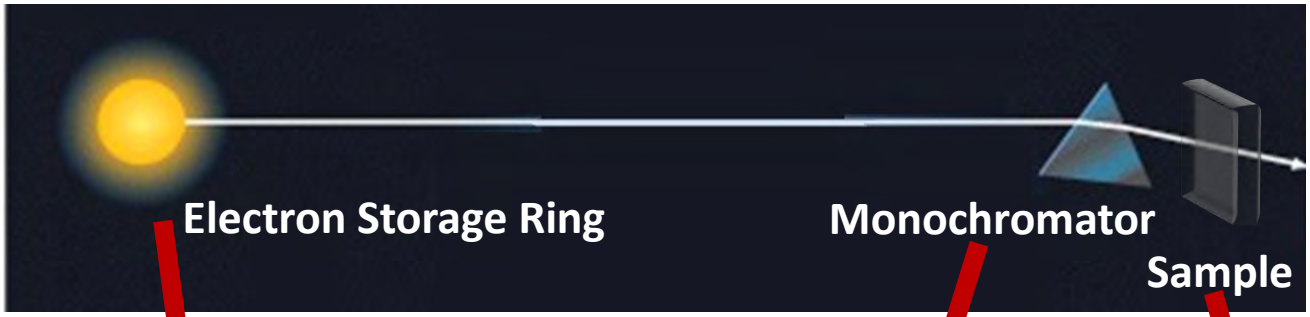

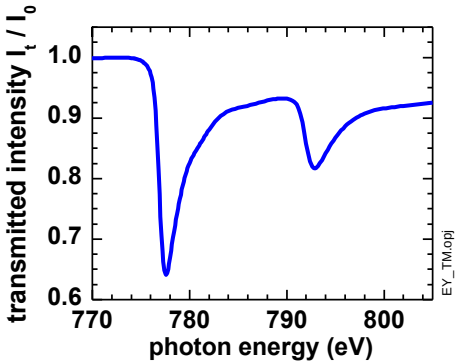

X-Ray Absorption – Detection Modes

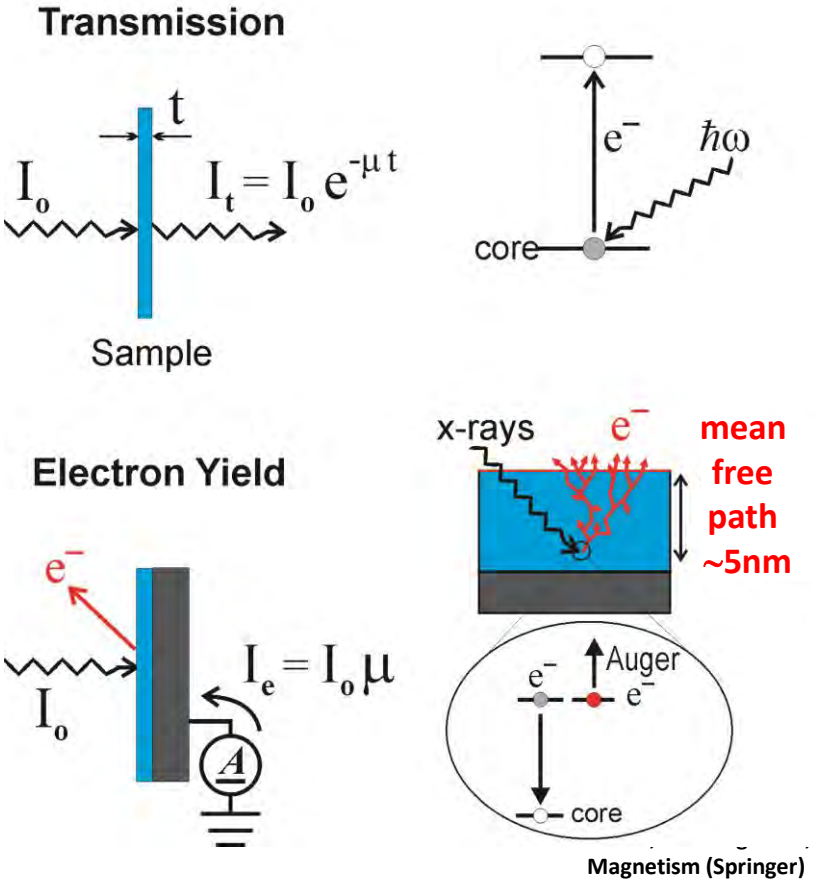

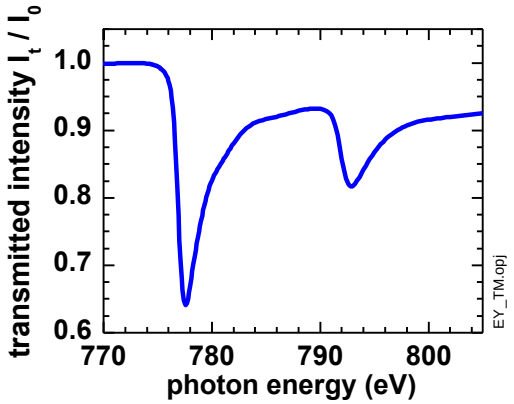

Photons absorbed

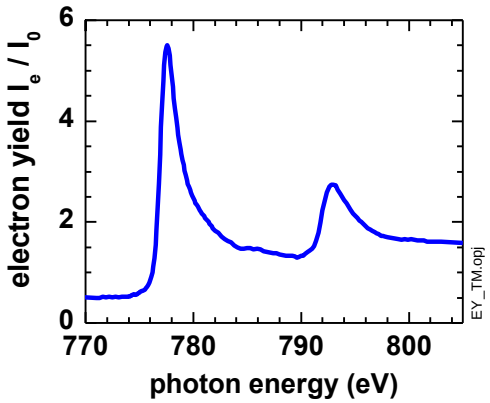

Electrons generated

Electron yield:

+ Absorbed photons create core holes subsequently filled by Auger electron emission
+ Auger electrons create low-energy secondary electron cascade through inelastic scattering
+ Emitted electrons ∝ probability of Auger electron creation ∝ absorption probability

Soft X-Ray Absorption – Probing Depth

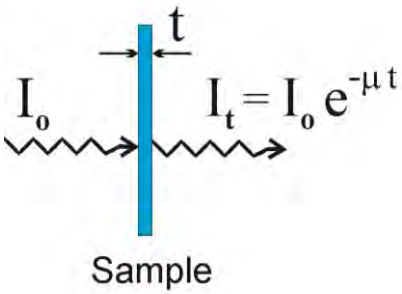

Element	10eV below L_3 1/μ [nm]	at L_3 1/μ [nm]	40 eV above L_3 1/μ [nm]
Fe	550	17	85
Co	550	17	85
Ni	625	24	85

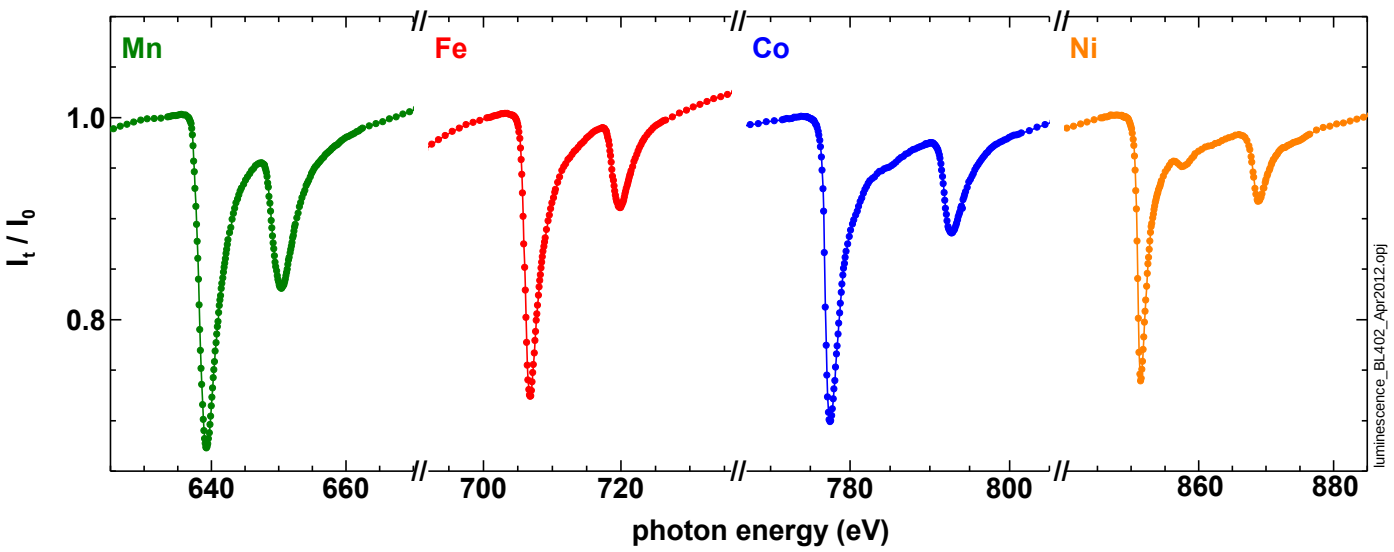

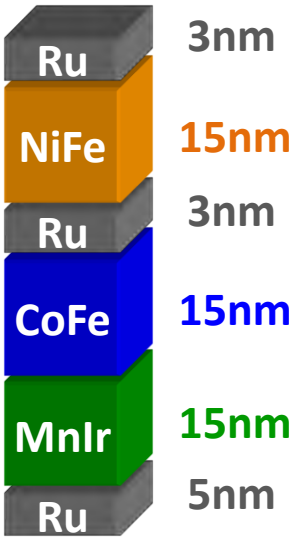

~10-20 nm layer thick films supported by substrates transparent to soft X rays

X-Ray Absorption – Detection Modes and Probing Depth

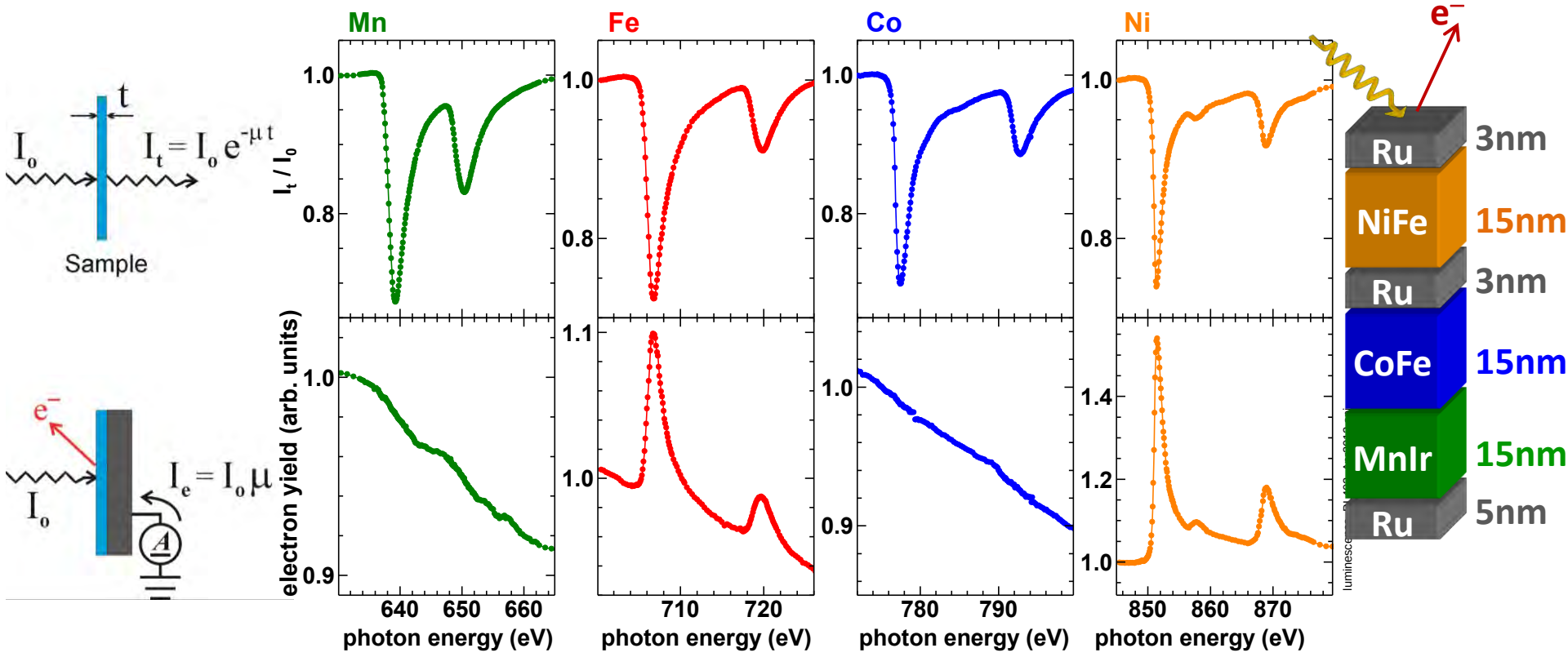

+ Electron sample depth: 2-5 nm in Fe, Co, Ni

  ⇒ 60% of the electron yield originates form the topmost 2-5 nm

X-Ray Absorption – Fundamentals

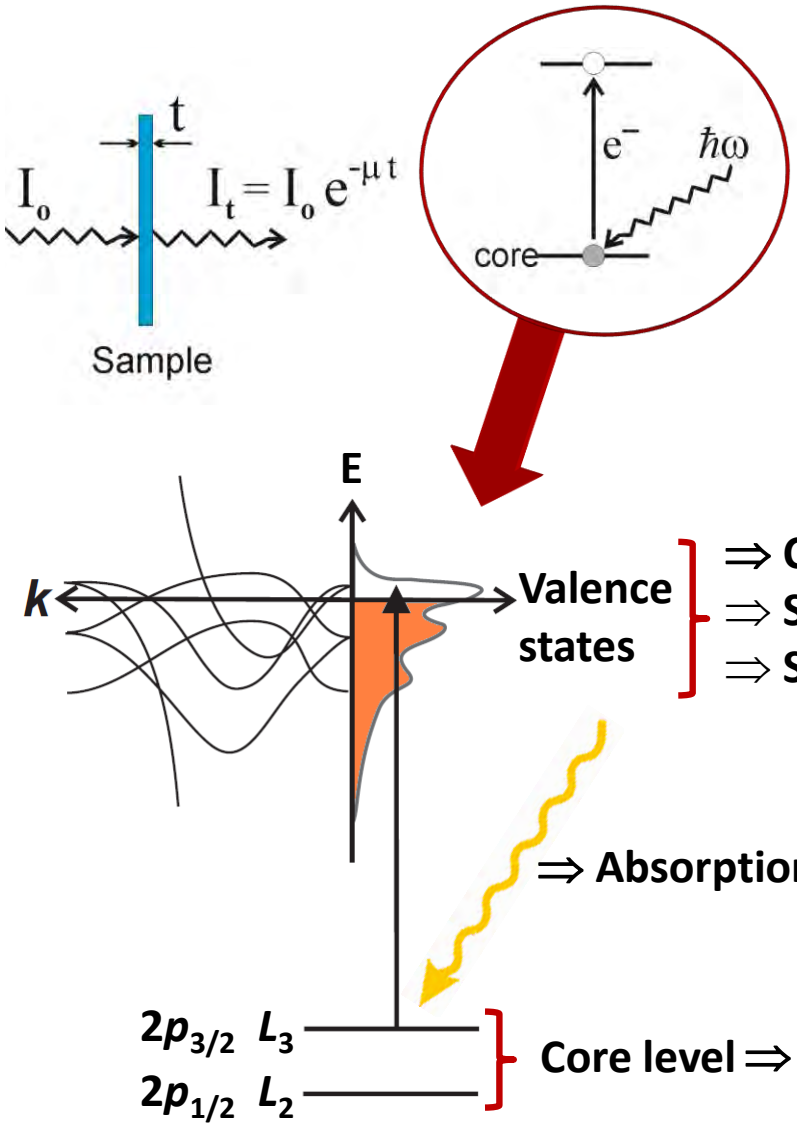

Experimental Concept:

Monitor reduction in X-ray flux transmitted through sample as function of photon energy

⇒ Charge state of absorber Fe^{2+}, Fe^{3+}

⇒ Symmetry of lattice site of absorber: O_h, T_d

⇒ Sensitive to magnetic order

⇒ Absorption probability: X-ray energy, X-ray polarization, experimental geometry

Core level ⇒ Atomic species of absorber Fe, Co, Ni, ….

X-Ray Absorption – Fundamentals

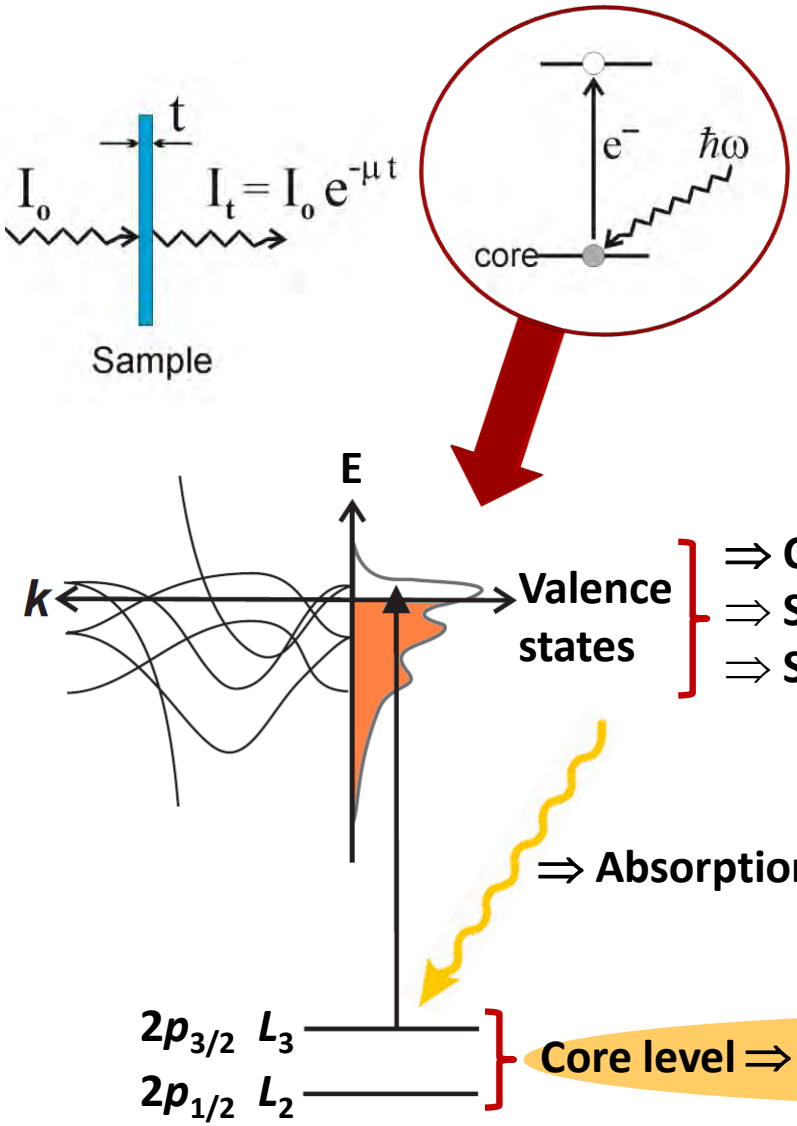

Experimental Concept:

Monitor reduction in X-ray flux transmitted through sample as function of photon energy

⇒ **Charge state of absorber Fe^{2+}, Fe^{3+}**

⇒ **Symmetry of lattice site of absorber: O_h, T_d**

⇒ **Sensitive to magnetic order**

⇒ **Absorption probability: X-ray energy, X-ray polarization, experimental geometry**

Core level ⇒ Atomic species of absorber Fe, Co, Ni, ….

‘White Line’ Intensity

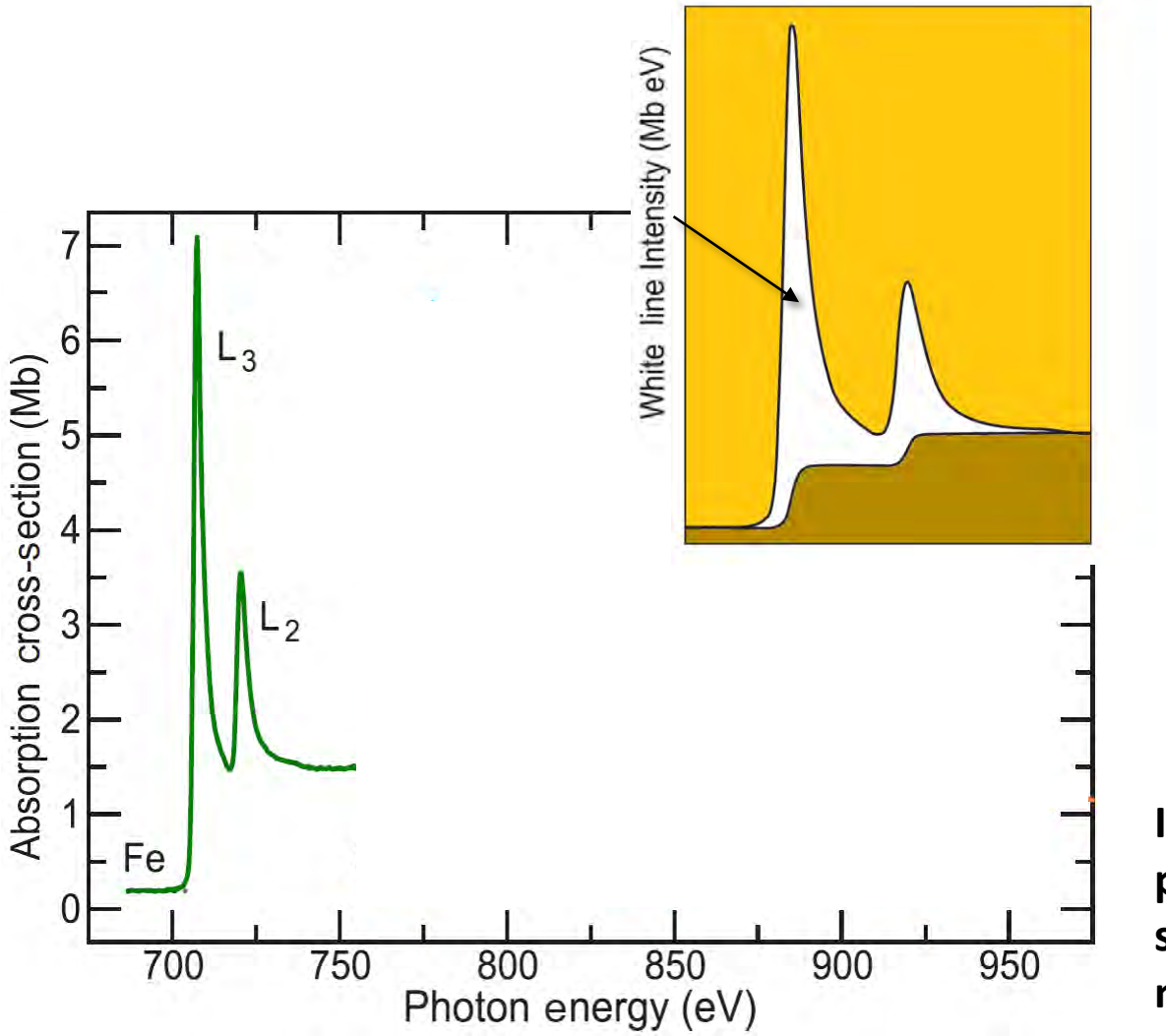

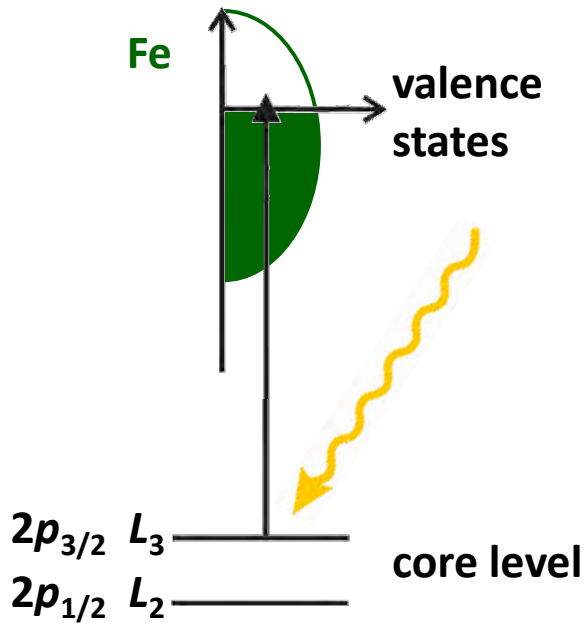

Intensity of $L_{3,2}$ resonances is proportional to number of *d* states above the Fermi level, i.e. number of holes in the *d band.*

‘White Line’ Intensity

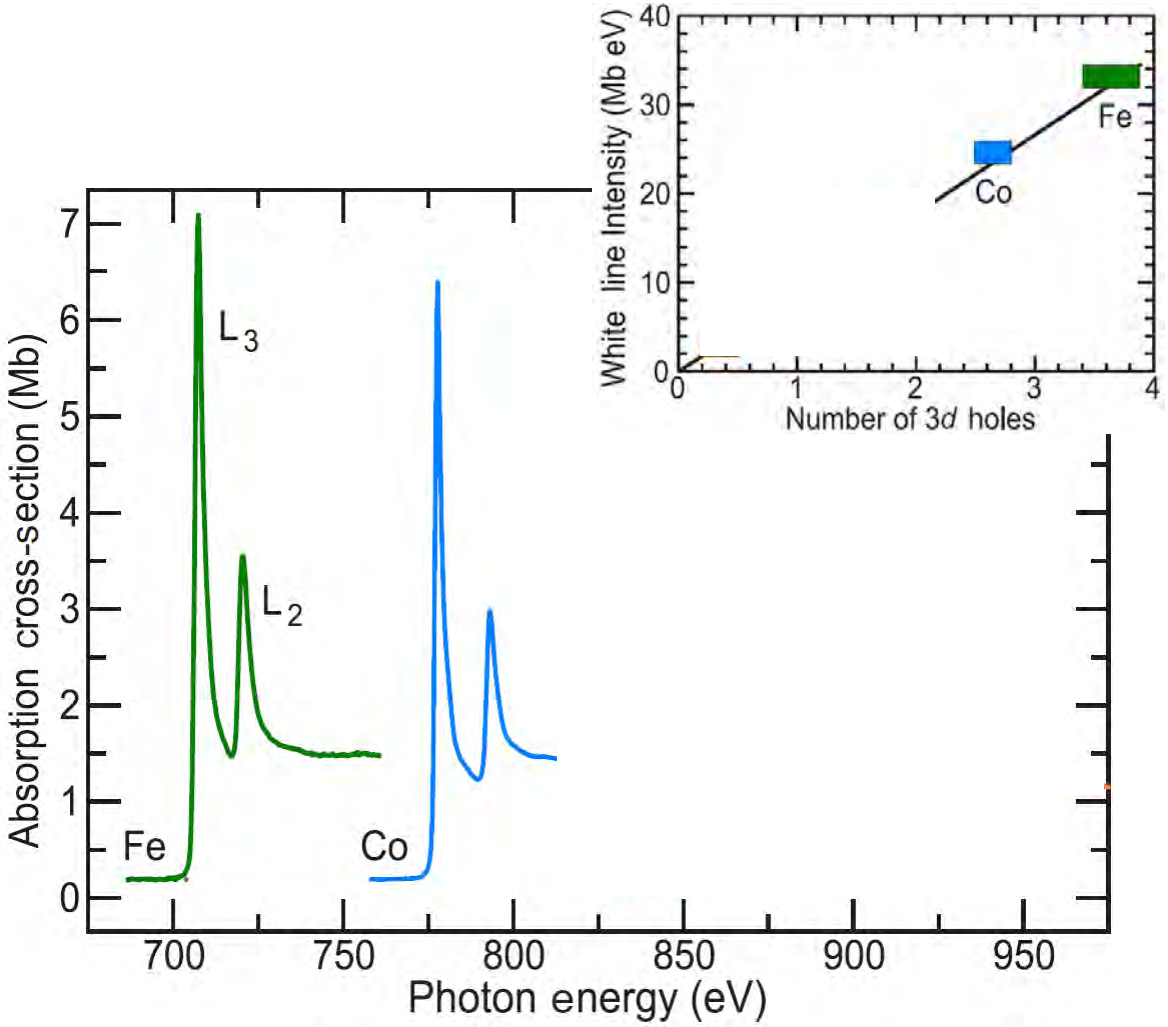

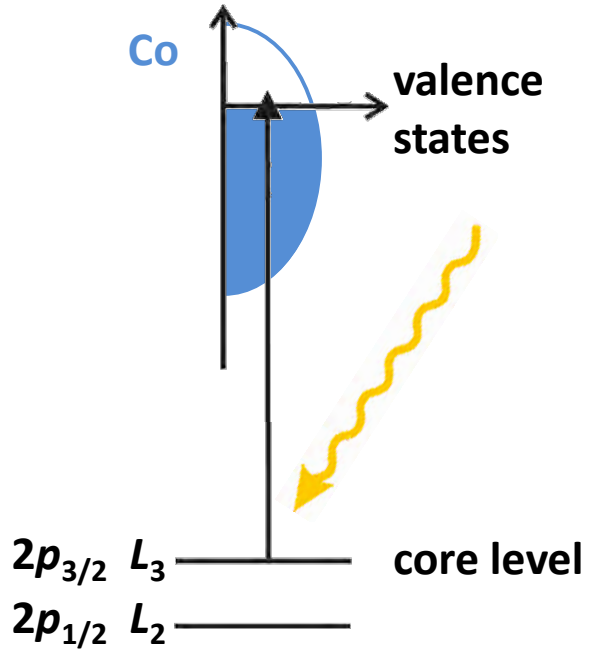

Intensity of $L_{3,2}$ resonances is proportional to number of *d* states above the Fermi level, i.e. number of holes in the *d band.*

‘White Line’ Intensity

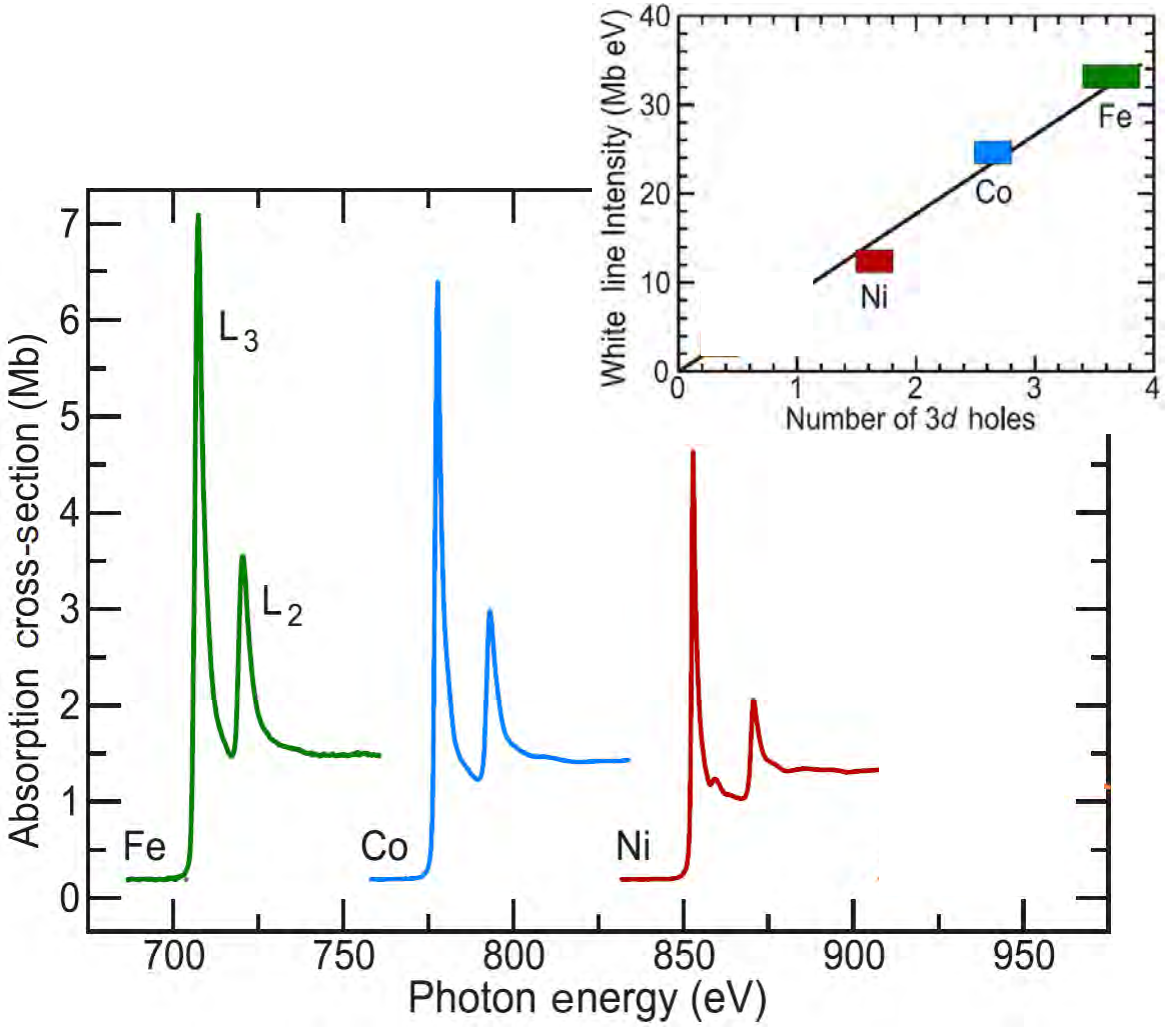

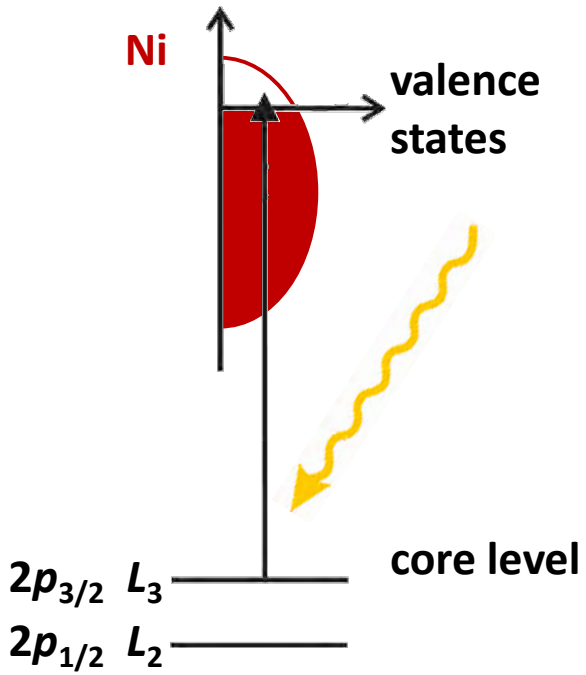

Intensity of $L_{3,2}$ resonances is proportional to number of *d* states above the Fermi level, i.e. number of holes in the *d band.*

‘White Line’ Intensity

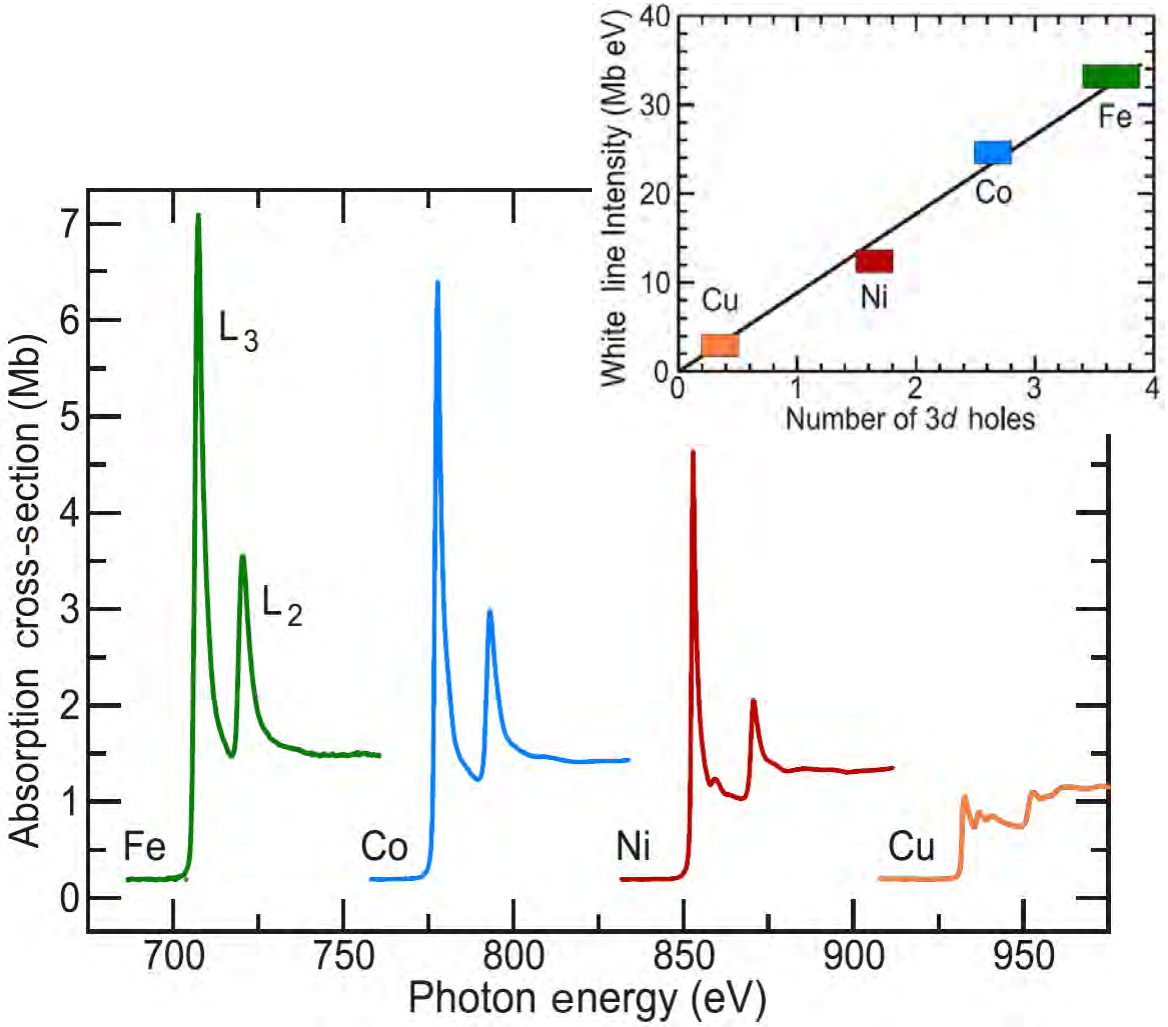

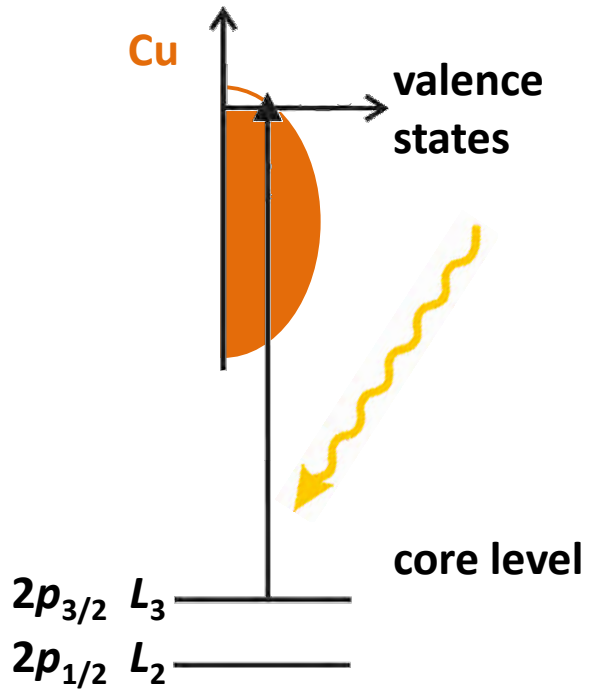

Intensity of $L_{3,2}$ resonances is proportional to number of *d* states above the Fermi level, i.e. number of holes in the *d band.*

X-Ray Absorption – Fundamentals

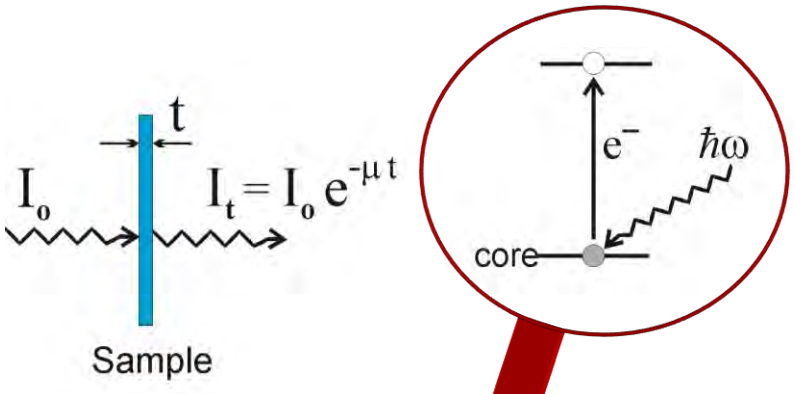

Experimental Concept:

Monitor reduction in X-ray flux transmitted through sample as function of photon energy

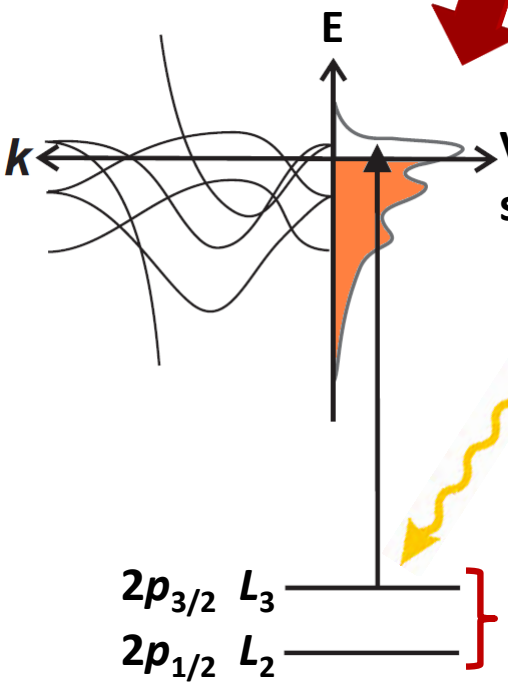

⇒ **Charge state of absorber Fe^{2+}, Fe^{3+}, …**

⇒ **Symmetry of lattice site of absorber: O_h, T_d**

⇒ **Sensitive to magnetic order**

⇒ **Absorption probability: X-ray energy, X-ray polarization, experimental geometry**

Core level ⇒ Atomic species of absorber Fe, Co, Ni, ….

X-ray Absorption – Valence State

Influence of the charge state of the absorber

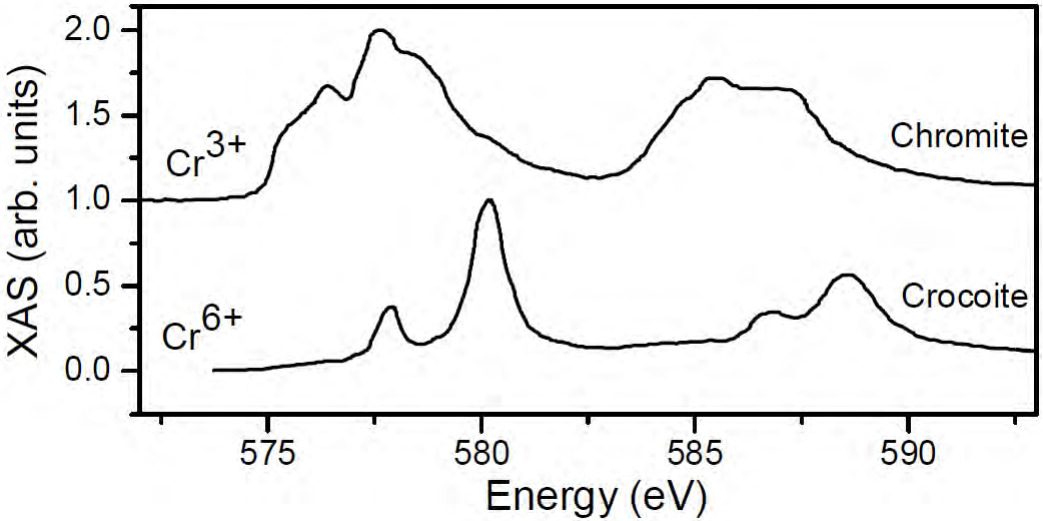

N. Telling *et al.*,
Appl. Phys. Lett. 95, 163701 (2009)

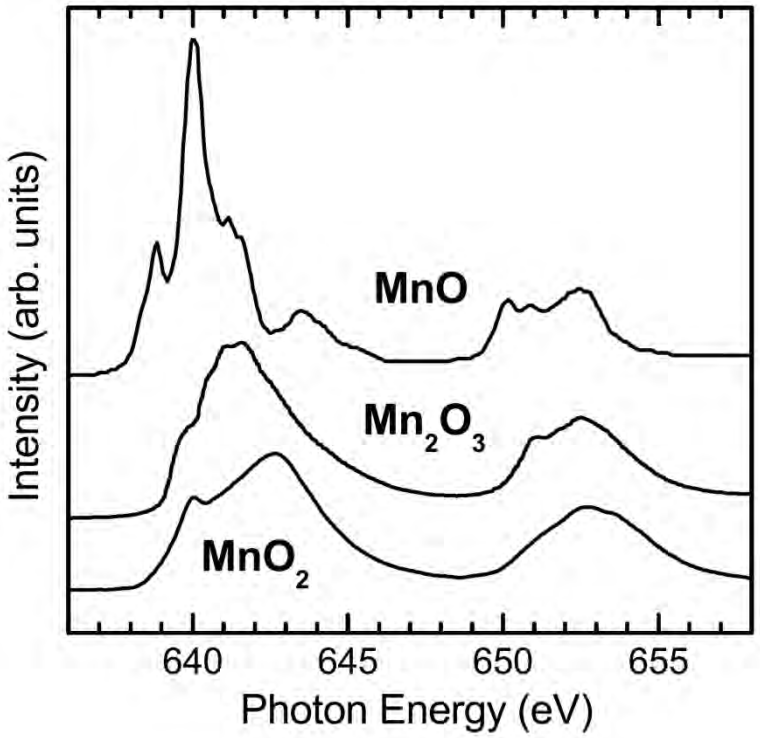

J.-S. Kang et al., Phys. Rev. B 77, 035121 (2008)

X-Ray Absorption – Configuration Model

Ni^{2+} in NiO: $2p^6\,3d^8 \rightarrow 2p^5\,3d^9$

Configuration model, e.g. *L* edge absorption :

+ **Excited from ground/initial state configuration, $2p^6 3d^8$ to exited/final state configuration, $2p^5 3d^9$**
+ **Omission of all full subshells (spherical symmetric)**
+ **Takes into account correlation effects in the ground state as well as in the excited state**
+ **Leads to multiplet effects/structure**

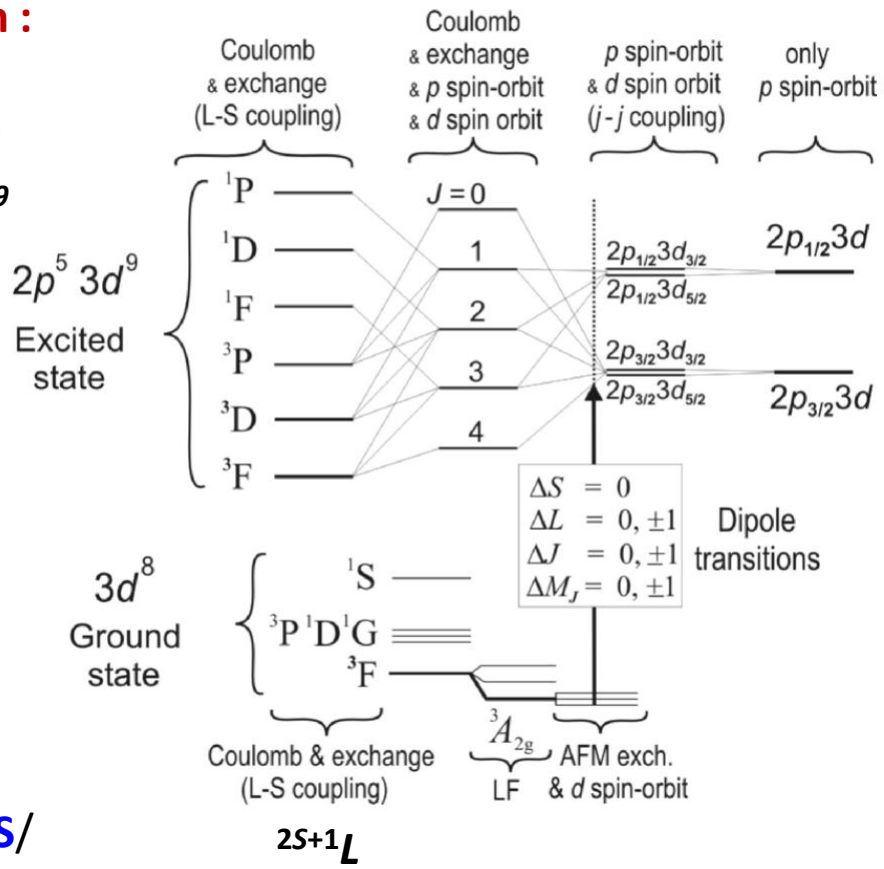

http://www.anorg.chem.uu.nl/CTM4XAS/

J. Stöhr, H.C. Siegmann, Magnetism (Springer)

X-Ray Absorption – Fundamentals

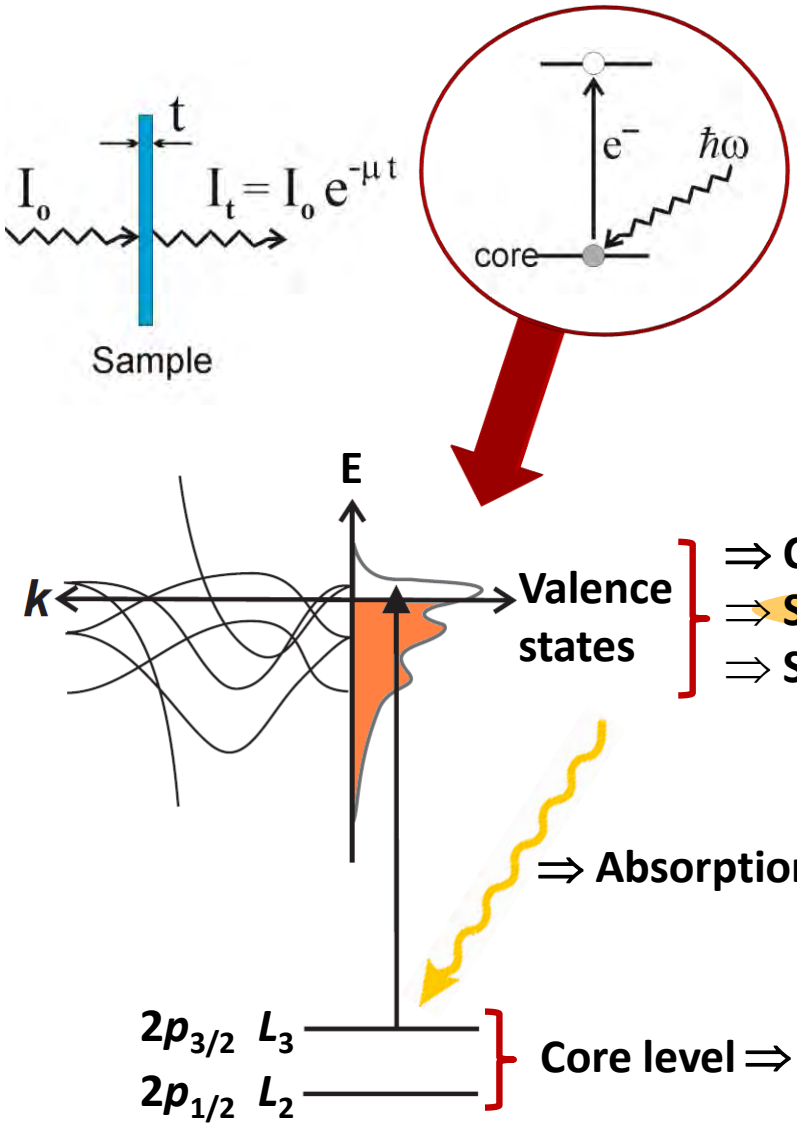

Experimental Concept:

Monitor reduction in X-ray flux transmitted through sample as function of photon energy

⇒ **Charge state of absorber Fe^{2+}, Fe^{3+}**

⇒ **Symmetry of lattice site of absorber: O_h, T_d**

⇒ **Sensitive to magnetic order**

⇒ **Absorption probability: X-ray energy, X-ray polarization, experimental geometry**

Core level ⇒ Atomic species of absorber Fe, Co, Ni, ….

Sensitivity To Site Symmetry: Ti^{4+} $L_{3,2}$

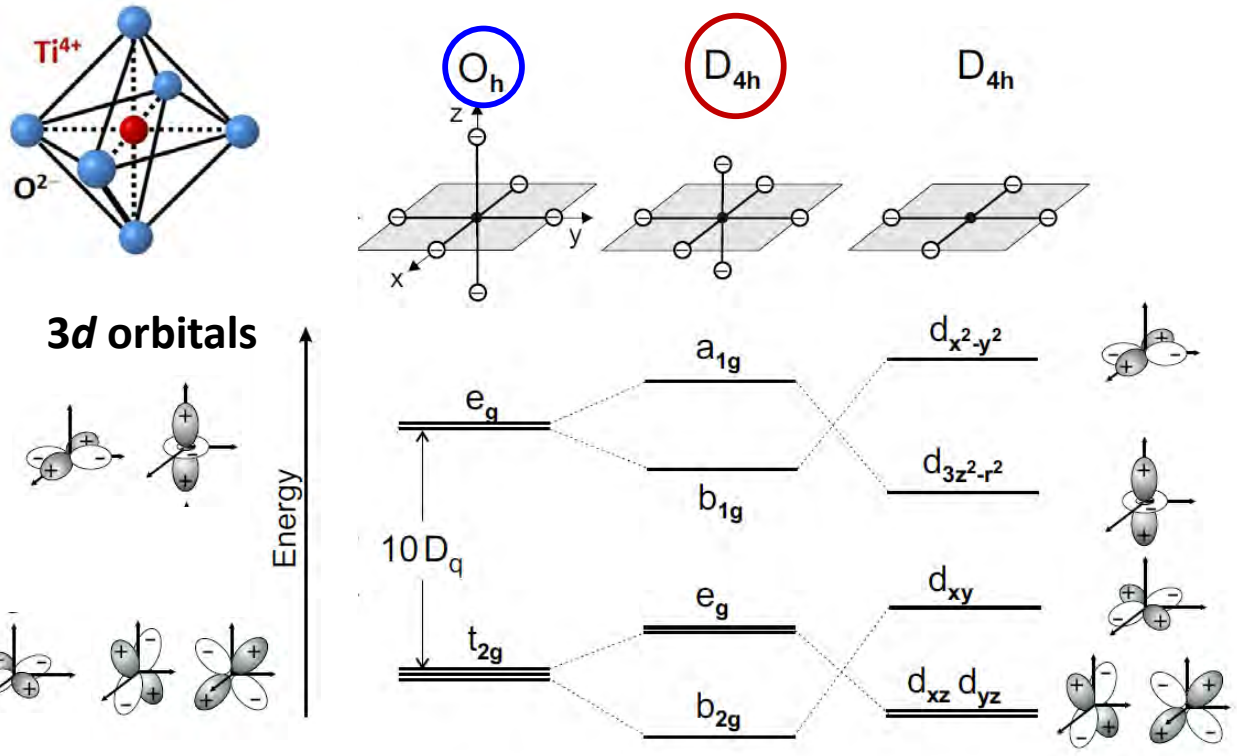

J. Stöhr, H.C. Siegmann, Magnetism (Springer)

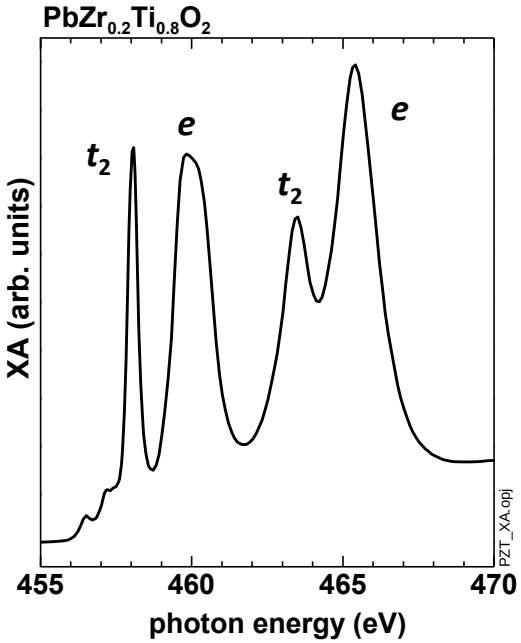

+ Electric dipole transitions: $d^0 \rightarrow 2p^5 3d^1$

+ Crystal field splitting 10*Dq* acting on 3*d* orbitals:

Octahedral symmetry:

e orbitals towards ligands → higher energy

t_2 orbitals between ligands → lower energy

Tetragonal symmetry:

e orbitals → $b_2 = d_{xy}$, $e = d_{yz}, d_{yz}$

t_2 orbitals → $b_1 = d_{x^2-y^2}$, $a_1 = d_{3z^2-r^2}$

X-Ray Absorption – Lattice Symmetry

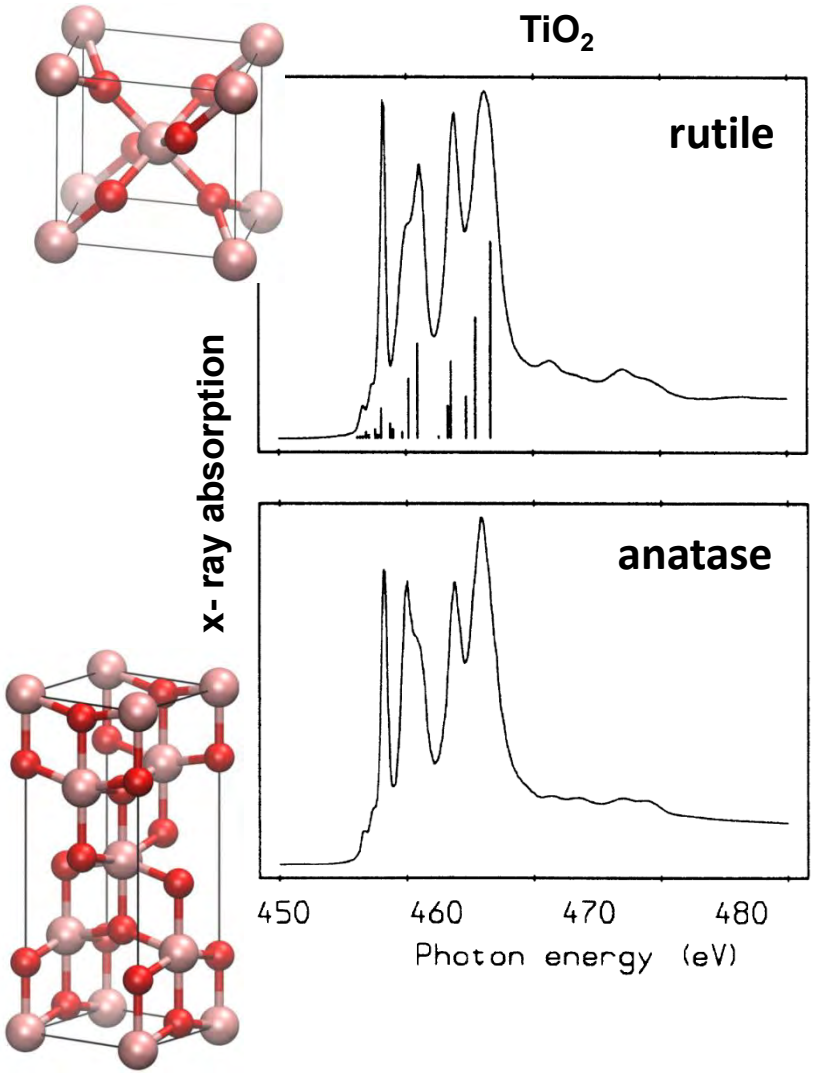

Influence of lattice site symmetry at the absorber

G. Van der Laan
Phys. Rev. B 41, 12366 (1990)

X-Ray Absorption – Fundamentals

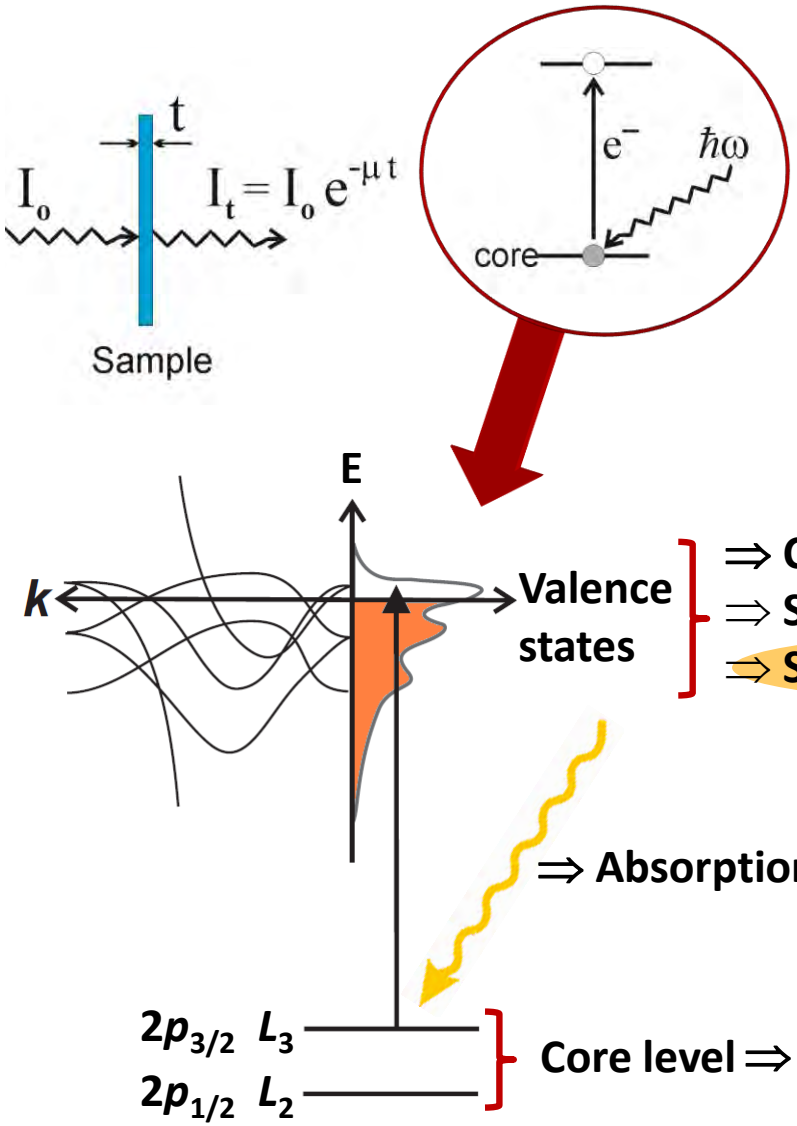

Experimental Concept:

Monitor reduction in X-ray flux transmitted through sample as function of photon energy

⇒ **Charge state of absorber Fe^{2+}, Fe^{3+}**

⇒ **Symmetry of lattice site of absorber: O_h, T_d**

⇒ **Sensitive to magnetic order**

⇒ **Absorption probability: X-ray energy, X-ray polarization, experimental geometry**

Core level ⇒ Atomic species of absorber Fe, Co, Ni, ….

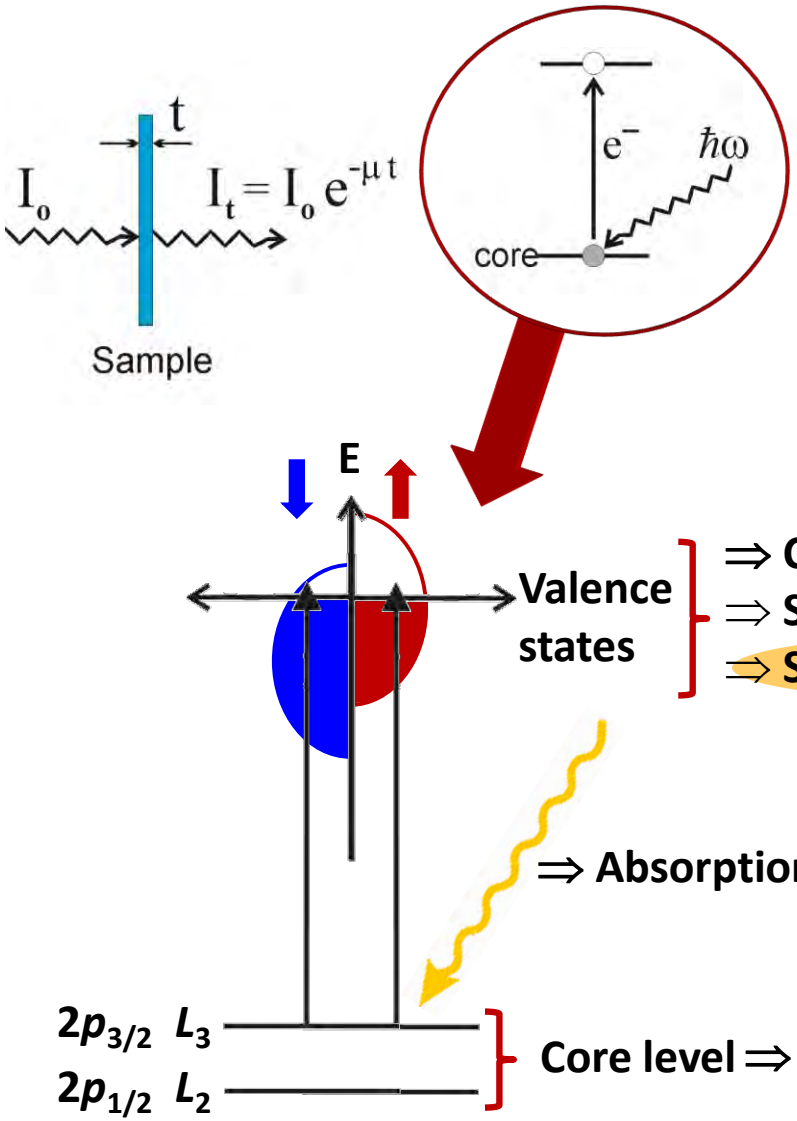

Experimental Concept:

Monitor reduction in X-ray flux transmitted through sample as function of photon energy

⇒ **Charge state of absorber Fe^{2+}, Fe^{3+}**

⇒ **Symmetry of lattice site of absorber: O_h, T_d**

⇒ **Sensitive to magnetic order**

⇒ **Absorption probability: X-ray energy, X-ray polarization, experimental geometry**

Core level ⇒ Atomic species of absorber Fe, Co, Ni, ….

Stoner Model For Ferromagnetic Metals

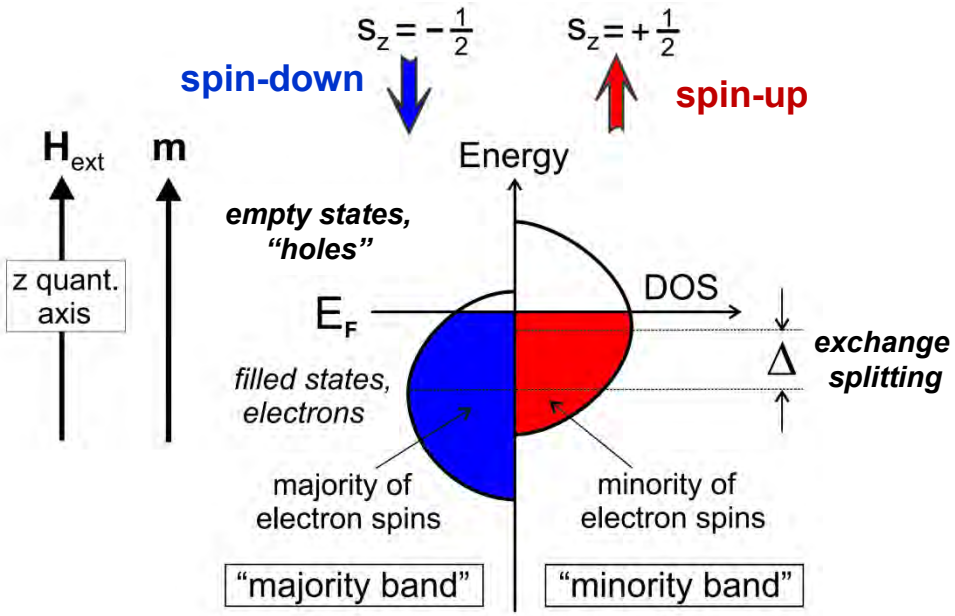

J. Stöhr, H.C. Siegmann, Magnetism (Springer)

3*d* shell

+ **Magnetic moments in Fe, Co, Ni well described by Stoner model: *d*-bands containing up and down spins shifted relative to each other by exchange splitting**
+ **Spin-up and spin-down bands filled according to Fermi statistics**
+ **Magnetic moment |m| determined by difference in number of electrons in majority and minority bands**

$$|m| \propto \mu_B (n_e^{maj} - n_e^{min})$$

Origin of X-ray Magnetic Circular Dichroism

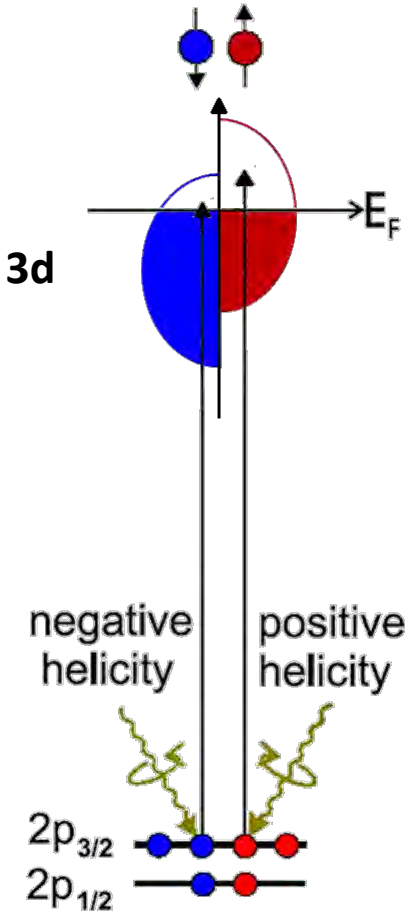

2-Step Model for photoexcitation of electrons from $2p_{3/2}$, $2p_{1/2}$ to $3d$ states by absorption of circularly polarized X rays:

+ Transfer of angular momentum of incident circular polarized X rays to excited electrons (angular momentum conservation, selection rules)
+ Spin polarization of excited electrons opposite for incident X rays with opposite helicity.
+ Unequal spin-up and spin-down populations in exchange split valence shell acts as detector for spin of excited electrons.

Origin of X-ray Magnetic Circular Dichroism

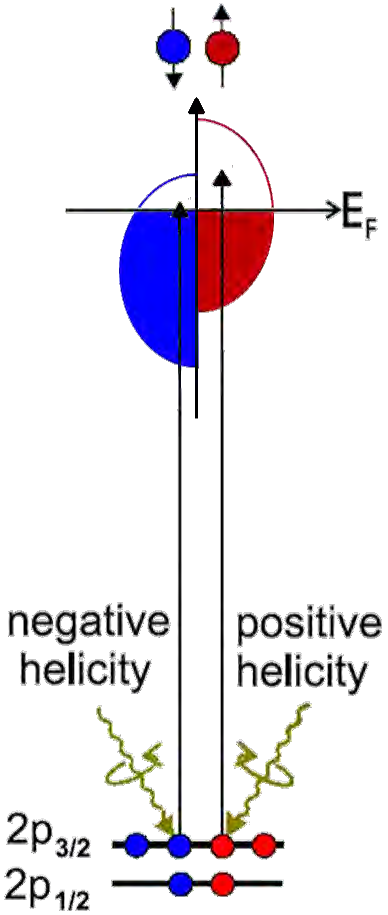

+ Calculate transition probabilities from filled $2p_{3/2}$ and $2p_{1/2}$ states to empty states in *d*-band for circularly polarized X rays using Fermi's Golden Rule

Origin of X-ray Magnetic Circular Dichroism

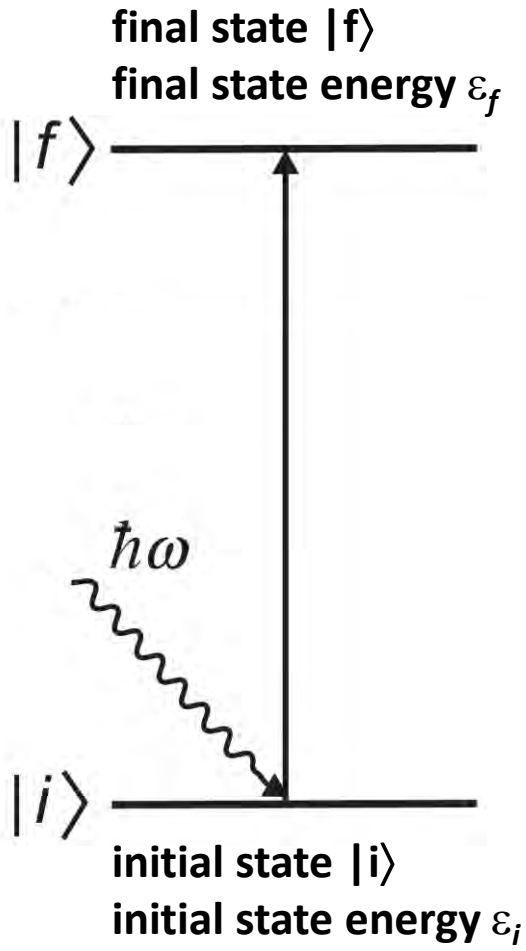

+ Wave functions describe electronic and photon states
  Energies include electronic and photon energies
+ Calculate transitions probabilities T_{if}
  considering photon as time-dependent perturbation,
  i.e. an electromagnetic (EM) field

Fermi's Golden Rule

$$T_{if} = \frac{2\pi}{\hbar} \left| \langle f | \mathcal{H}_{\text{int}} | i \rangle \right|^2 \delta(\varepsilon_i - \varepsilon_f) \rho(\varepsilon_f)$$

$\rho(\varepsilon_f)$ = density of final states per unit energy

T_{if} Dimension [time^{-1}]

$$\mathcal{H}_{\text{int}} = \frac{e}{m_e} \boldsymbol{p} \cdot \boldsymbol{A}$$

Origin of X-ray Magnetic Circular Dichroism

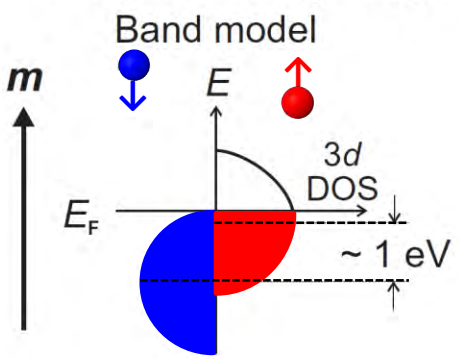

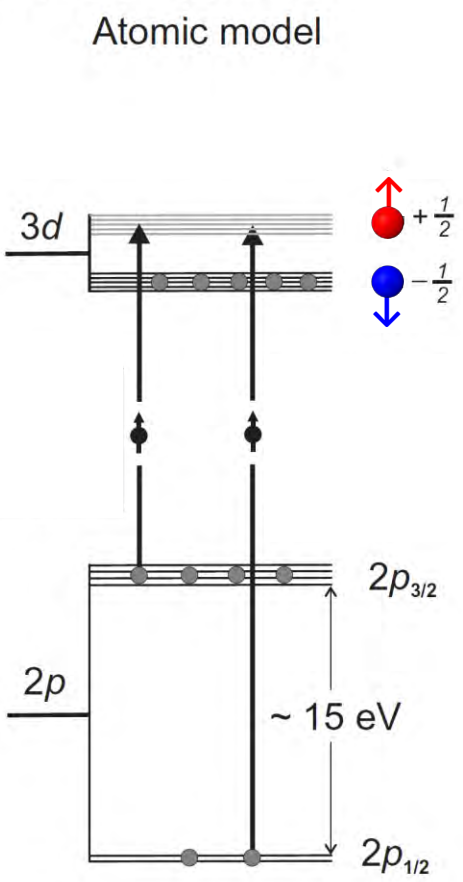

J. Stöhr, H.C. Siegmann, Magnetism (Springer)

X-ray absorption of circularly polarized photons with angular momentum $q = \pm 1$ in units of ħ

+ **Consider strong ferromagnet with one filled spin band:**
  - **All spin down *d* states filled**
  - **Spin up *d* states partially filled**

+ **This specific case: Only spin up electron excited**

Origin of X-ray Magnetic Circular Dichroism

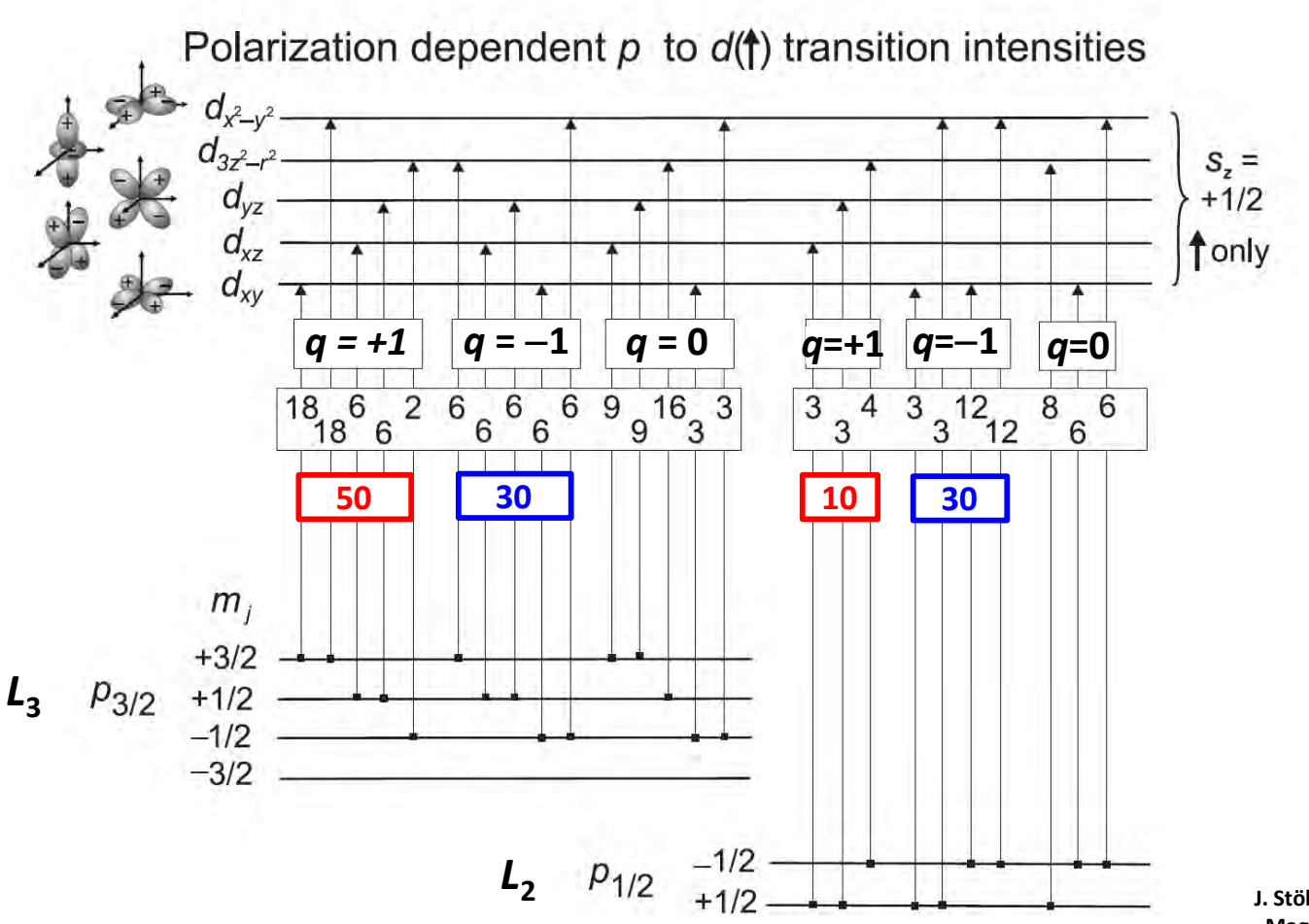

J. Stöhr, H.C. Siegmann, Magnetism (Springer)

L_3: X rays with q = +/–1 excite 62.5%/37.5% of the spin up electrons

L_2: X rays with q = +/–1 excite 25%/75% of the spin up electrons

Origin of X-ray Magnetic Circular Dichroism

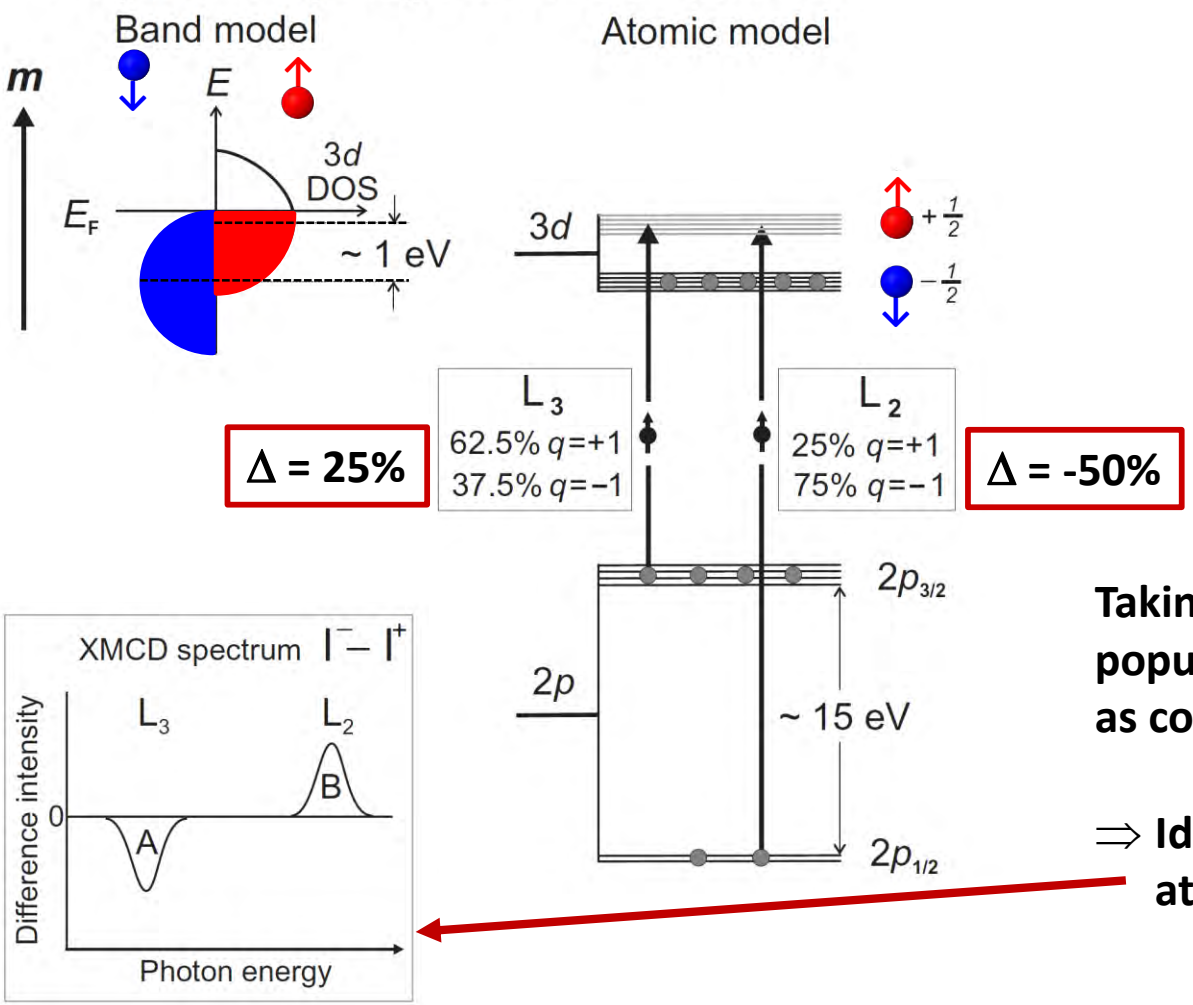

J. Stöhr, H.C. Siegmann, Magnetism (Springer)

Taking into account 2x higher population of $2p_{3/2}$ state as compared to $2p_{1/2}$ state:

⇒ Identical magnitude XMCD at L_3 and L_2 with opposite sign

X-Ray Magnetic Circular Dichroism (XMCD)

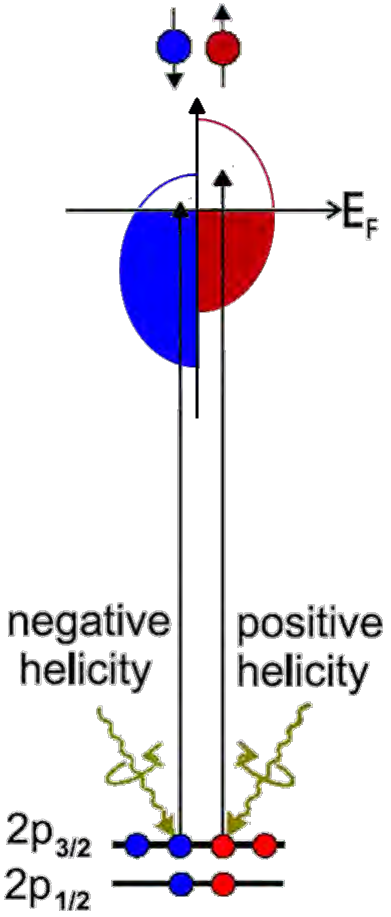

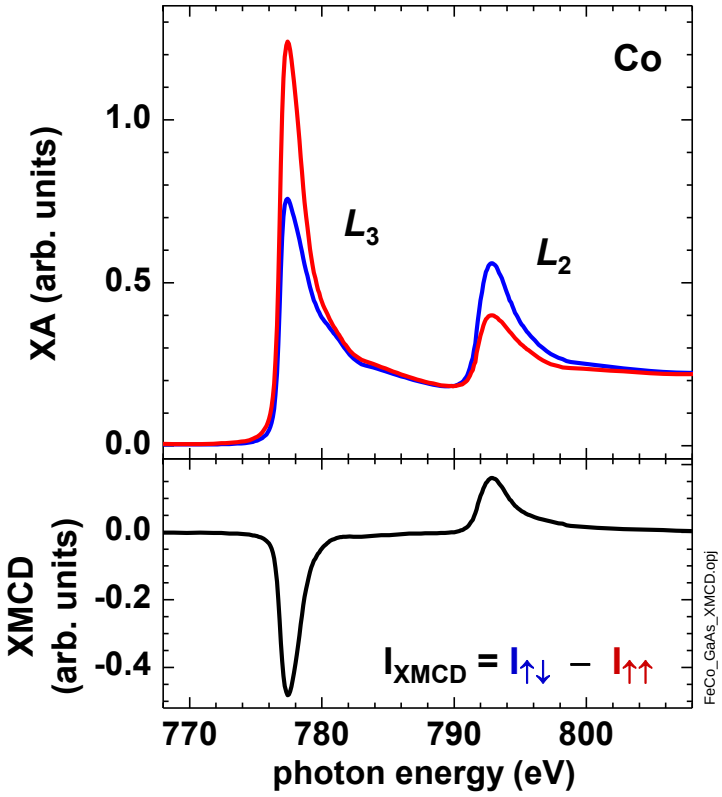

Magnitude of XMCD depends on

- **+ expectation value of 3*d* magnetic moment**
- **+ degree of circular photon polarization, P_{circ}**
- **+ geometry**

X-Ray Magnetic Circular Dichroism (XMCD)

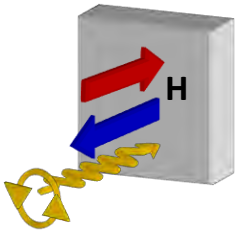

circularly polarized

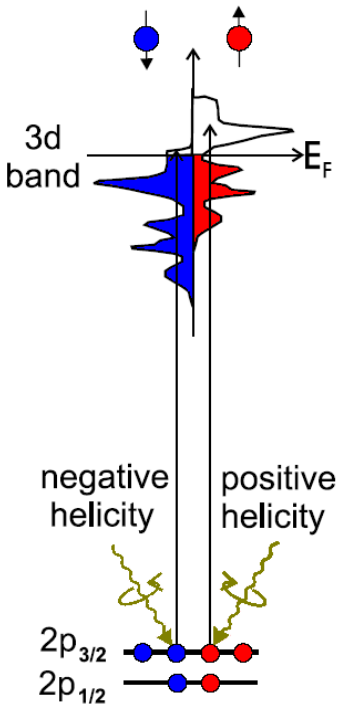

J. Stöhr, H.C. Siegmann, Magnetism (Springer)

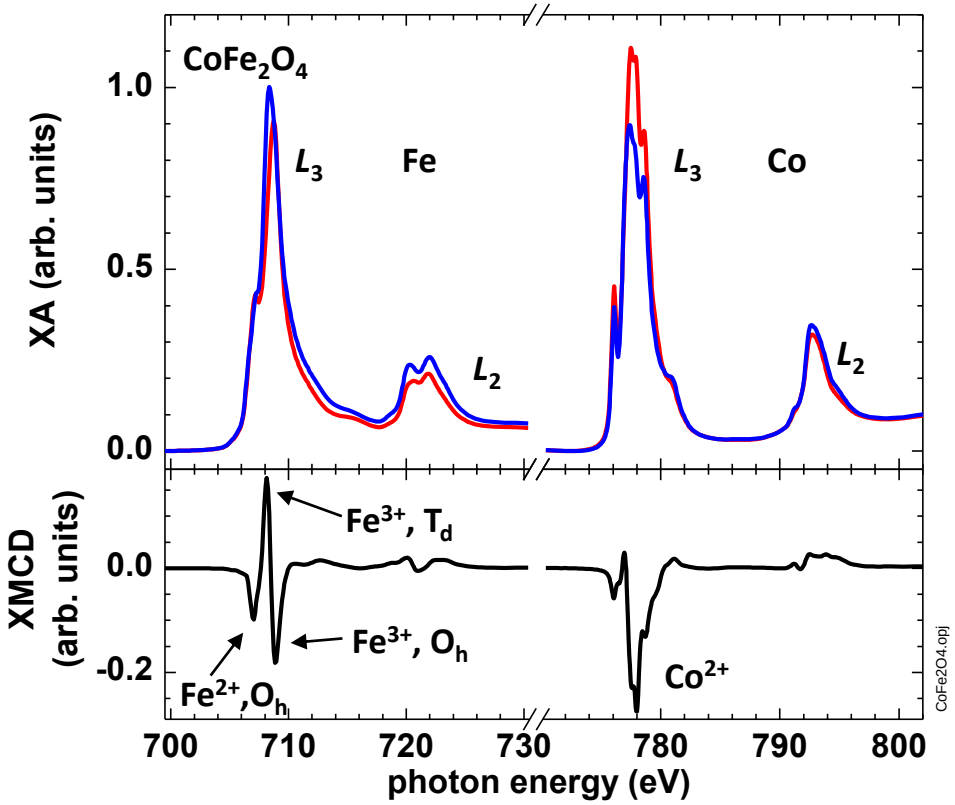

+ XMCD provides magnetic information resolving elements Fe, Co, …
valence states: Fe^{2+}, Fe^{3+}, …
lattice sites: octahedral, O_h, tetrahedral, T_d,

Magnetic Bionanospinels

+ Geobacter sulfurreducens bacteria form magnetite nanocrystals (15nm) via extracellular reduction of amorphous Fe(III)-bearing minerals

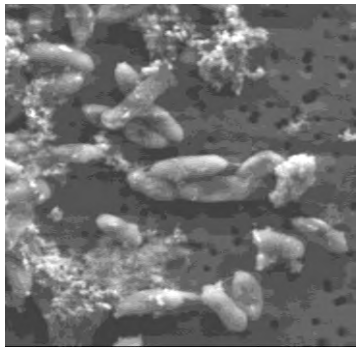

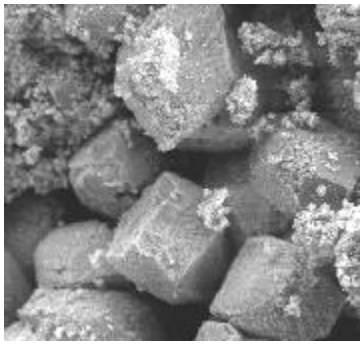

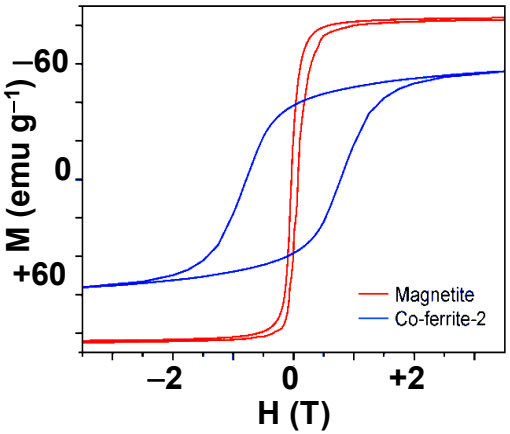

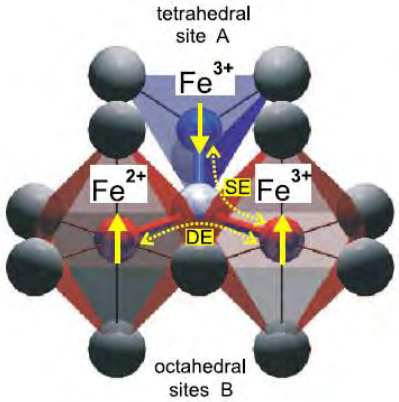

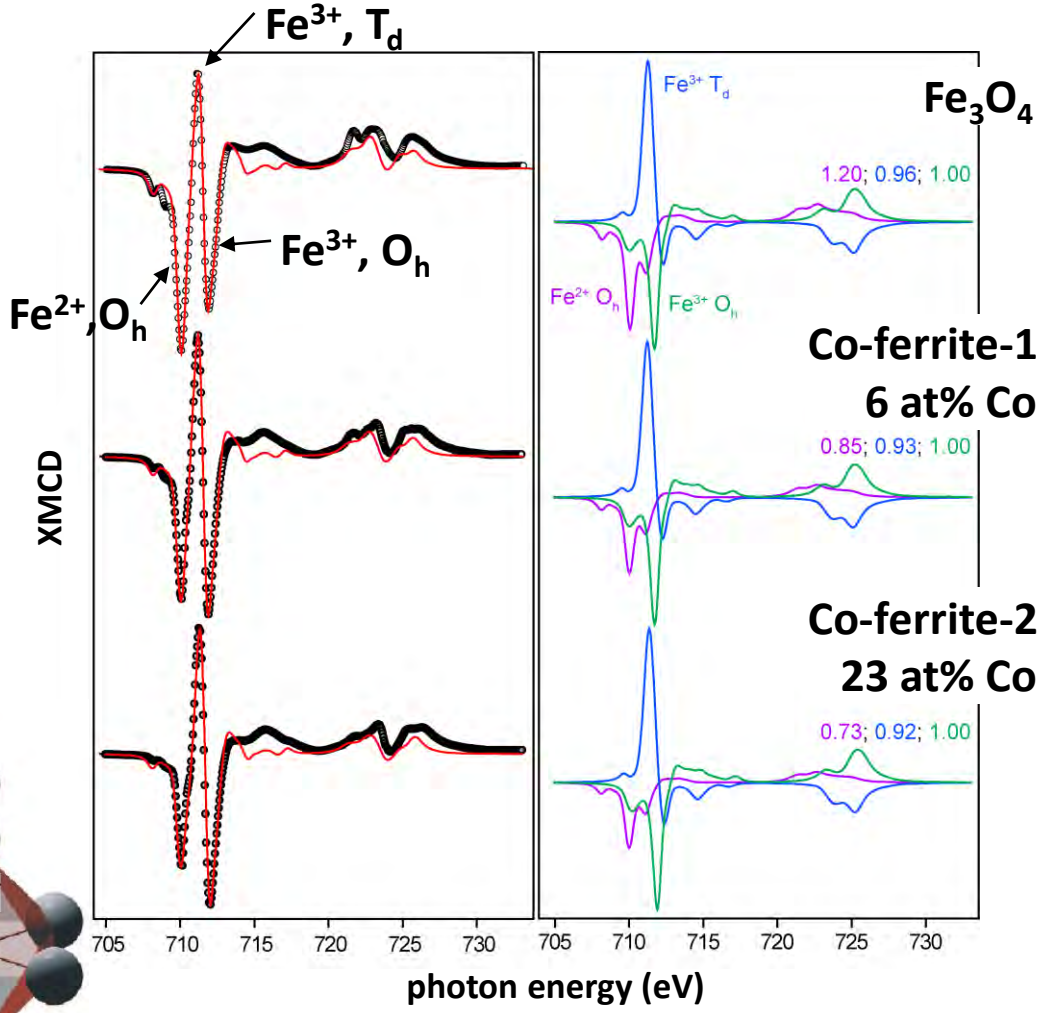

V. Cocker *et al.*,
Eur. J. Mineral. 19, 707–716 (2007)

Magnetic Bionanospinels

+ **Geobacter sulfurreducens bacteria form magnetite nanocrystals (15nm) via extracellular reduction of amorphous Fe(III)-bearing minerals**

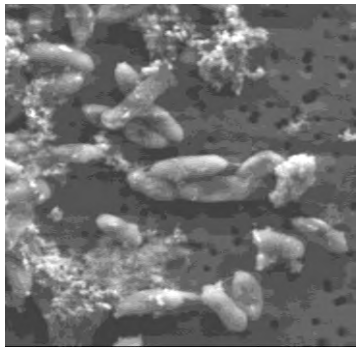

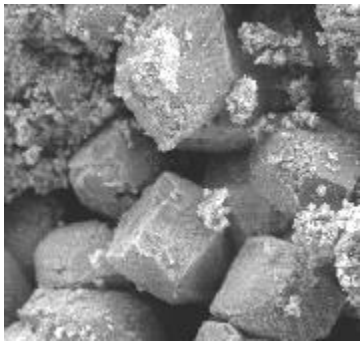

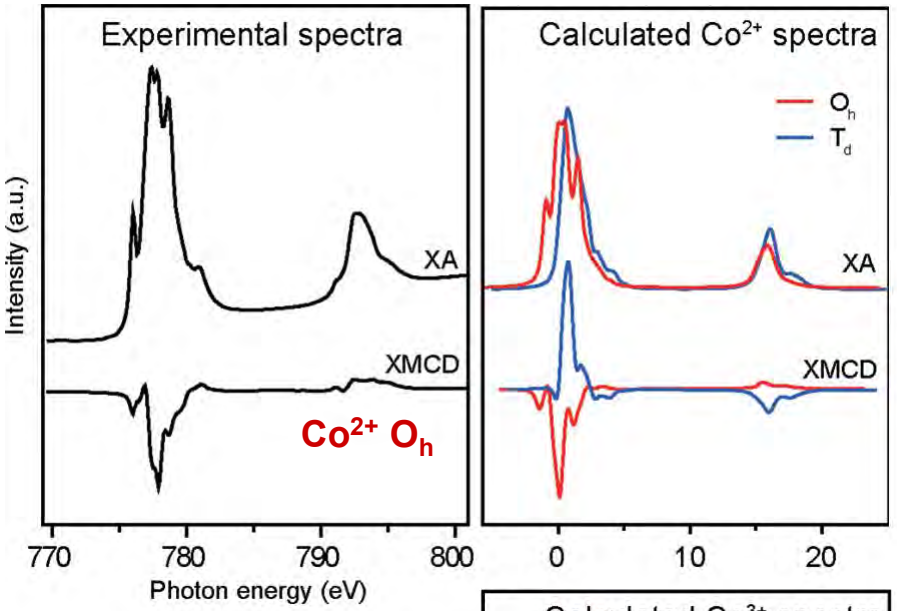

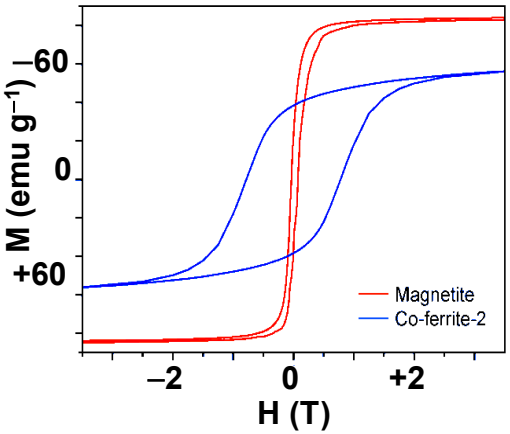

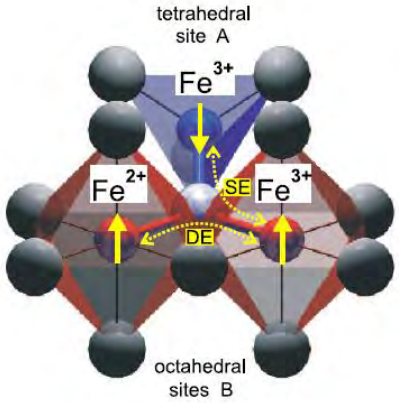

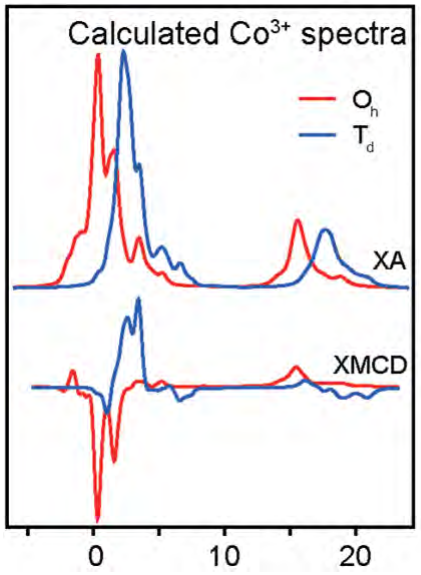

Co-doped TiO_2

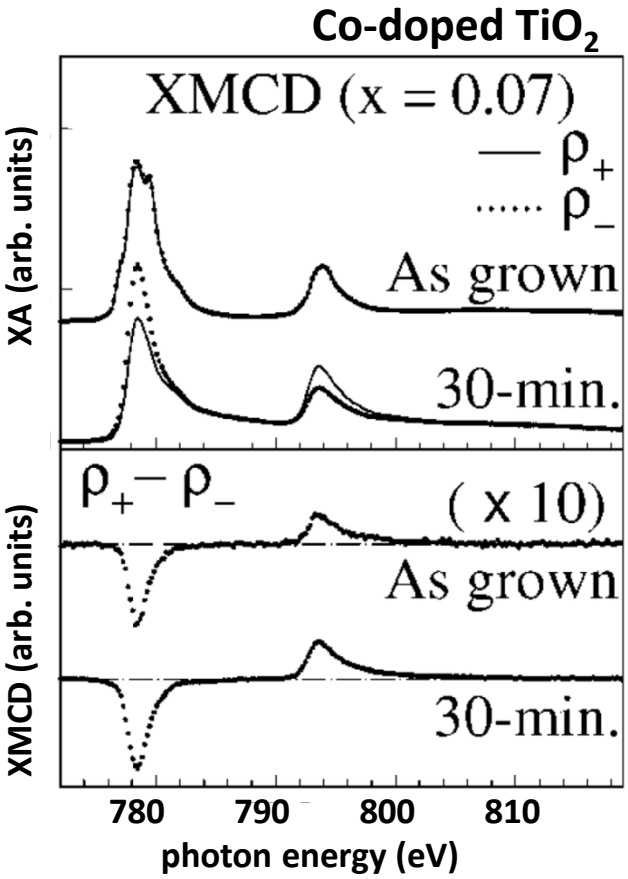

J.-Y. Kim *et al.*,
Phys. Rev. Lett. 90, 017401 (2003)

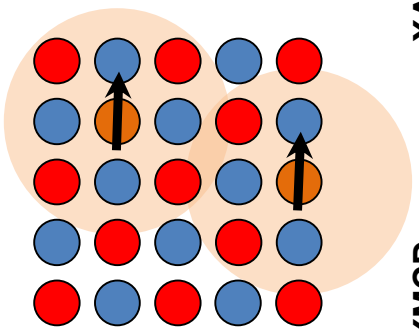

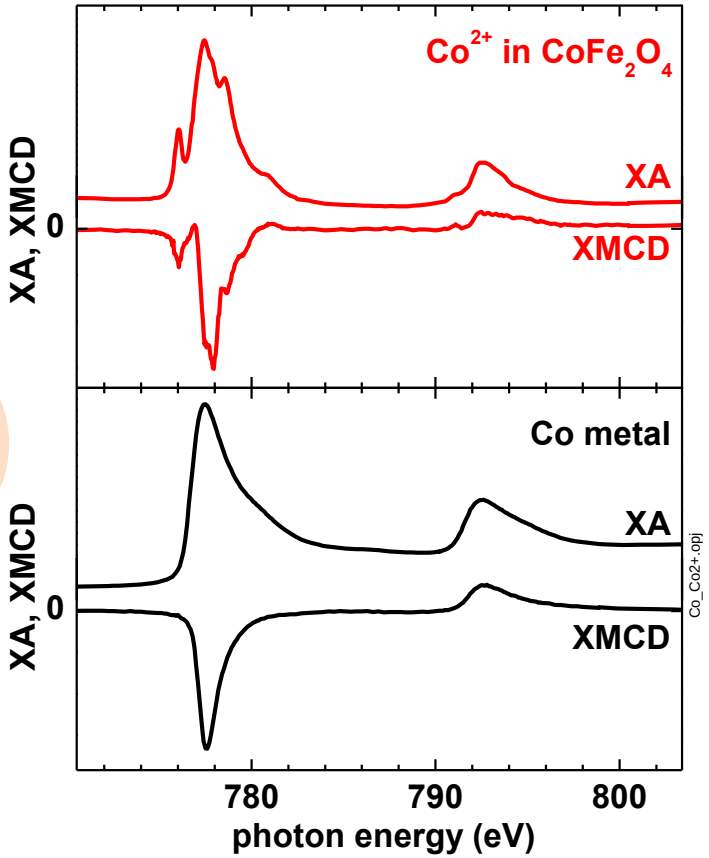

+ Comparing XMCD spectra with model compounds and/or calculations
⇒ Identifying magnetic phases

Induced Moments At Co/Cu Interfaces

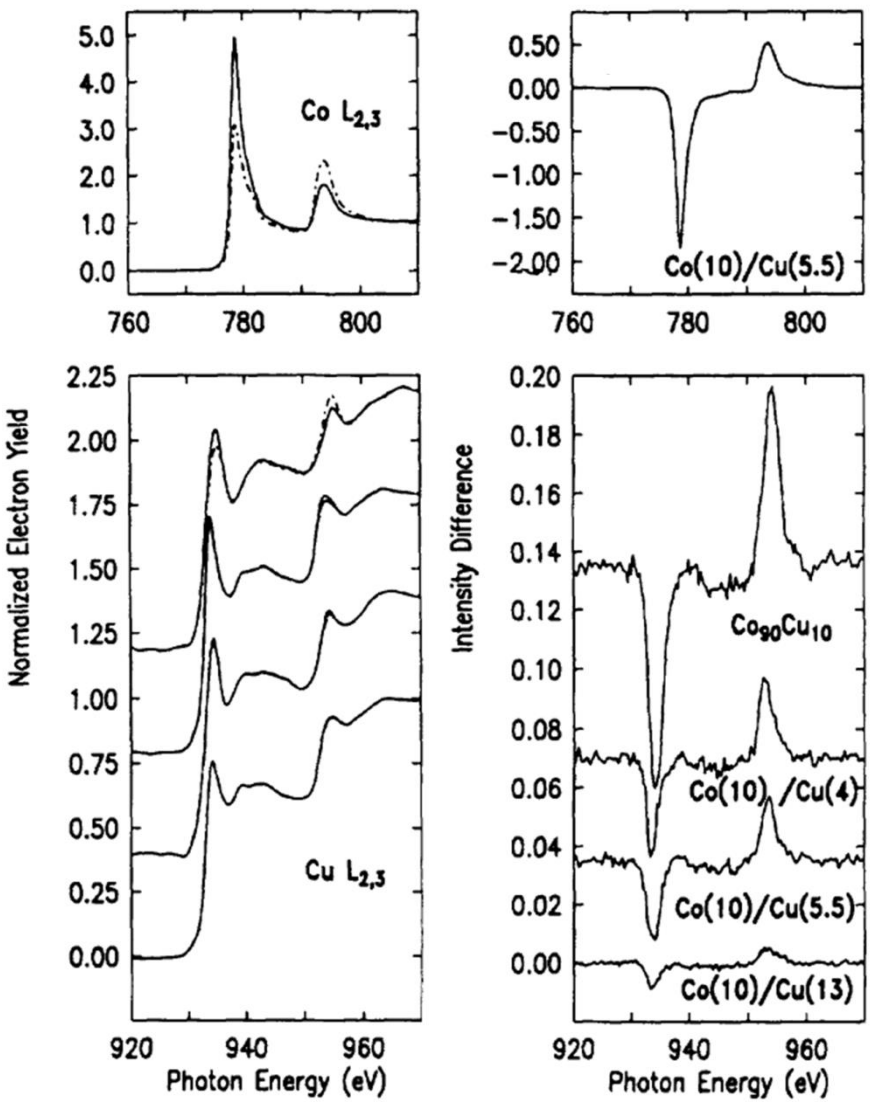

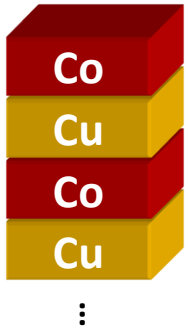

+ **The element-specificity makes XMCD measurements an ideal tool to determine induced moments at interfaces between magnetic and non-magnetic elements.**

M. G. Samant *et al.*,
Phys. Rev. Lett. 72, 1112 (1994)

Magnetic Interfaces

+ Weak Mn XMCD signal

⇒ Uncompensated Mn at Co/IrMn interface

+ Same sign of XMCD signal for Co and Mn

⇒ Parallel coupling of Co and Mn moments

+ Nominal thickness of uncompensated interface moments: (0.5±0.1)ML

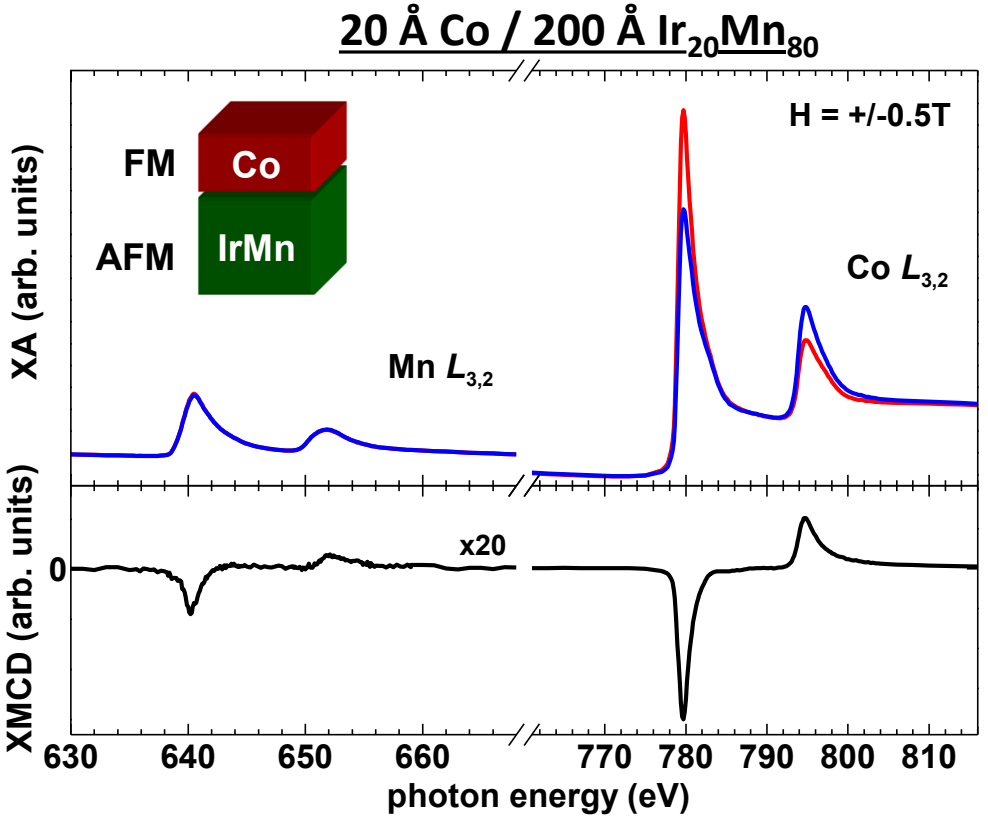

H. Ohldag *et al.*,
Phys. Rev. Lett. 91, 017203 (2003)

Band Filling In Ga_xFe_{1-x}

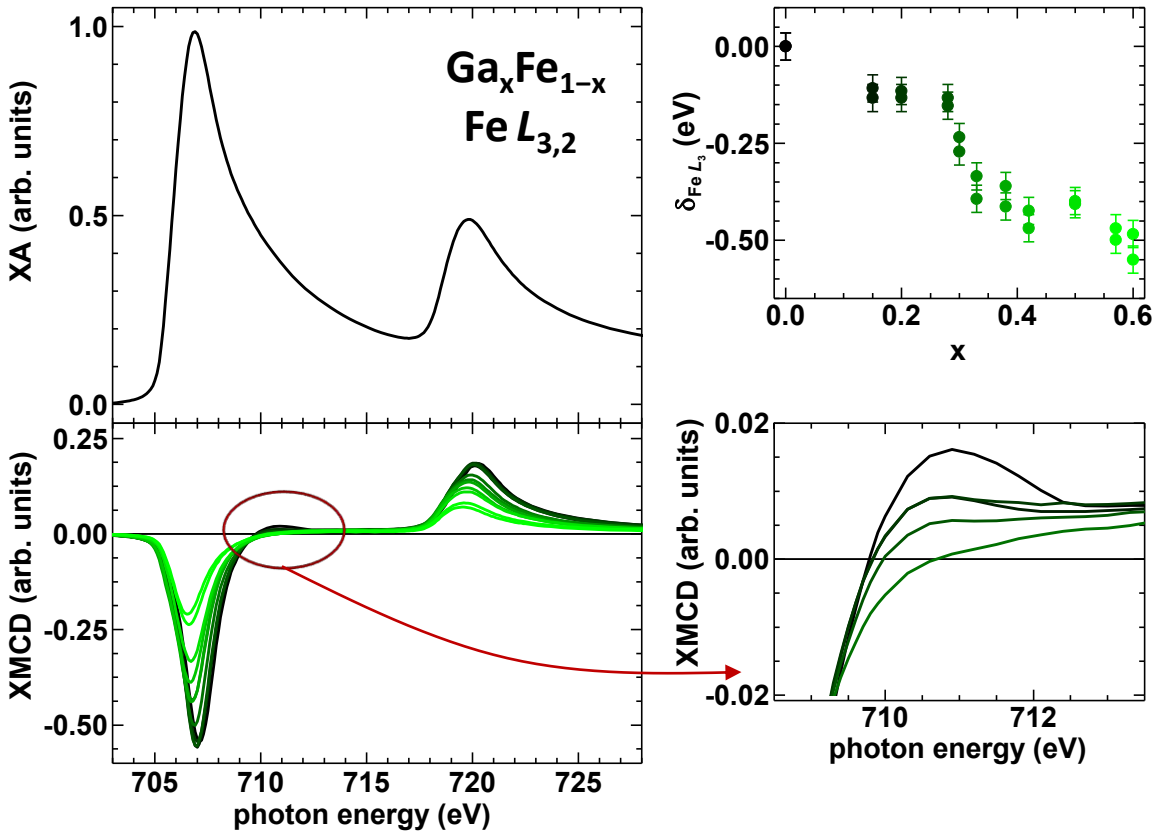

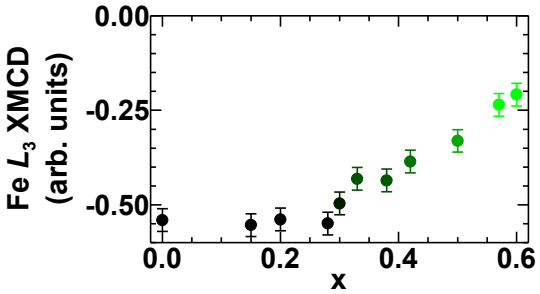

E. Arenholz *et al.*,
Phys. Rev. B 82, 180405 (2010)

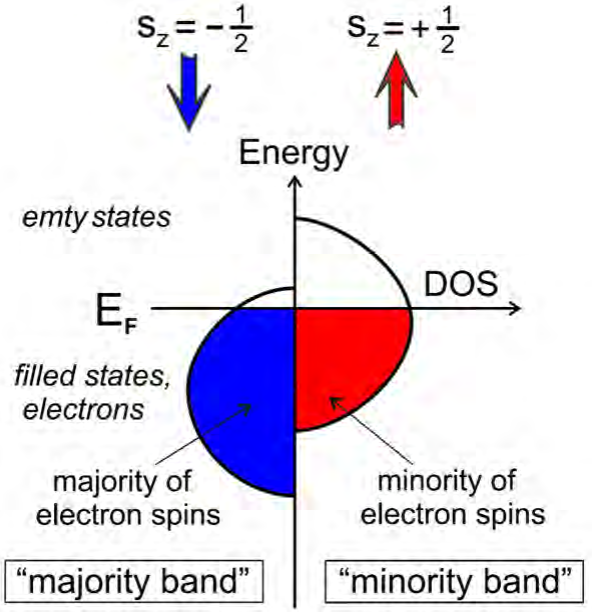

J. Stöhr, H.C. Siegmann,
Magnetism (Springer)

+ Fe majority-spin filled for x=0.3
+ x > 0.3: Fe moment decrease strongly,
  Formation of D03 precipitates

Composition Dependence of $Fe_{1-x}Mn_x$

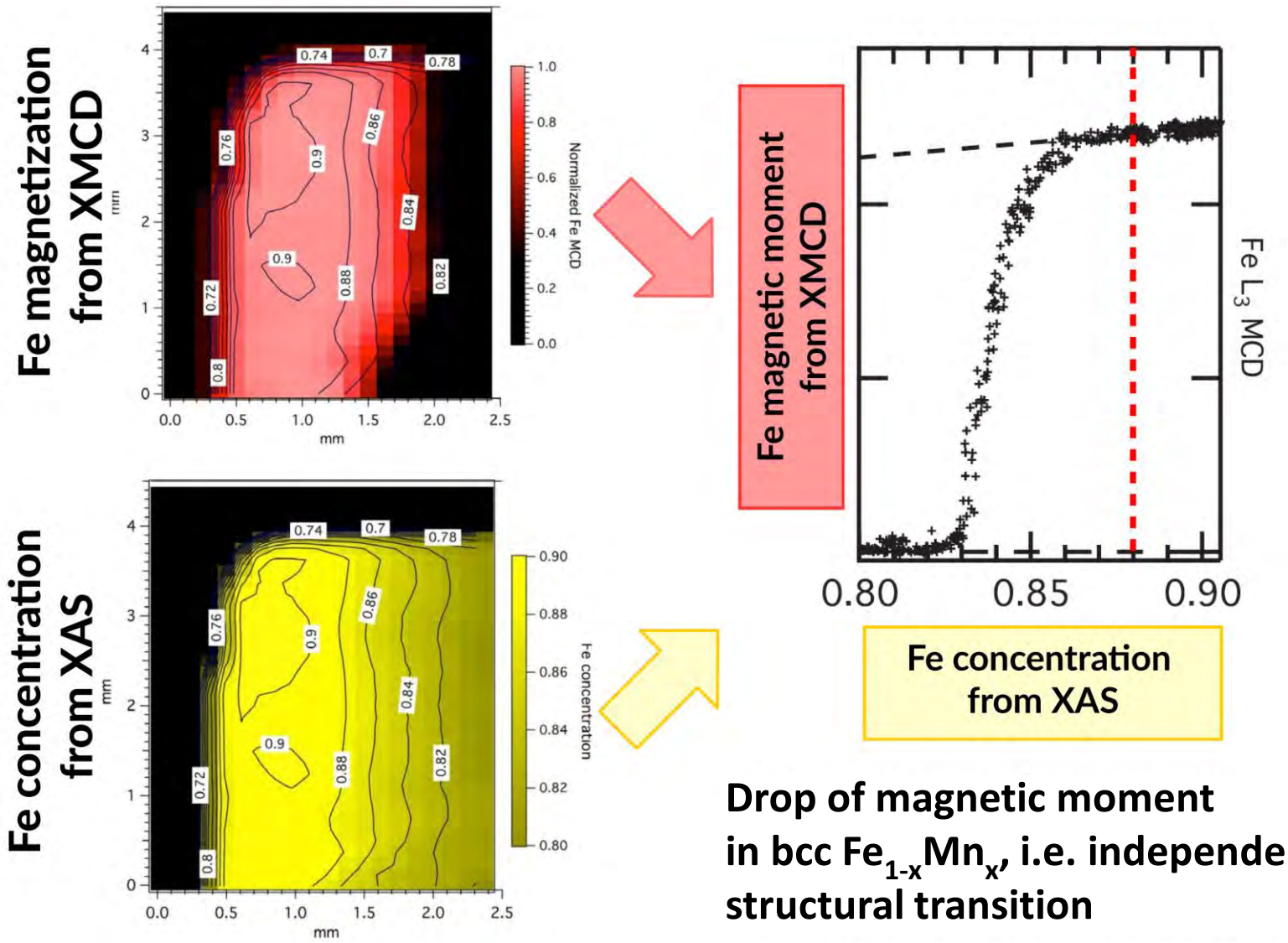

Drop of magnetic moment in bcc $Fe_{1-x}Mn_x$, i.e. independent of structural transition

Sum Rules

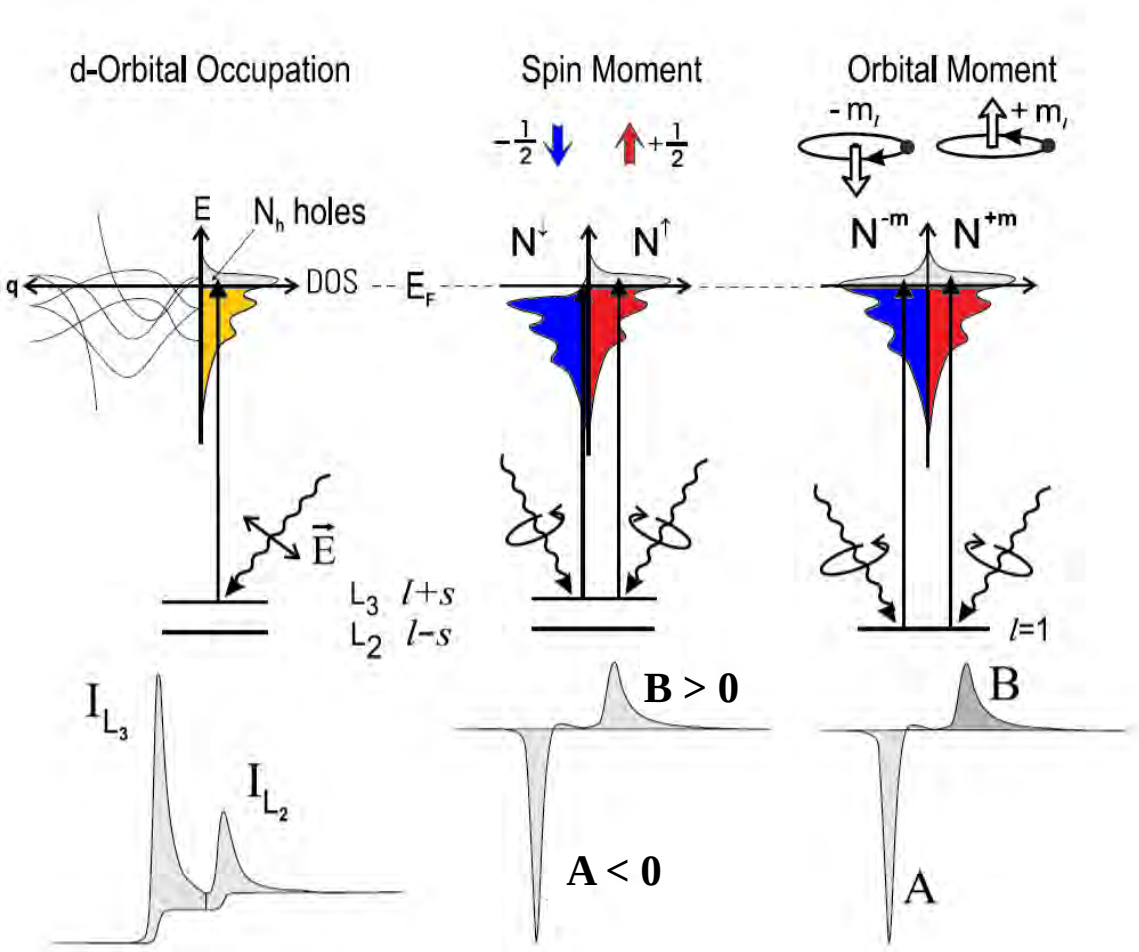

$N_h = \langle I_{L3} + I_{L2} \rangle / C$

$m_S = \mu_B \langle -A + 2B \rangle / C$

$m_L = -2\mu_B \langle A + B \rangle / 3C$

+ **Theoretically derived sum rules correlate XMCD spectra with spin and orbital moment providing unique tool for studying magnetic materials.**

J. Stöhr, H.C. Siegmann, Magnetism (Springer)

Orbital Moment Of Co Nanoparticles

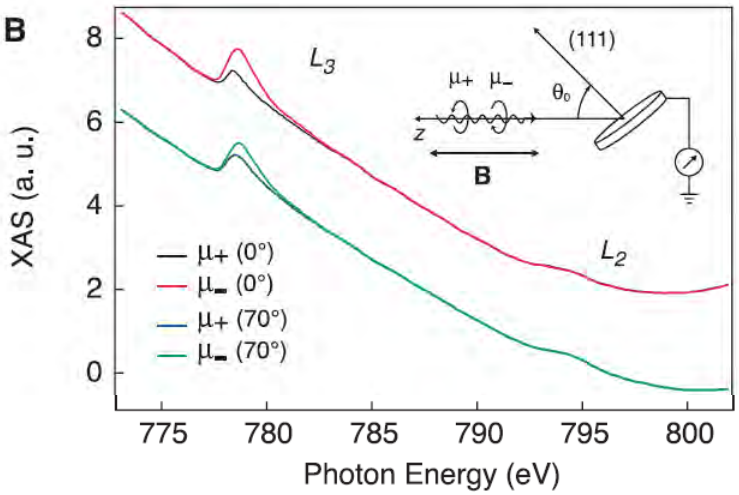

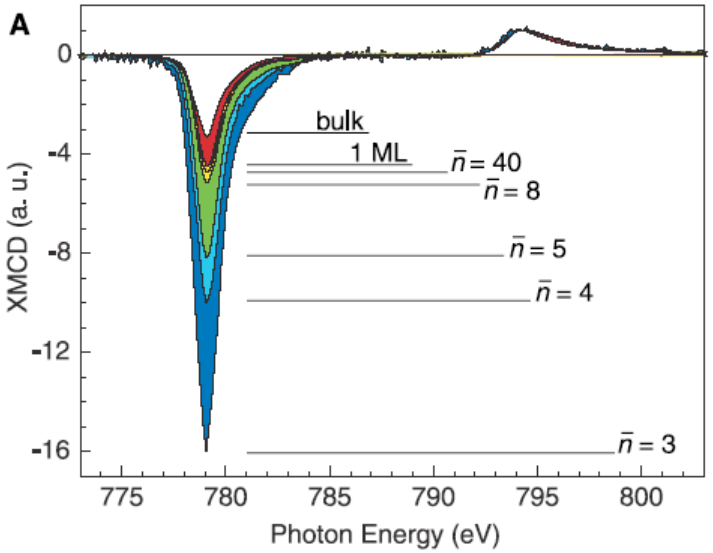

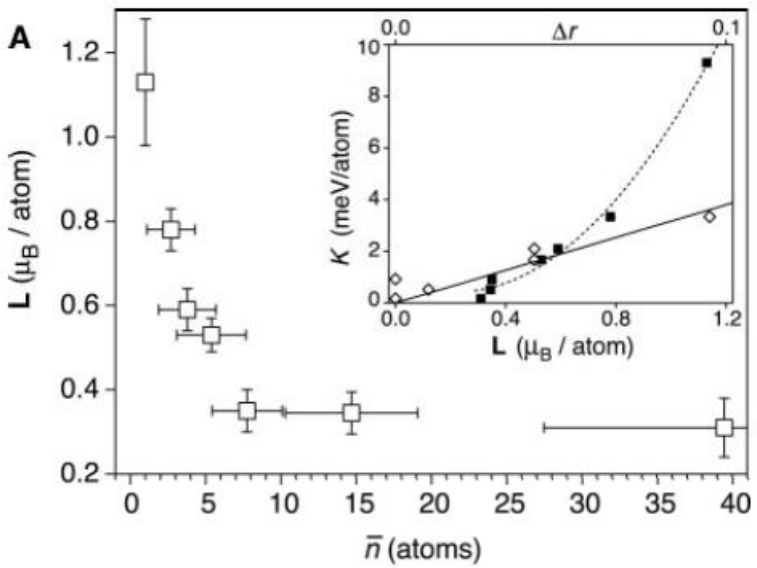

+ **Strong variation of orbital and spin magnetic moment observable as change in relative L_3 and L_2 intensity in XMCD spectrum.**
+ **Co atoms and nanoparticles on Pt have enhanced orbital moments up to 1.1 μ_B**

P. Gambardella *et al.*,
Science 300, 1130 (2003)

Element-specific Magnetization Reversal

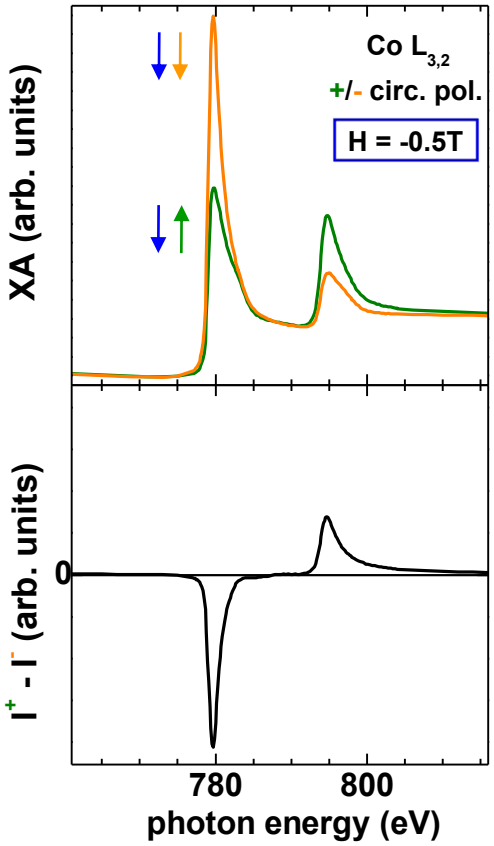

+ Monitoring field dependence of XMCD

⇒ Element-specific information on magnetization reversal in complex magnetic nanostructures.

Element-specific Magnetization Reversal

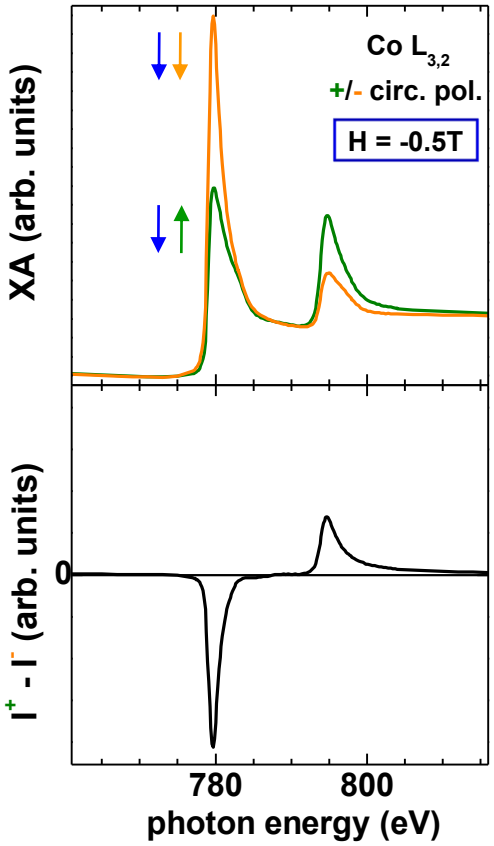

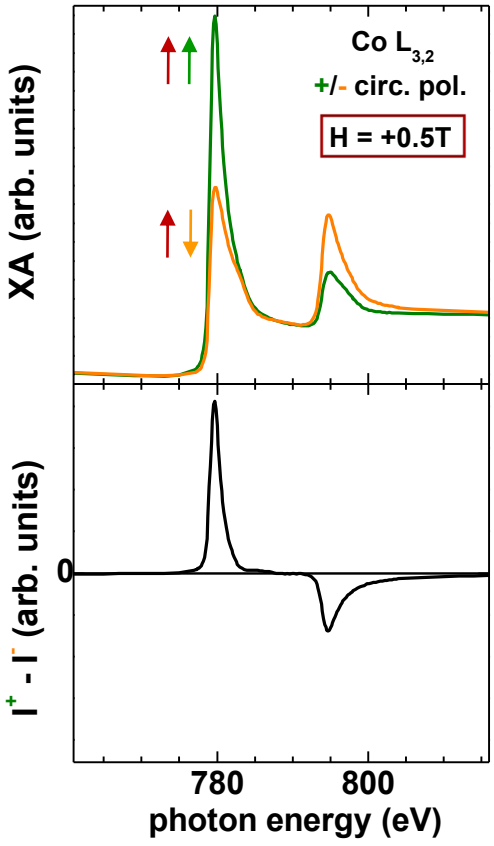

+ Monitoring field dependence of XMCD

⇒ Element-specific information on magnetization reversal in complex magnetic nanostructures.

Element-specific Magnetization Reversal

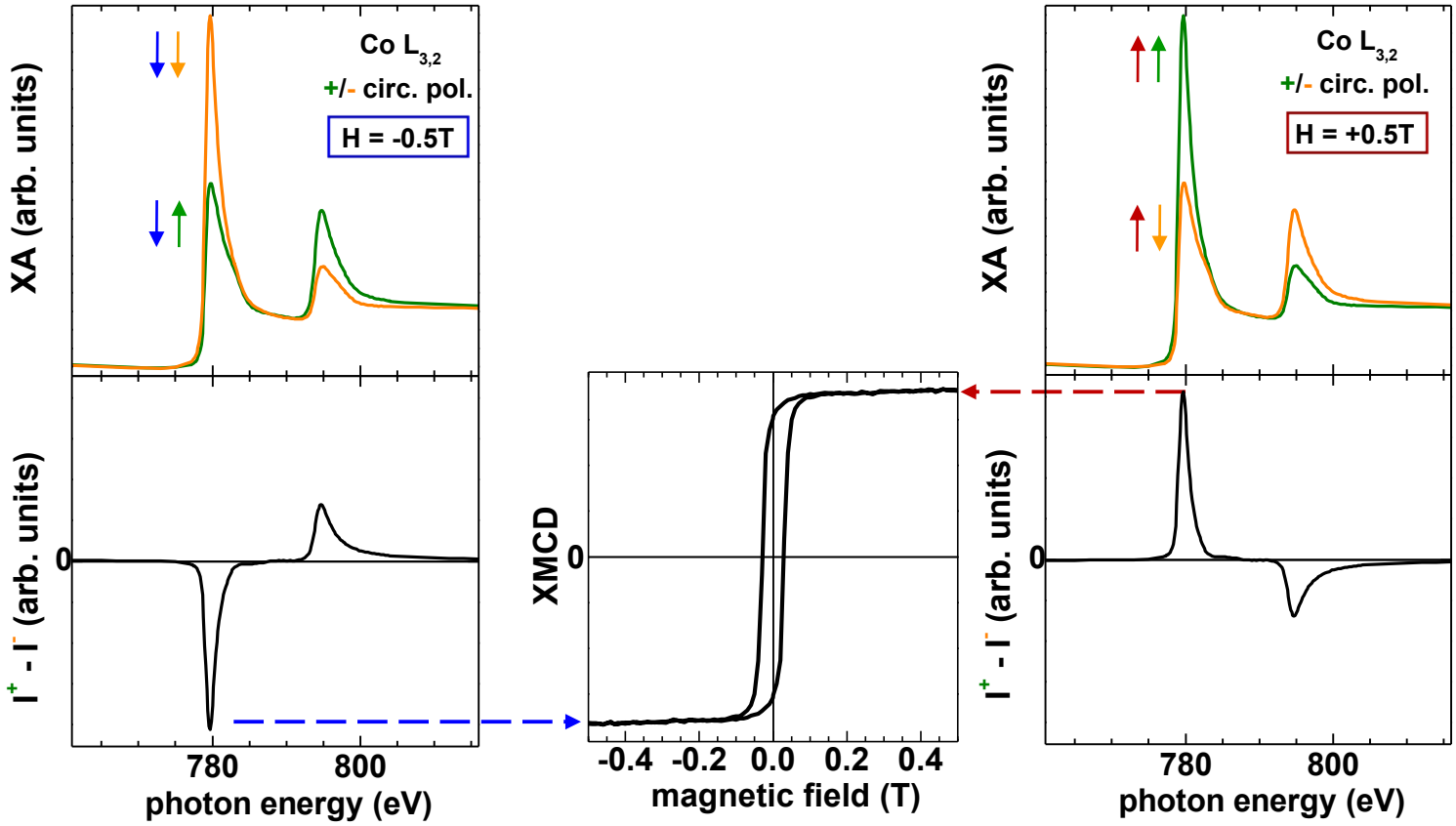

+ Monitoring field dependence of XMCD

⇒ Element-specific information on magnetization reversal in complex magnetic nanostructures.

Element-Specific Magnetization Reversal

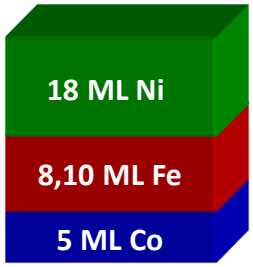

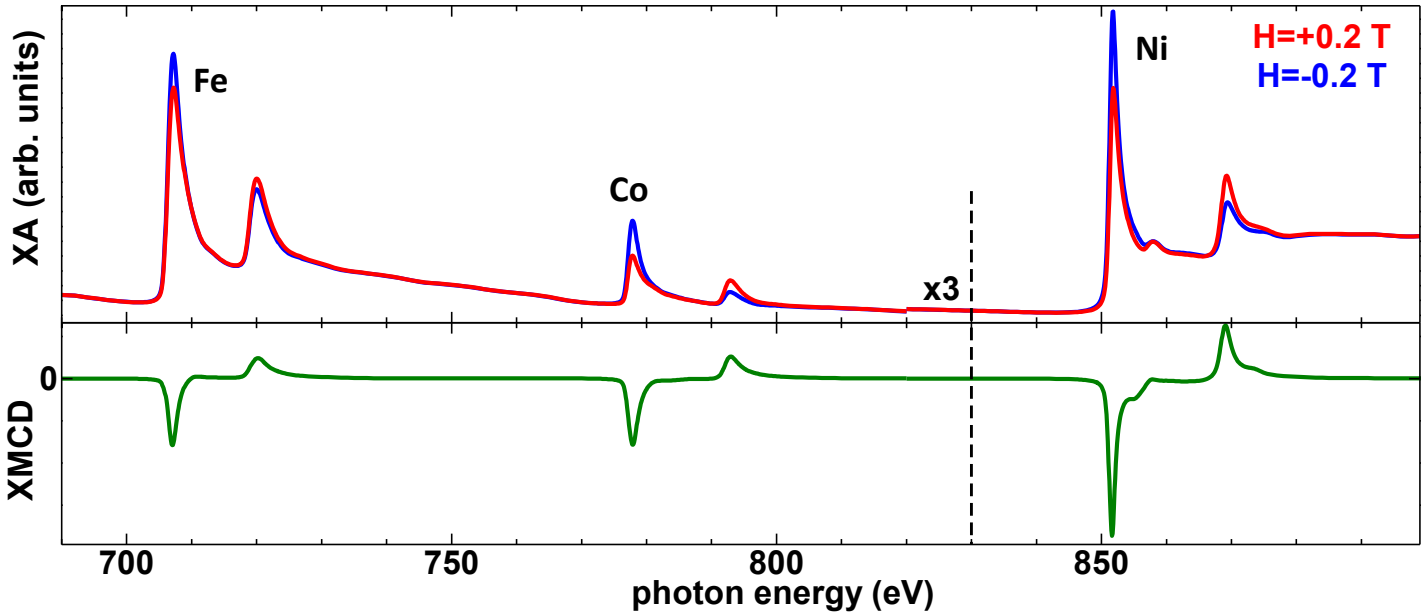

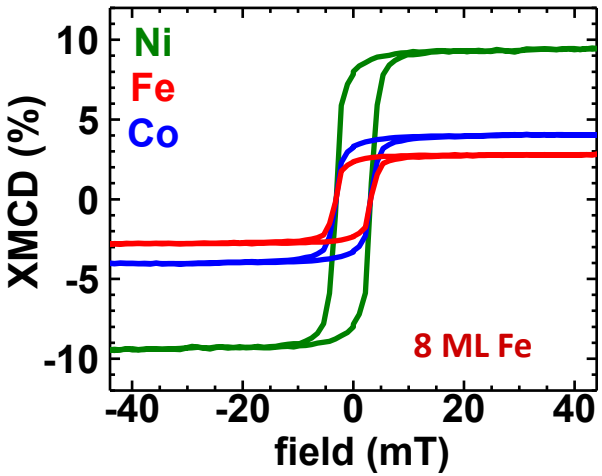

Element-specific Magnetization Reversal

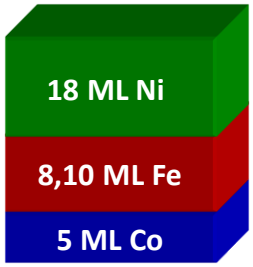

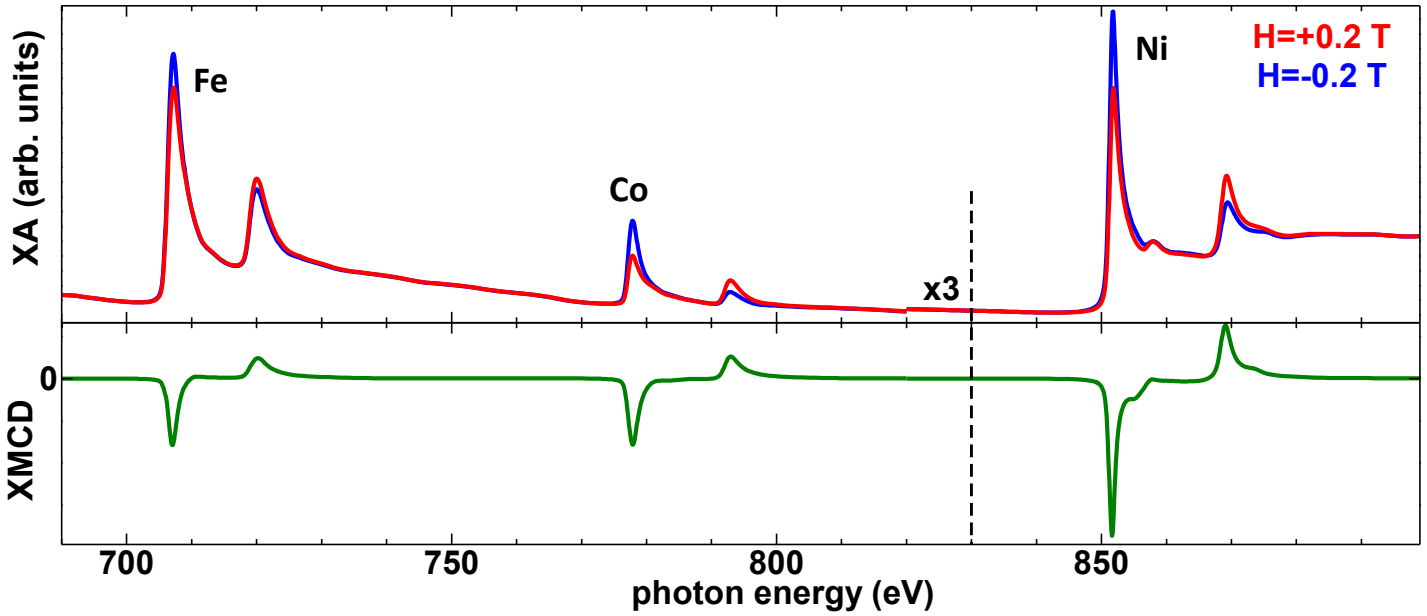

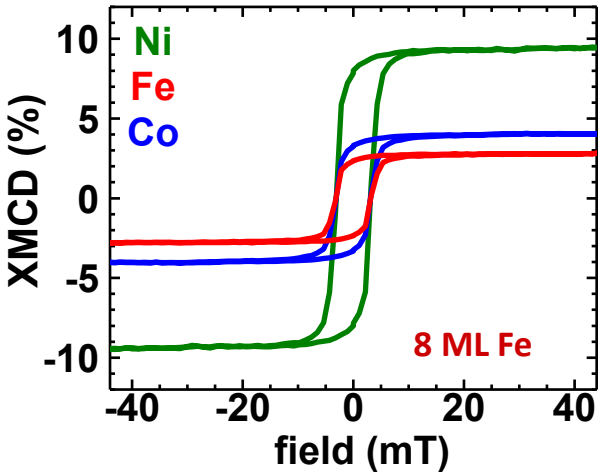

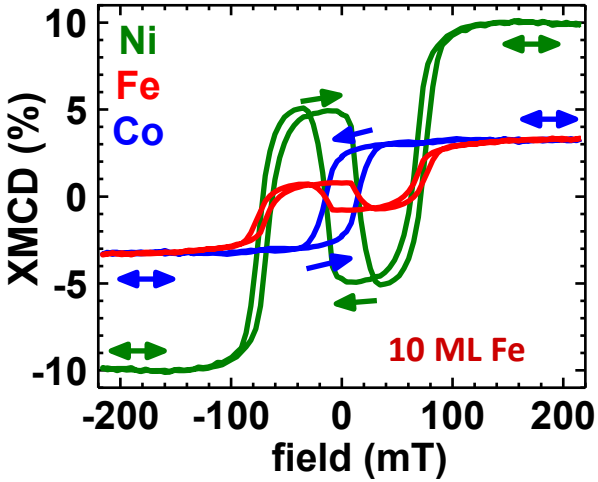

X-Ray Ferromagnetic Resonance

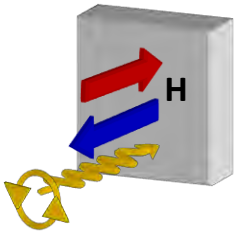

circularly polarized

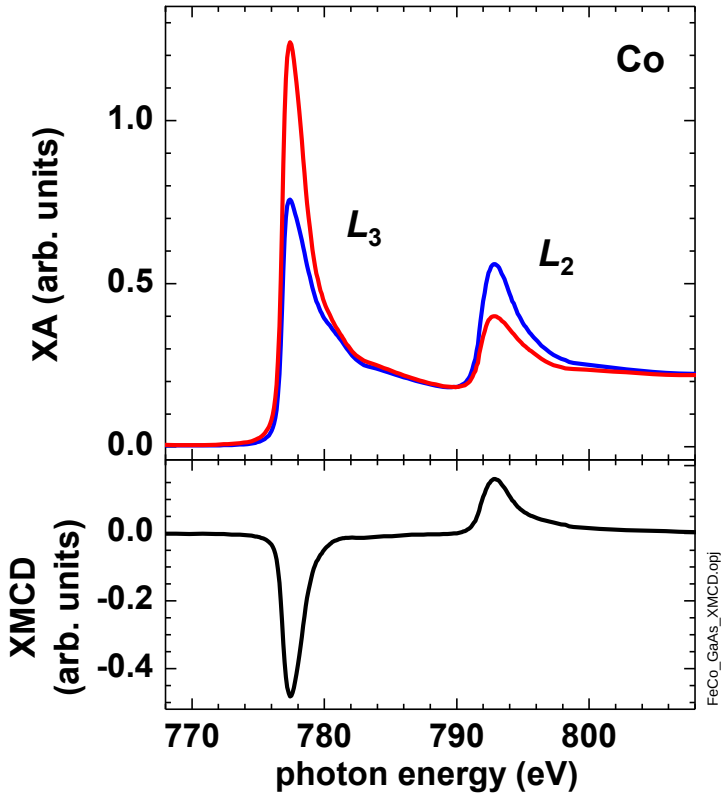

+ **In fact:**
  Magnetic moments are not fully aligned with applied fields but precess around them.

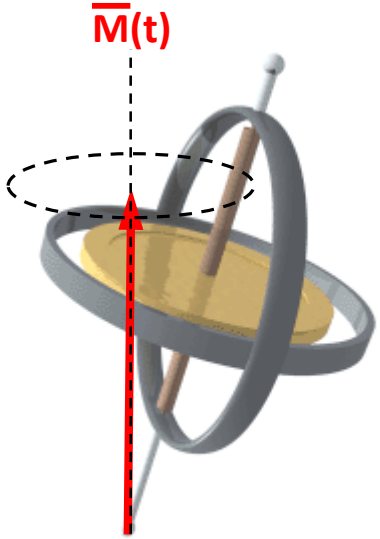

X-Ray Ferromagnetic Resonance

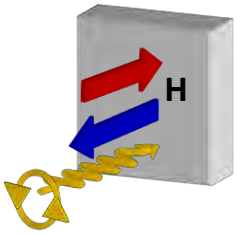

circularly polarized

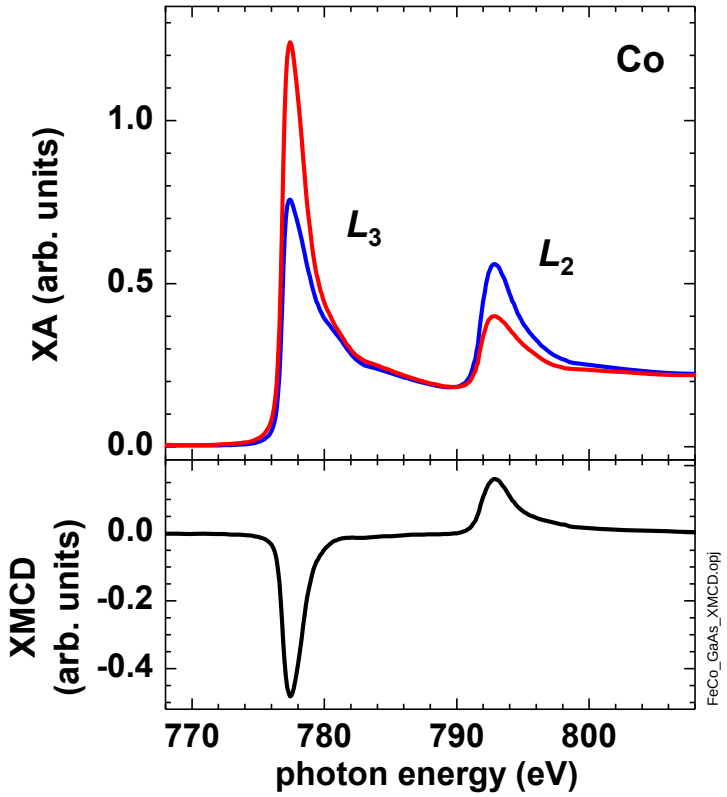

+ In fact:
  Magnetic moments are not fully aligned with applied fields but precess around them.

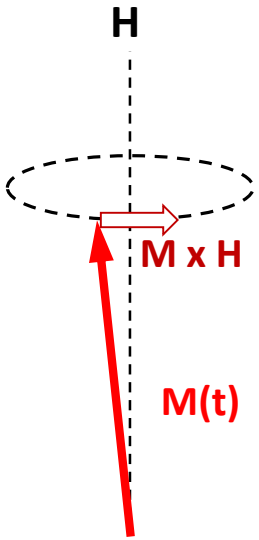

+ Is it possible to measure the pression of magnetic moments making use of the pulsed nature of synchrotron radiation and XMCD? (!)

X-Ray Ferromagnetic Resonance

Static XMCD

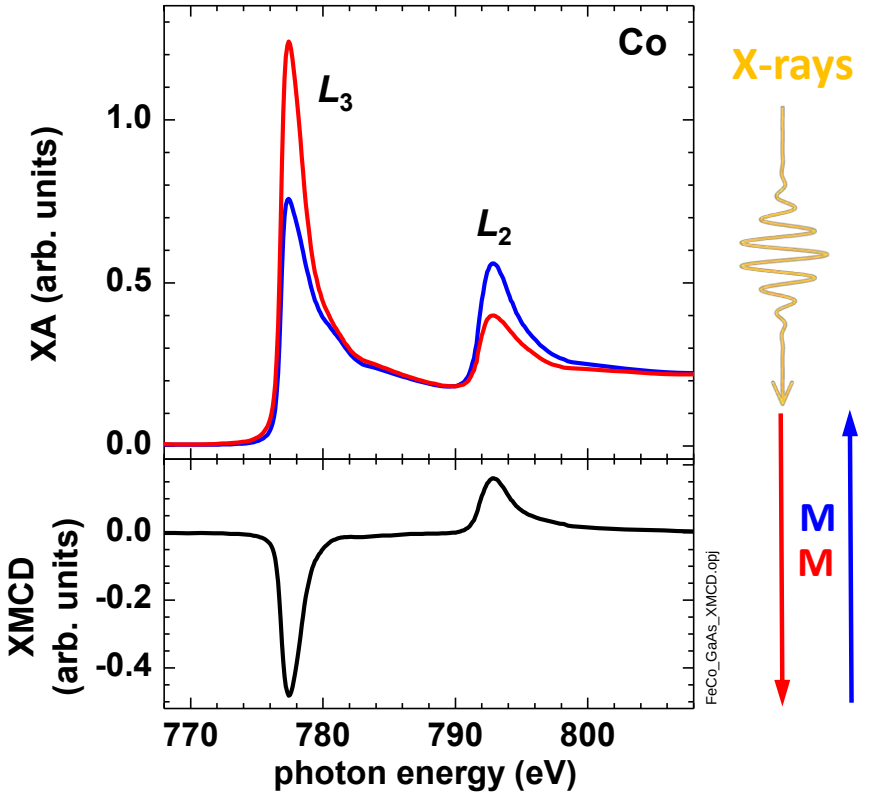

Dynamic XMCD

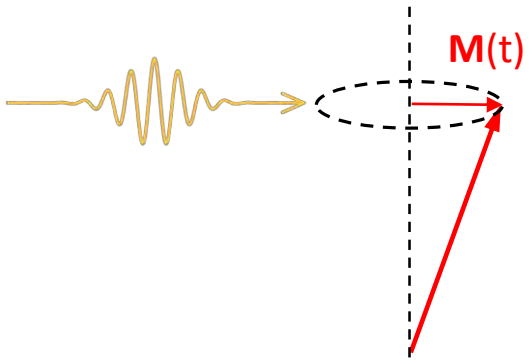

X-Ray Ferromagnetic Resonance

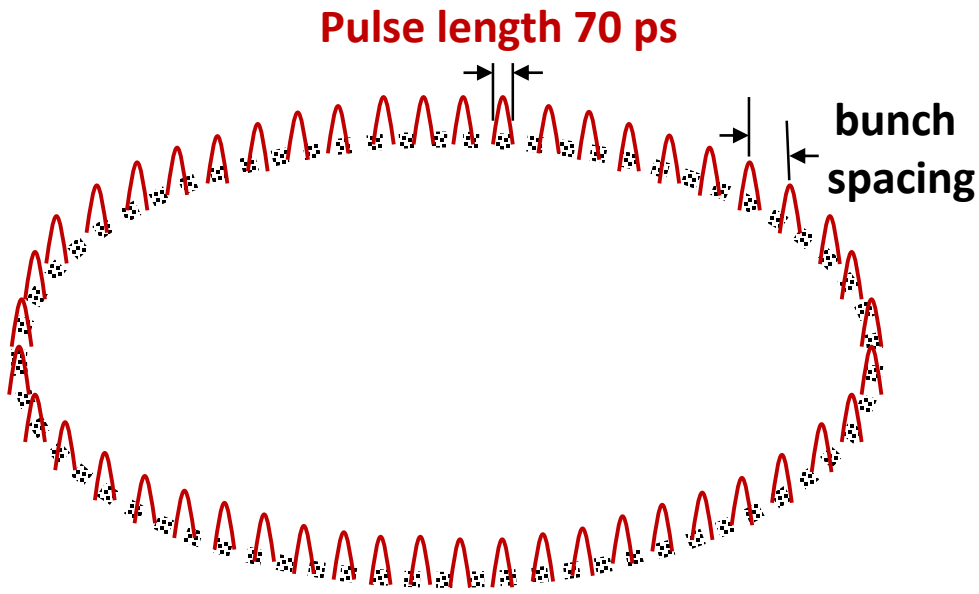

Pulsed nature of synchrotron radiation
Example: Advanced Light Source

- 256-320 bunches for 500mA beam current
- Bunch spacing: 2 ns (500MHz)
- Pulse length 70ps

X-Ray Ferromagnetic Resonance

Dynamic XMCD measurement, i.e. synchronize X-ray pulses with FMR precession

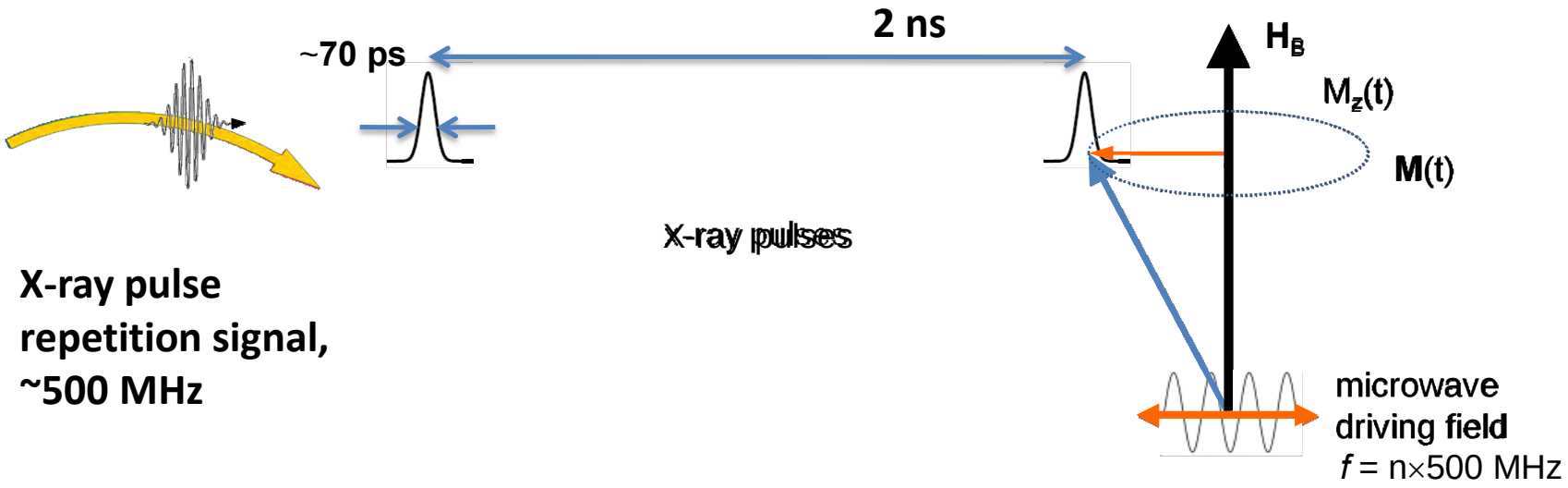

X-ray pulse repetition signal, ~500 MHz

X-Ray Ferromagnetic Resonance

Static XMCD

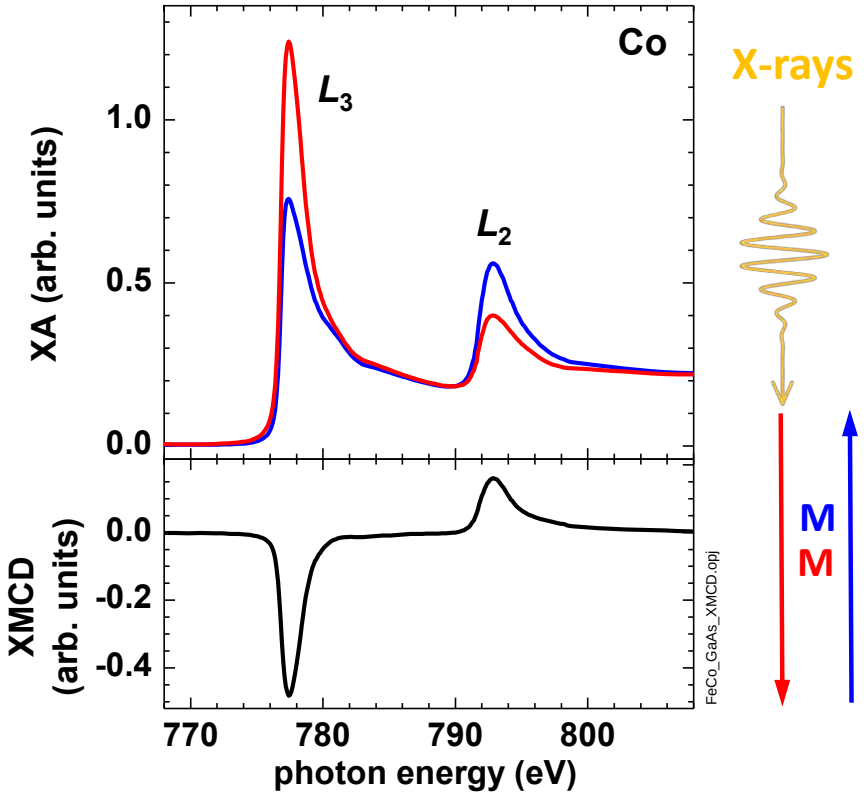

Dynamic XMCD

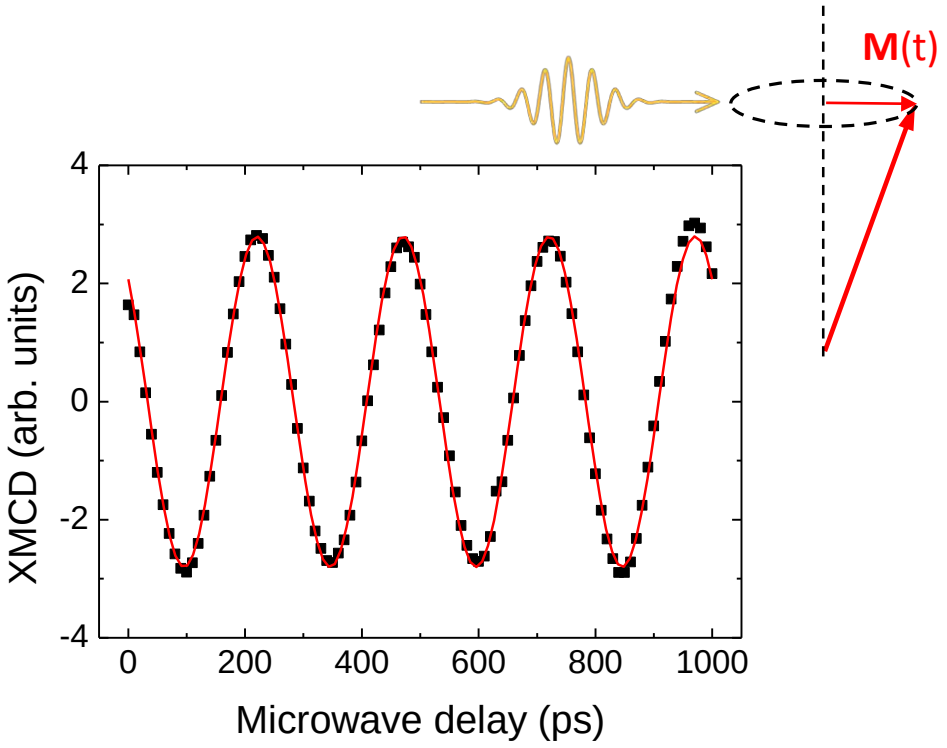

X-Ray Ferromagnetic Resonance

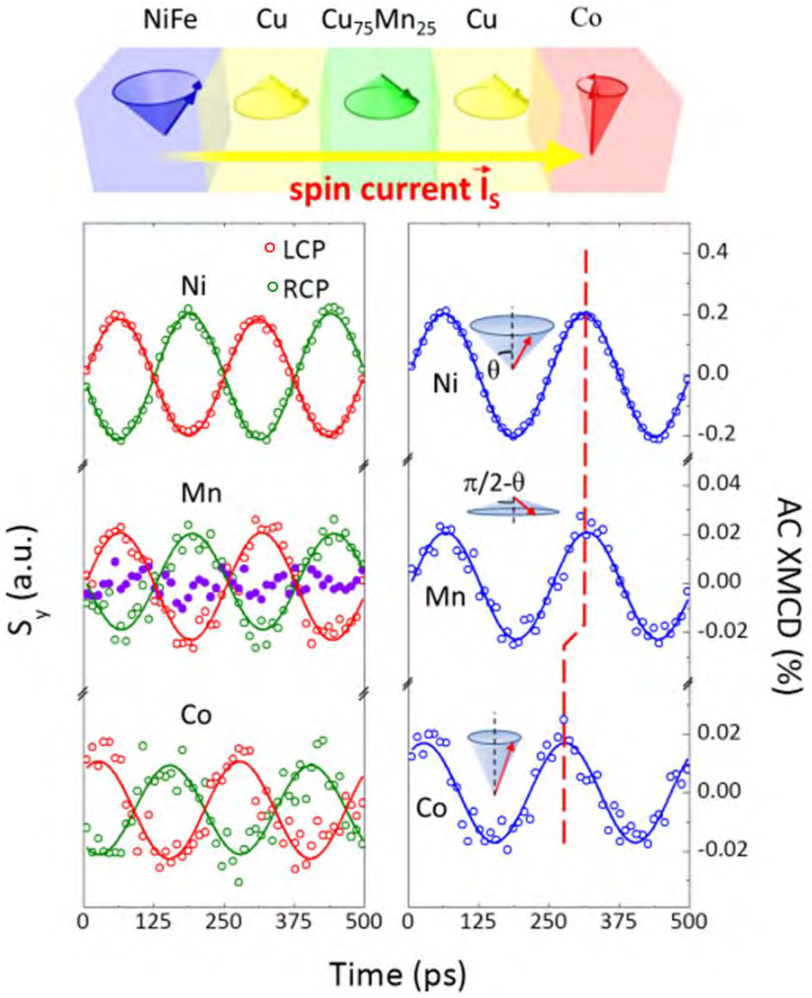

+ Precession is resonantly excited in the NiFe layer with an 4 GHz RF field.
+ The resonance field of the Co layer is higher, i.e. no precession is excited in the Co layer.
+ Precession in Py, $Cu_{75}Mn_{25}$, and Co layers are probed by XMCD using left- and right-circularly polarized X-rays at Ni, Mn, and Co edges, respectively.
+ The $Cu_{75}Mn_{25}$ spin precession is a direct indicator of the AC spin current through the structure.

X-Ray Linear Dichroism

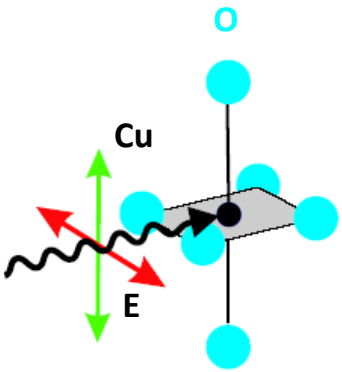

C. T. Chen *et al.*
PRL 68, 2543 (1992)

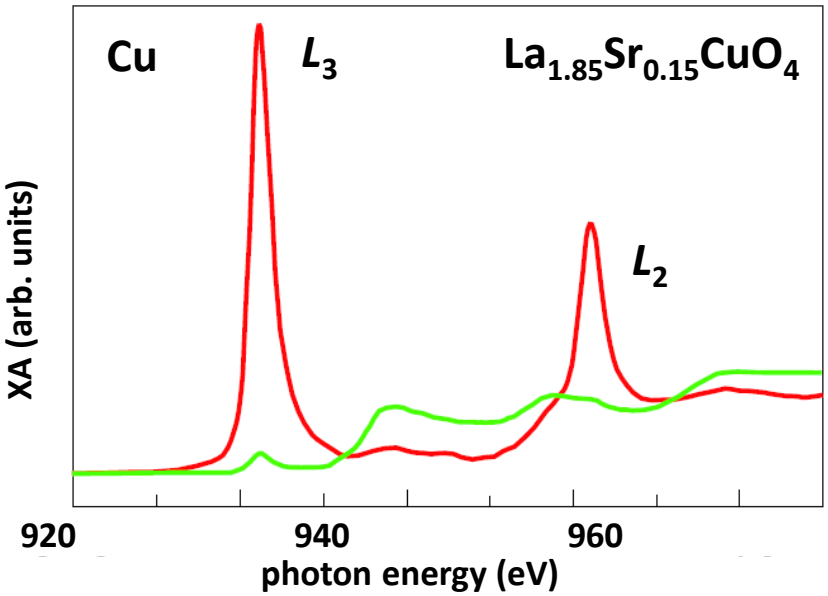

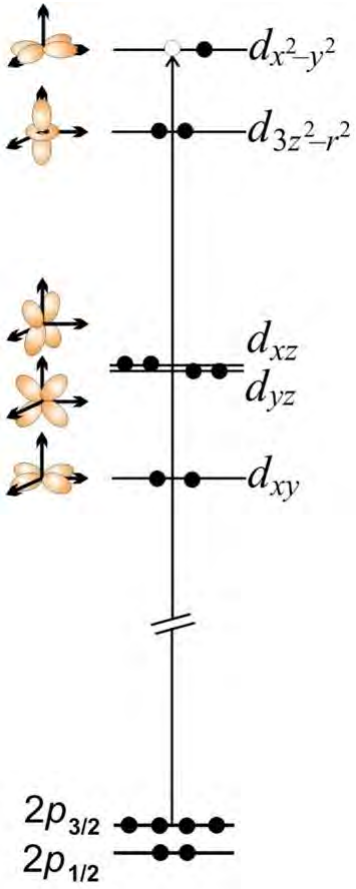

X-Ray Linear Dichroism:

+ Difference in X-ray absorption for different linear polarization direction relative to crystalline and/or spin axis.
+ Due to the anisotropic charge distribution about the absorbing atom caused by bonding and/or magnetic order.
+ "Search Light Effect": X-ray absorption of linear polarized X rays proportional to density of empty valence states in direction of electric field vector E.

Structural Changes In $PbZr_{0.2}Ti_{0.8}O_3$

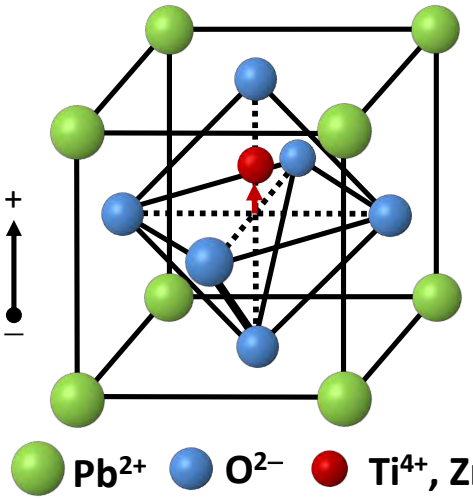

ferroelectric polarization

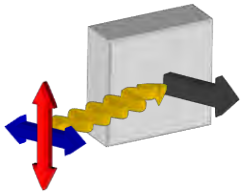

as grown

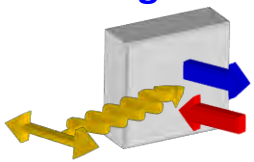

reversed

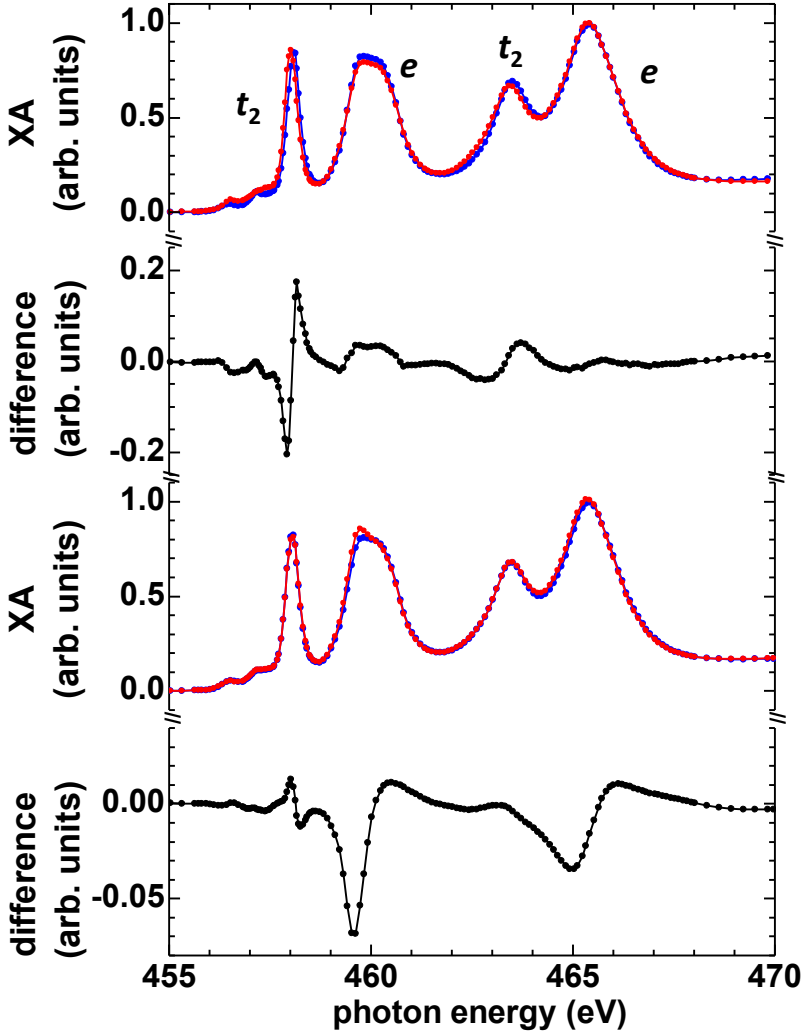

E. Arenholz *et al.*,
Phys. Rev. B 82, 140103 (2010)

+ Spontaneous electric polarization due to off-center shift of Ti^{4+}, Zr^{4+} associated with tetragonal distortion ⇔ linear dichroism

+ Reversing ferroelectric polarization changes XA ⇔ Change in tetragonal distortion

X-Ray Magnetic Linear Dichroism

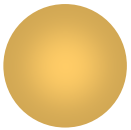

Isotropic *d* electron charge density
⇒ No polarization dependence

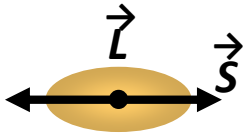

Magnetically aligned system
⇒ Spin-orbit coupling distorts charge density
⇒ Polarization dependence

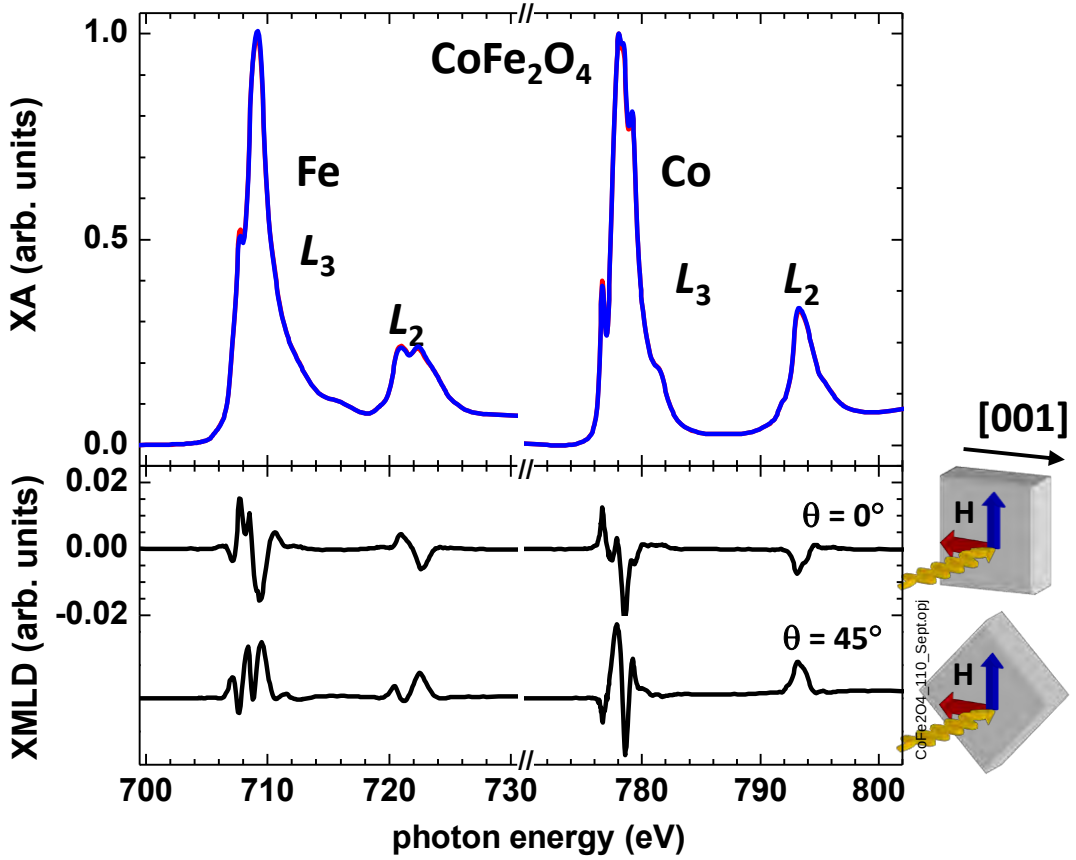

+ $I_{XMLD} = I_{||} - I_{\perp} \propto \langle m^2 \rangle$, $\langle m^2 \rangle$ = expectation value of square of atomic magnetic moment
+ XMLD allows investigating ferri- and ferromagnets as well as antiferromagnets
+ XMLD spectral shape and angular dependence are determined by magnetic order and lattice symmetry

X-Ray Magnetic Linear Dichroism

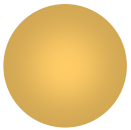

Isotropic *d* electron charge density
⇒ No polarization dependence

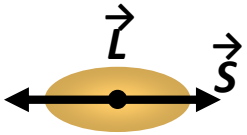

Magnetically aligned system
⇒ Spin-orbit coupling distorts charge density
⇒ Polarization dependence

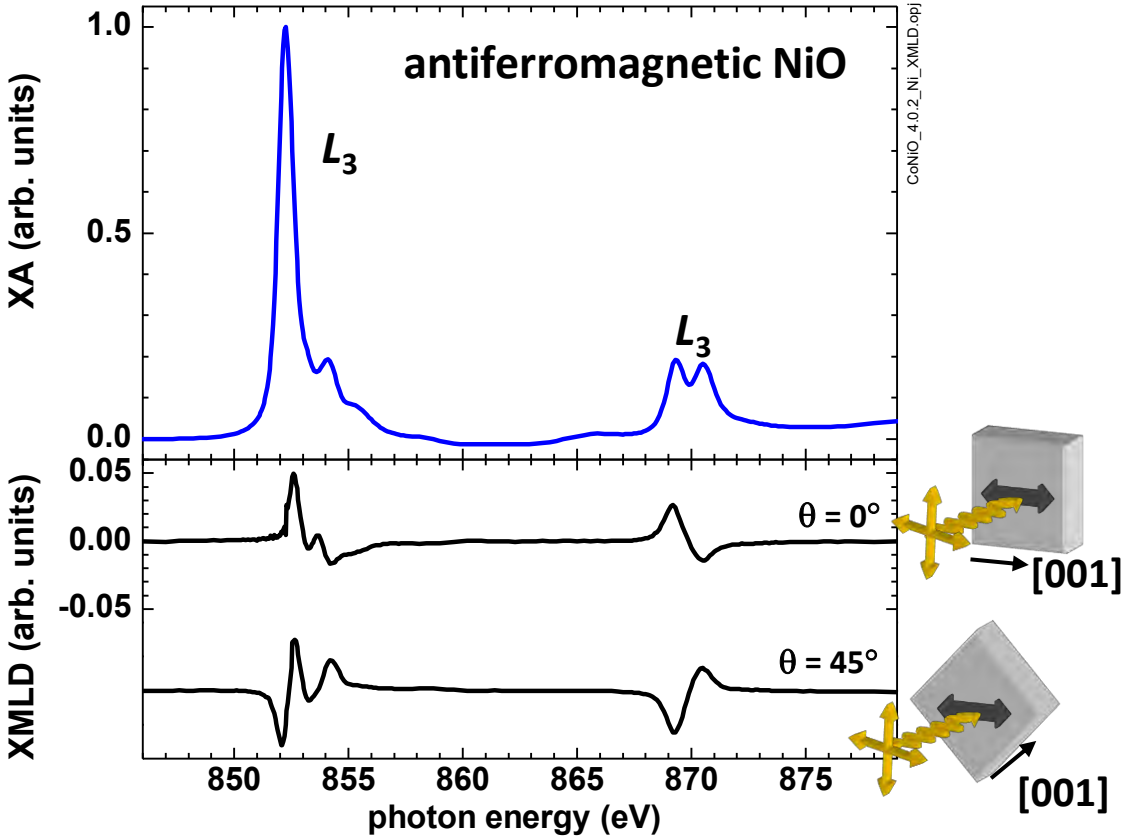

+ $I_{XMLD} = I_{||} - I_{\perp} \propto \langle m^2 \rangle$, $\langle m^2 \rangle$ = expectation value of square of atomic magnetic moment
+ XMLD allows investigating ferri- and ferromagnets as well as antiferromagnets
+ XMLD spectral shape and angular dependence are determined by magnetic order and lattice symmetry

Magnetic Coupling At Interfaces

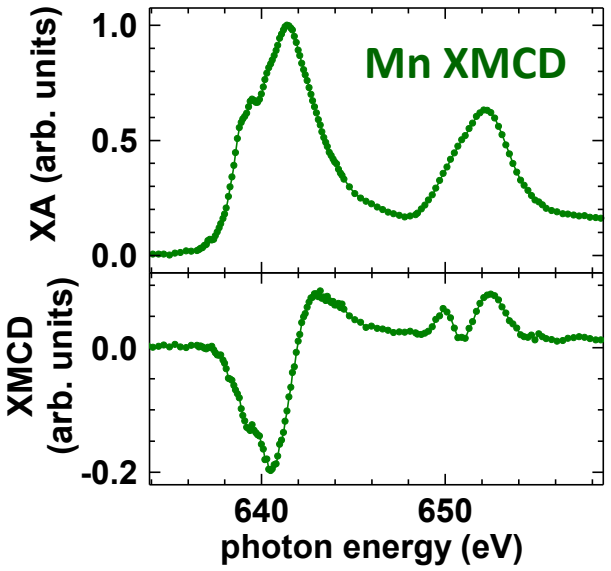

$La_{0.7}Sr_{0.3}MnO_3$ (LSMO)
ferromagnet
$La_{0.7}Sr_{0.3}FeO_3$ (LSFO)
antiferromagnet

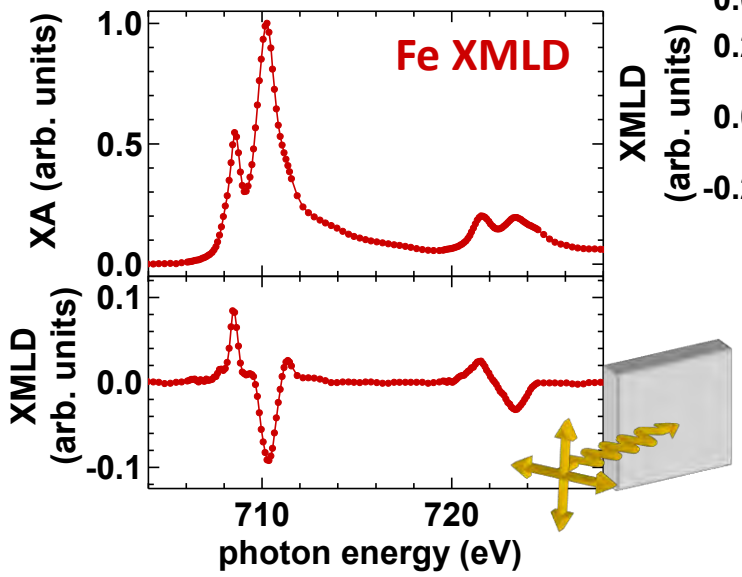

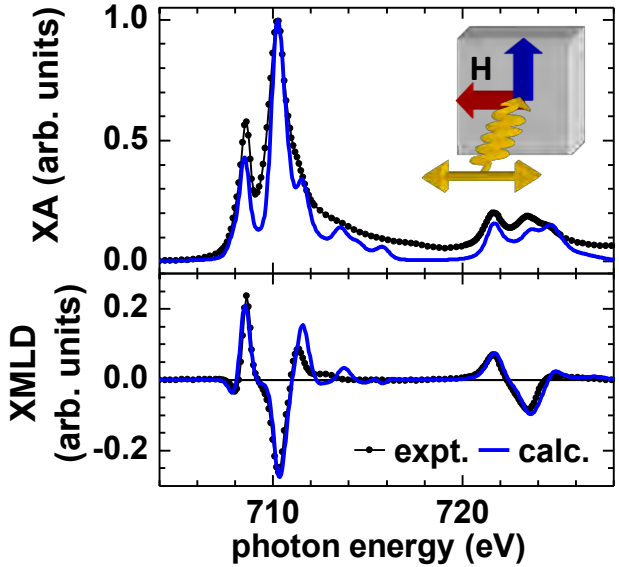

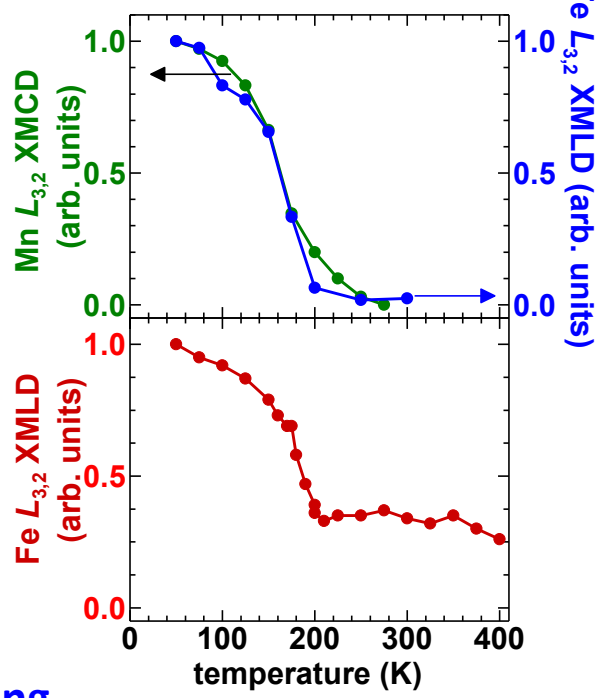

⇒ Perpendicular coupling at LSMO/LSFO interface

E. Arenholz *et al.*,
Appl. Phys. Lett. 94, 072503 (2009)

Planar Domain Wall

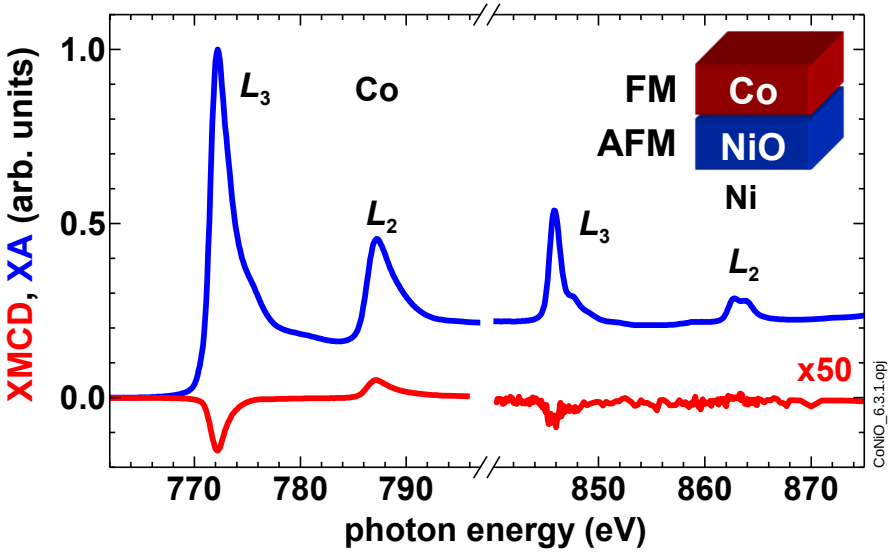

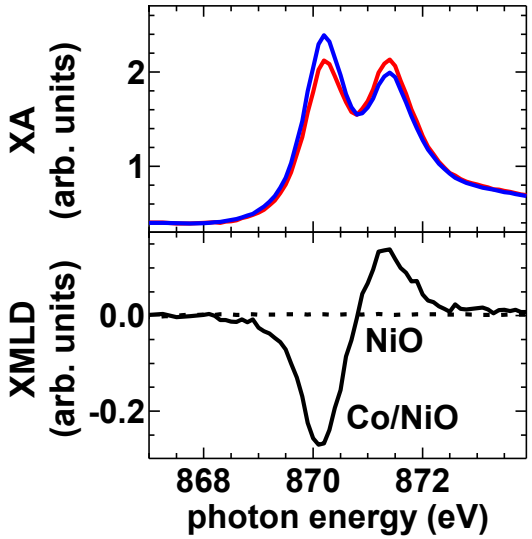

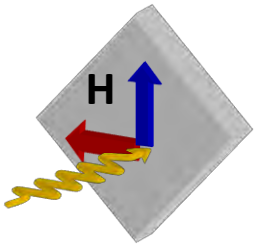

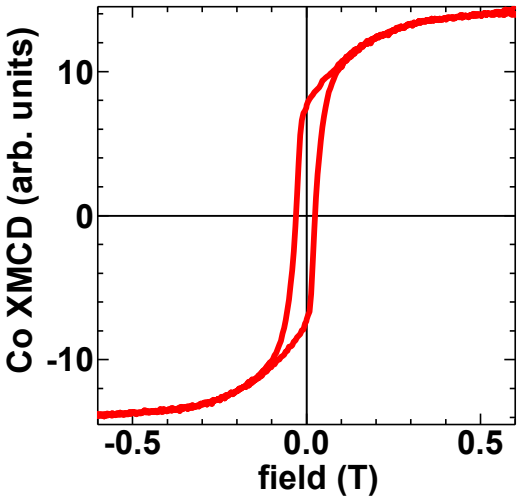

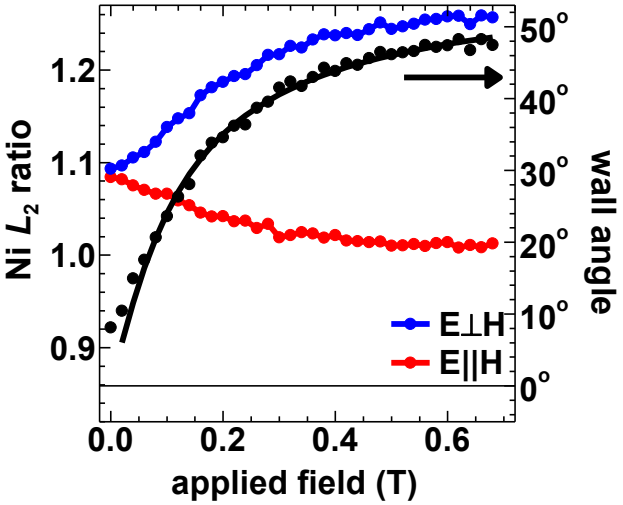

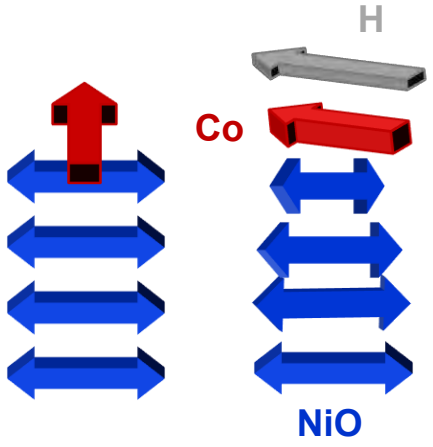

A. Scholl *et al.*,
Phys. Rev. Lett. 92, 247201 (2004)

Magnetic Microscopy

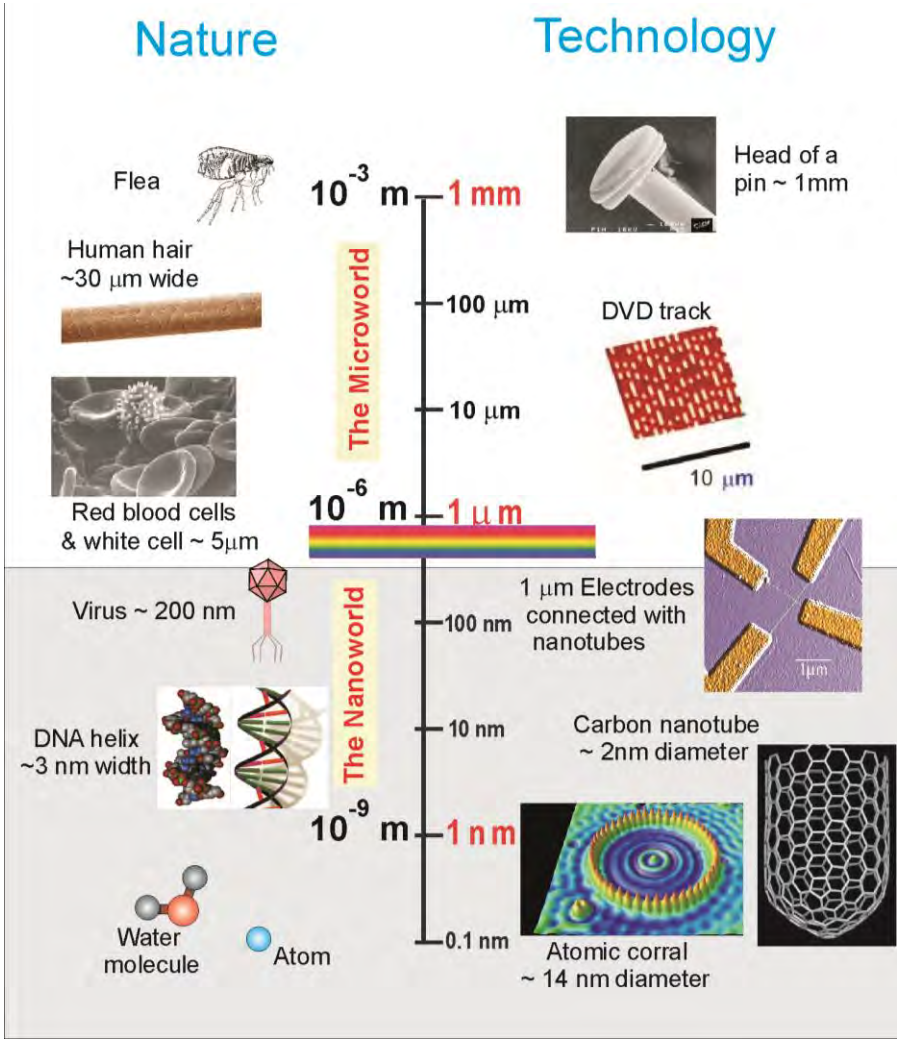

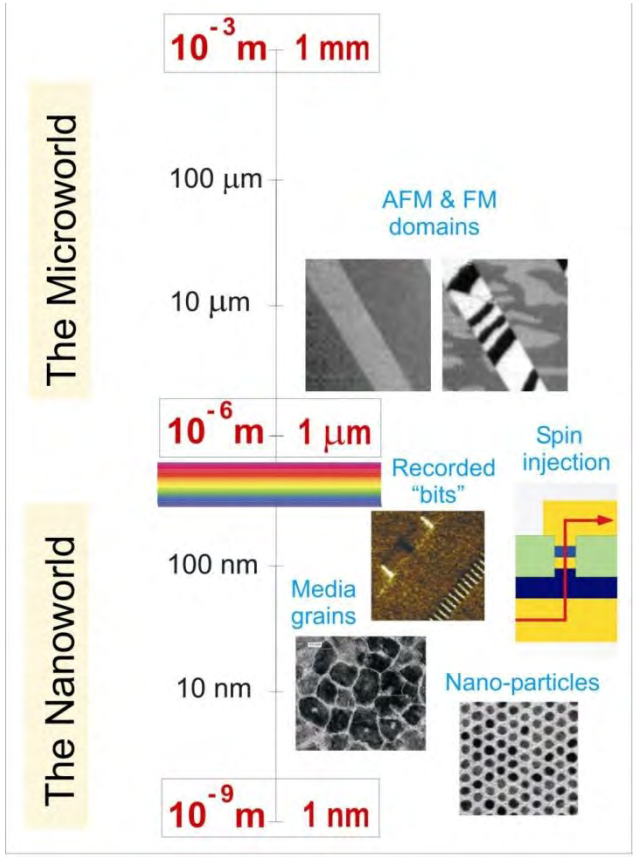

Magnetic Microscopy

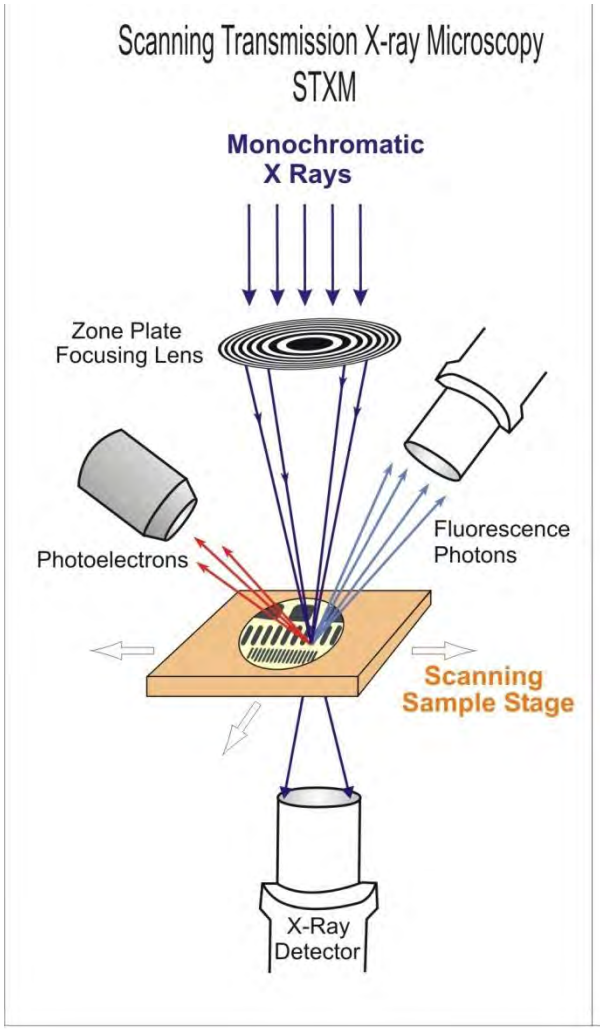

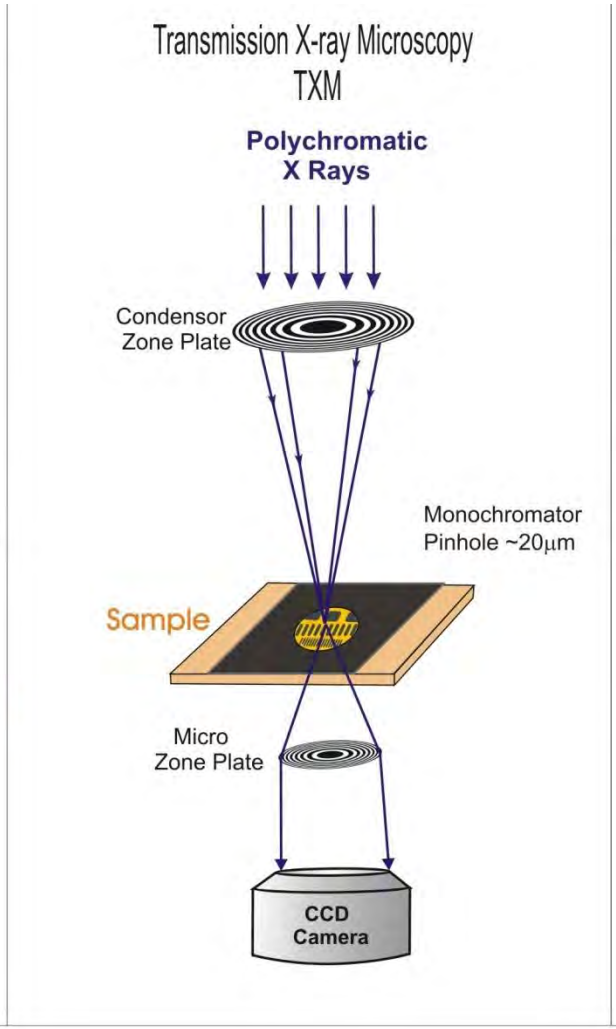

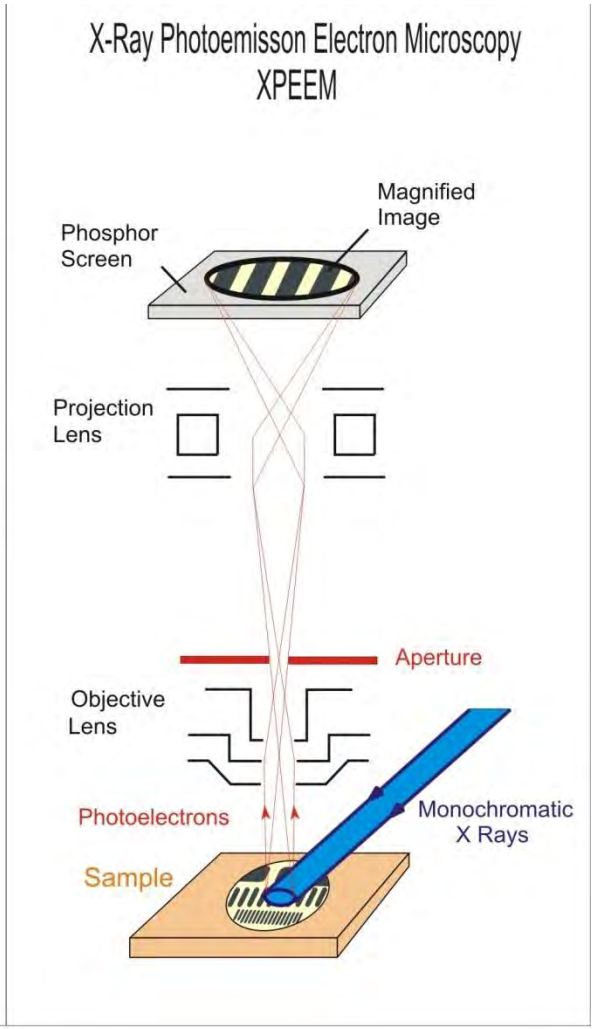

J. Stöhr, H.C. Siegmann, Magnetism (Springer)

10-50 nm spatial resolution

Imaging Magnetic Domains Using X-Rays

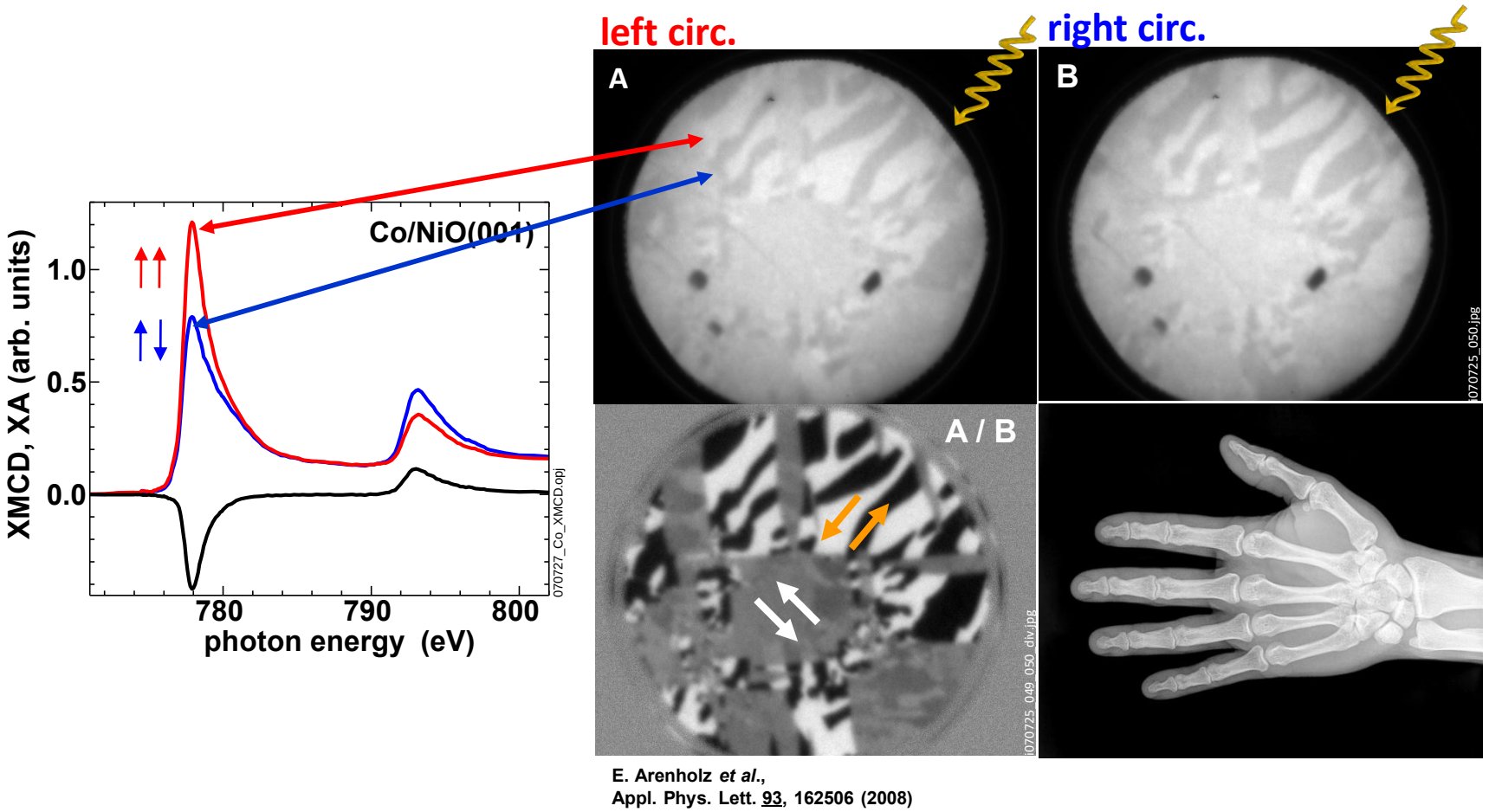

E. Arenholz *et al.*,
Appl. Phys. Lett. 93, 162506 (2008)

+ Images taken with left and right circularly polarized X-rays at photon energies with XMCD, i.e. Co L_3 edge, provide magnetic contrast and domain images.

Magnetic Coupling At Co/NiO Interface

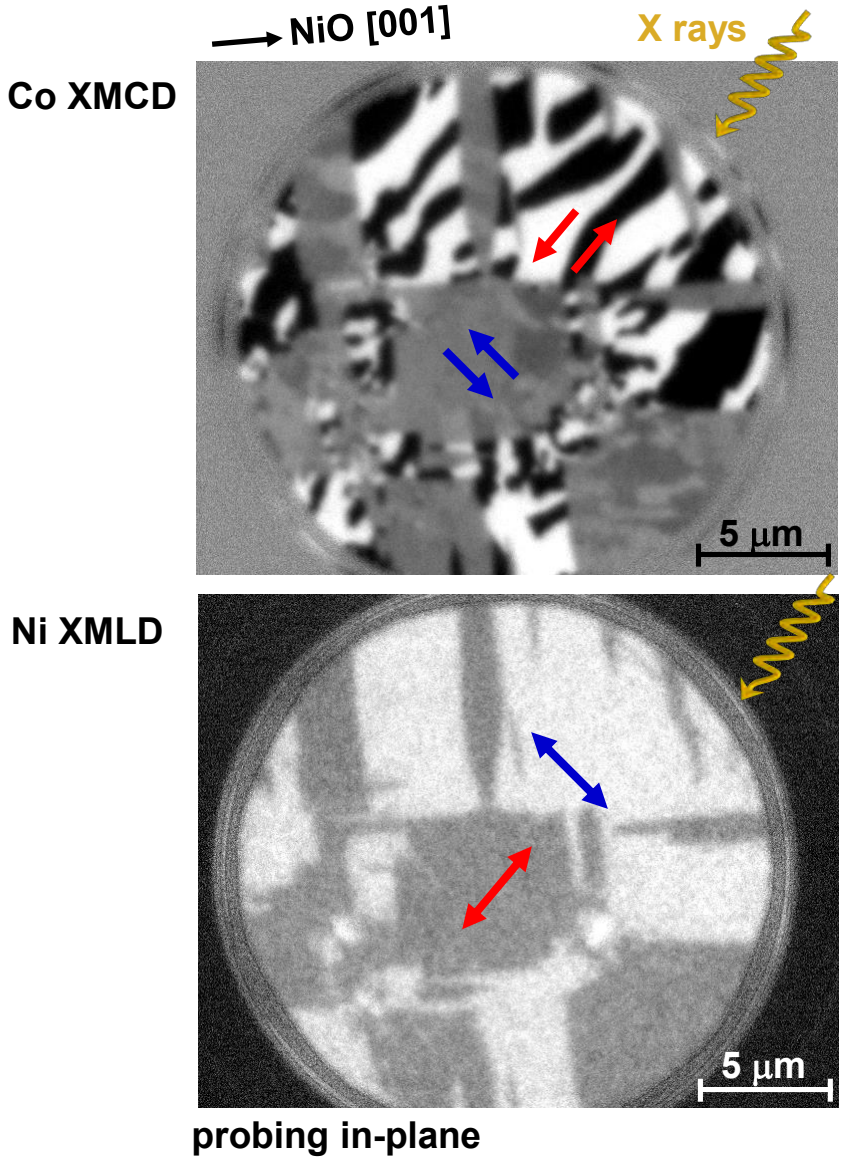

+ Taking into account the geometry dependence of the Ni XMLD signal

⇒ Perpendicular coupling of Co and NiO moments at the interface.

E. Arenholz *et al.*,
Appl. Phys. Lett. 93, 162506 (2008)

Magnetic Vortices

+ First direct observation of vortex state in antiferromagnetic CoO and NiO disks in Fe/CoO and Fe/NiO bilayers using XMCD and XMLD.
+ Two types of AFM vortices:
  - conventional curling vortex as in ferromagnets
  - divergent vortex, forbidden in ferromagnets
  - thickness dependence of magnetic interface coupling

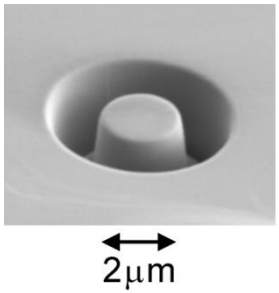

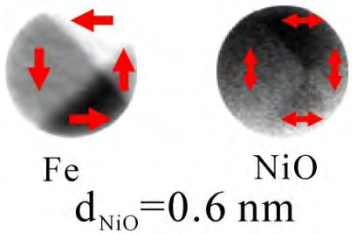

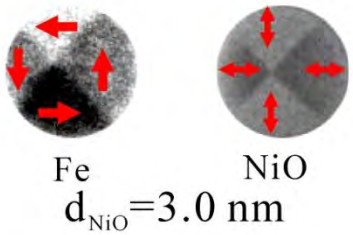

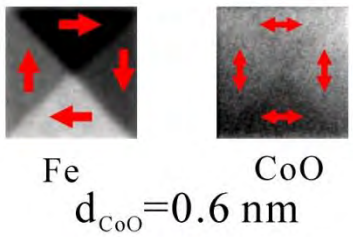

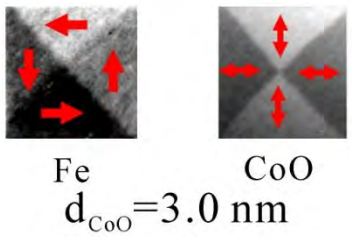

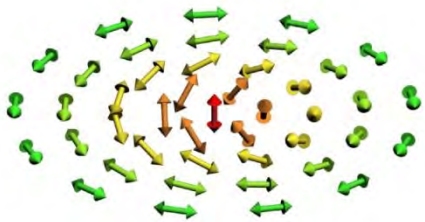

conventional curling vortex

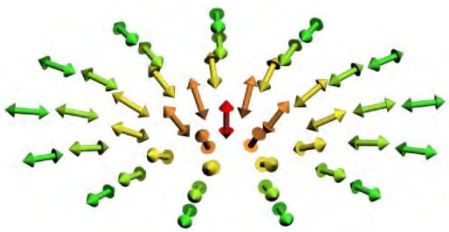

divergent vortex

J. Wu *et al.*,
Nature Phys. 7, 303 (2011)

Nanoscale Magnetic Phases

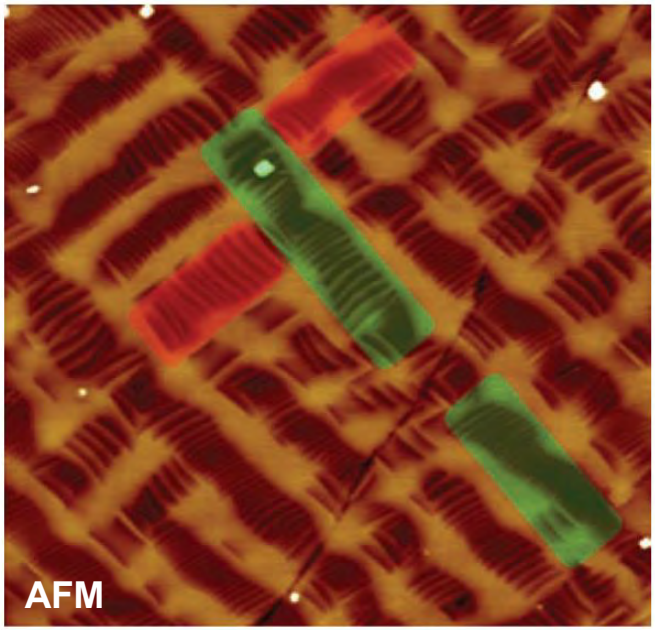

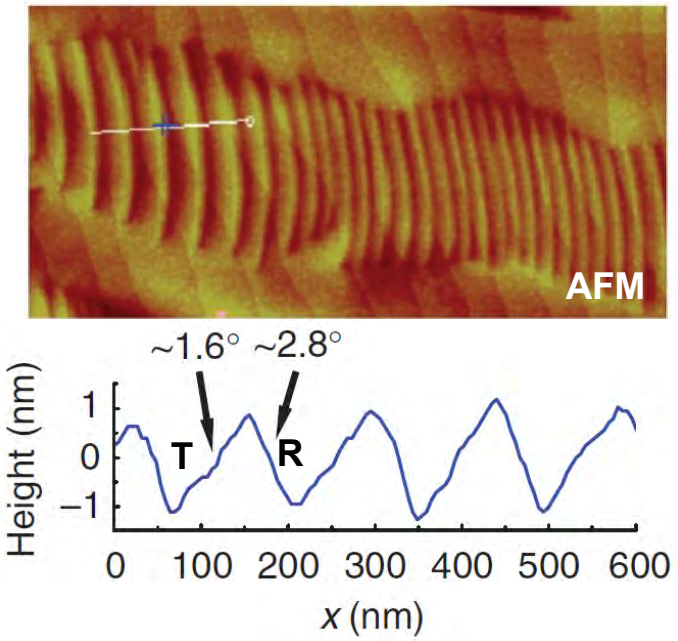

+ $BiFeO_3$ – multiferroic = ferroelectric + antiferromagnetic
+ Compressive strain on rhombohedral phase (R-phase) induced by substrate

⇒ tetragonal-like phase (T-phase)

+ Partial relaxation of epitaxial strain

⇒ Formation of a nanoscale mixture of T- and R-phases

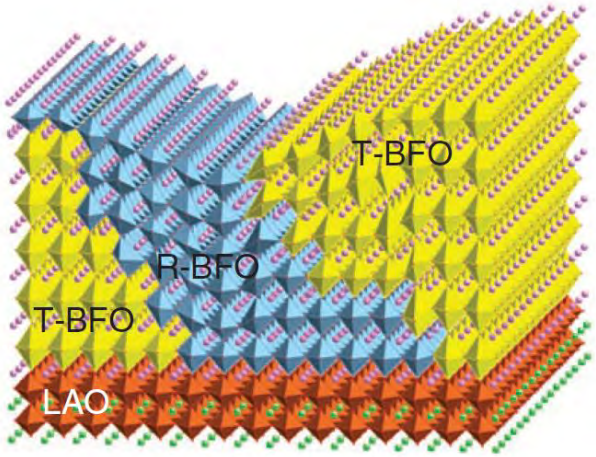

Q. He *et al.*, Nature Comm. 2, 225 (2011)

Nanoscale Magnetic Phases

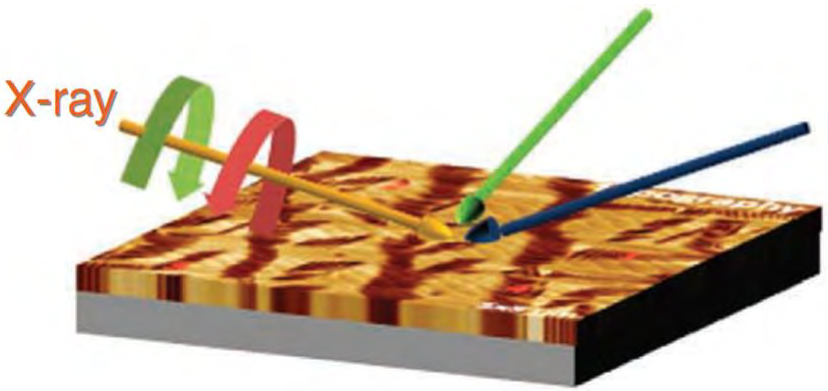

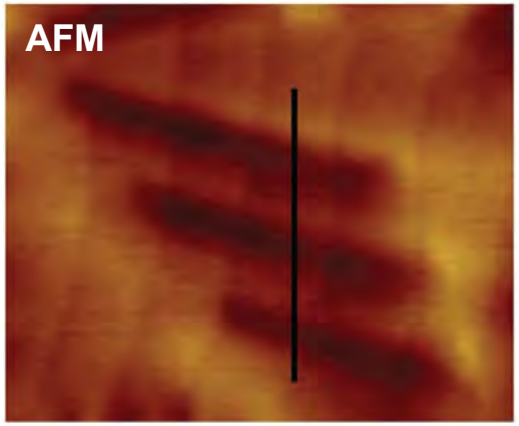

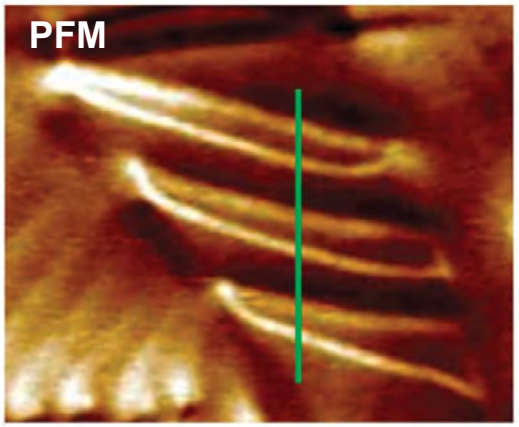

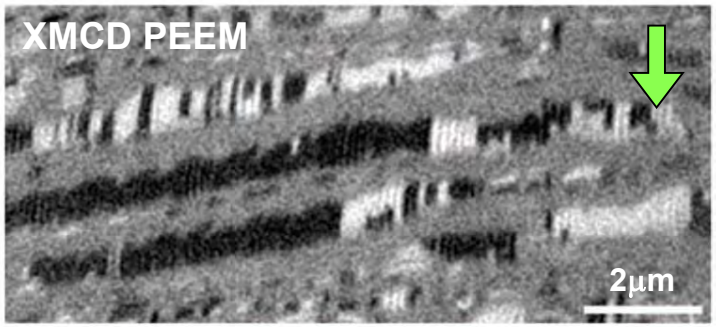

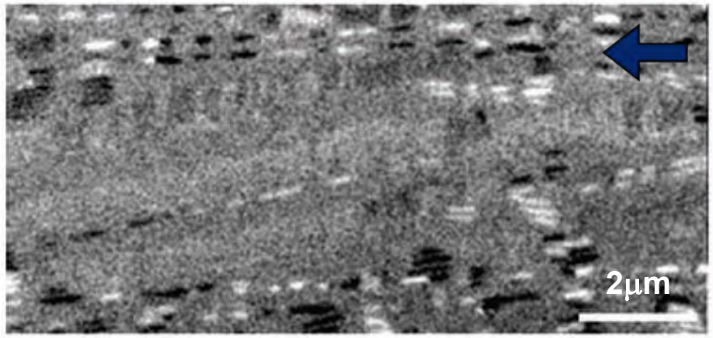

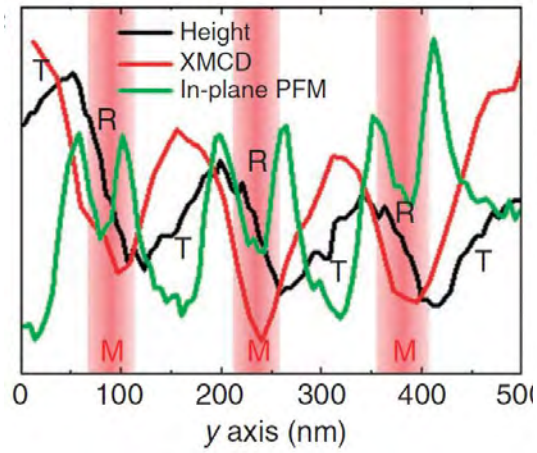

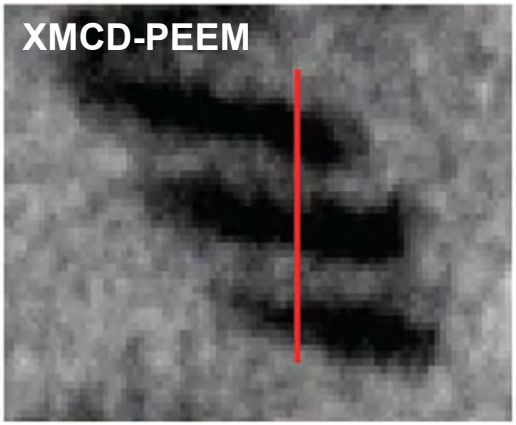

Q. He *et al.*,
Nature Comm. 2, 225 (2011)

+ **Highly distorted R-phase is the source of enhanced magnetic moment in the XMCD image.**

Ultrafast Magnetism

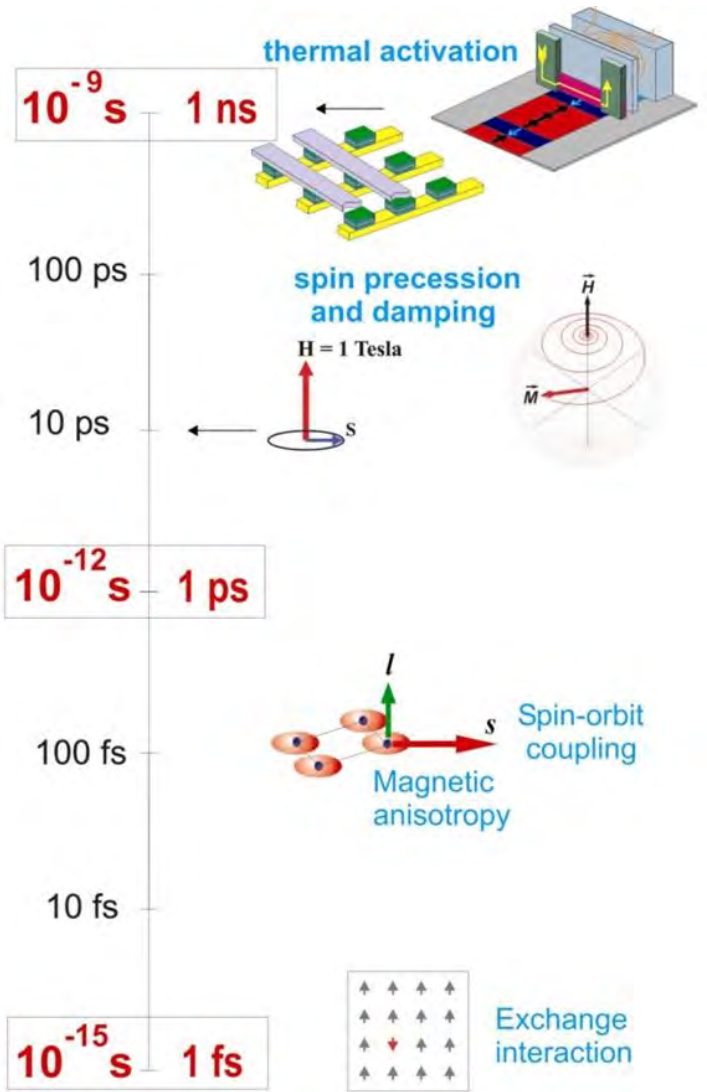

J. Stöhr, H.C. Siegmann, Magnetism (Springer)

+ Energy reservoirs in a ferromagnetic metal
+ Deposition of energy in one reservoir
⇒ Non-equilibrium distribution and subsequent relation through energy and angular momentum exchange

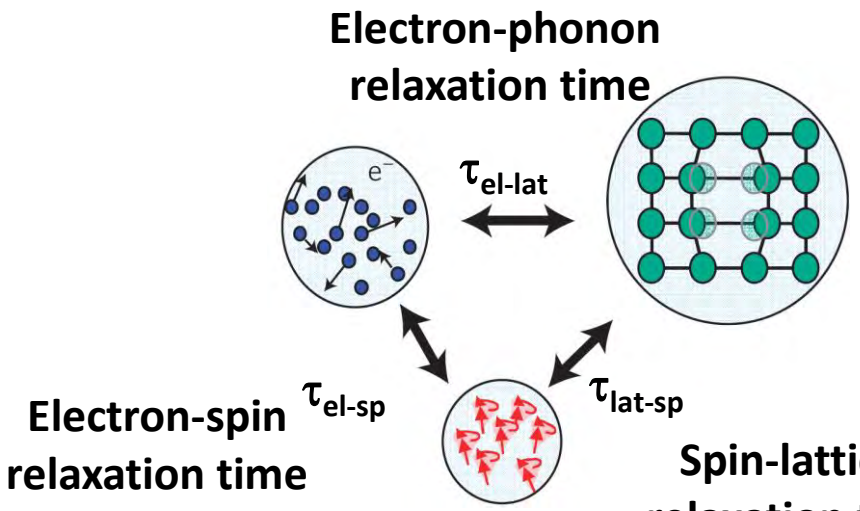

Ultrafast Dynamics Of Spin And Orbital Moments

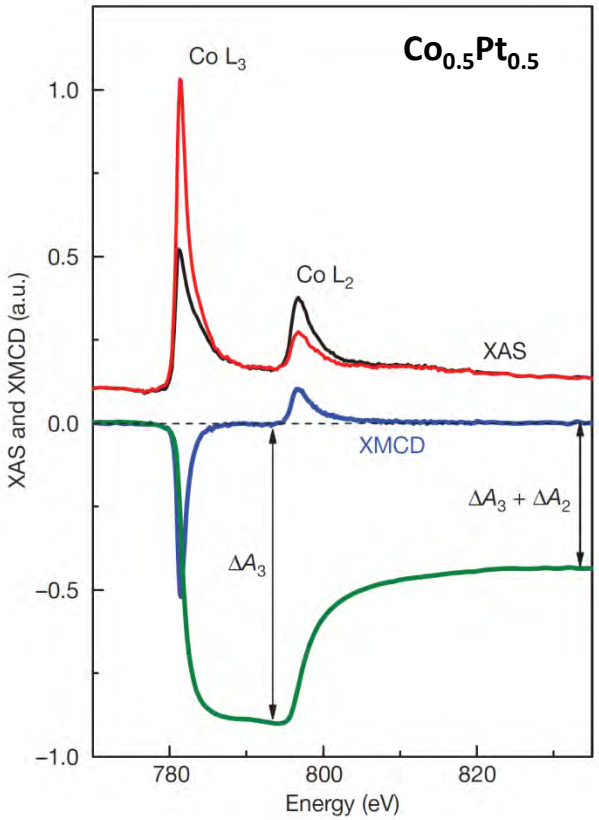

C. Boeglin, *et al.*,
Nature 465, 458 (2010)

+ Orbital (*L*) and spin (*S*) magnetic moments can change with total angular momentum is conserved.
+ Efficient transfer between *L* and S through spin–orbit interaction in solids
+ Transfer between *L* and *S* occurs on fs timescales.

+ $Co_{0.5}Pt_{0.5}$ with perpendicu magnetic anisotropy
+ 60 fs optical laser pulses change magnetization
+ Dynamics probed with XMCD using 120fs X-ray pulses

+ Linear relation connects Co L_3 and L_2 XMCD with L_z and S_z using sum rules

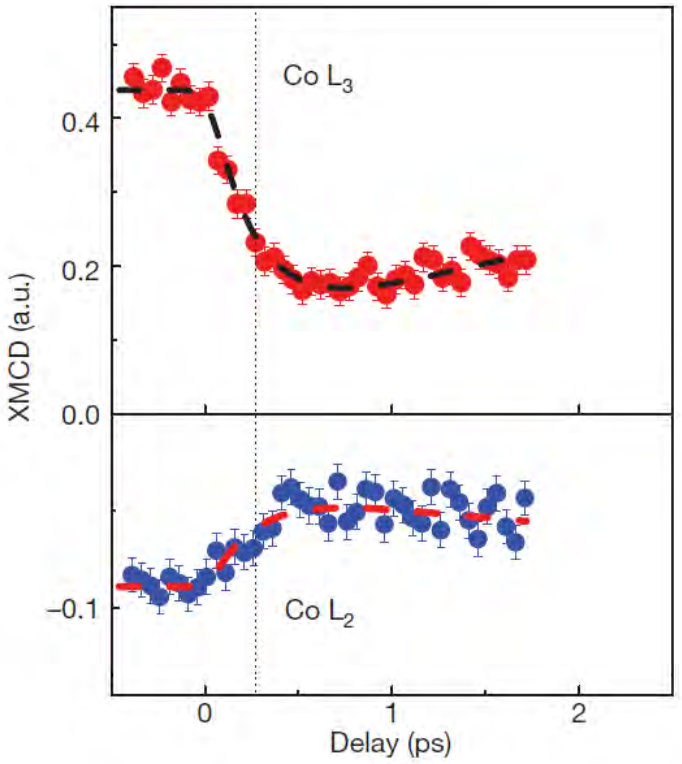

Ultrafast Dynamics Of Spin And Orbital Moments

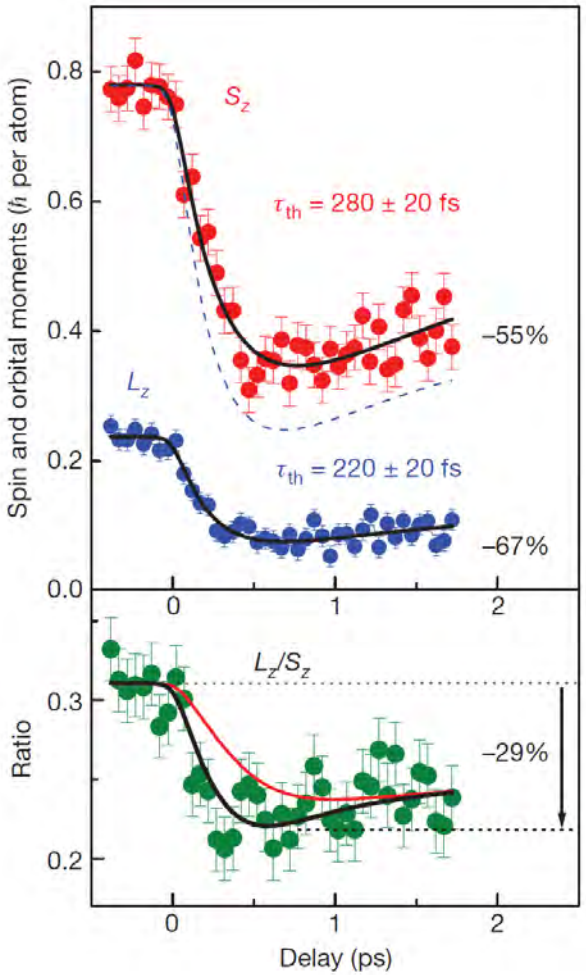

C. Boeglin, *et al.*,
Nature 465, 458 (2010)

+ Thermalization: Faster decrease of orbital moment
+ Theory: Orbital magnetic moment strongly correlated with magnetocrystalline anisotropy
+ Reduction in orbital moment
  ⇔ Reduction in magnetocrystalline anisotropy
+ Typically observed at elevated temperatures in static measurements as well

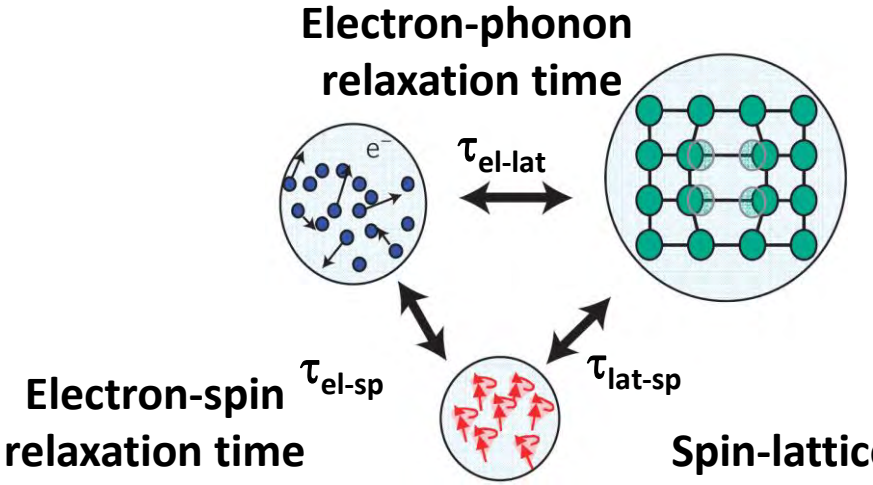

References And Further Reading

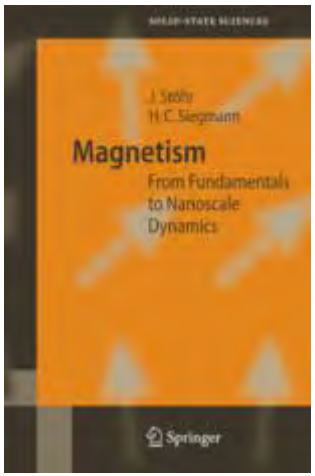

J. Stöhr, H.C. Siegmann
Magnetism– From Fundamentals to Nanoscale Dynamics
Springer